2010

PIP-OFDM System Design and Application for Cognitive Radio Communications

Cong Wang
Western University

PIP-OFDM System Design and Application for Cognitive Radio Communications

(Spine title: OFDM System with Precoded In-band Pilots)

(Thesis format: Monograph)

by

Cong Wang

Graduate Program
in
Engineering Science
Electrical and Computer Engineering

A thesis submitted in partial fulfillment
of the requirements for the degree of
Master of Engineering Science

The School of Graduate and Postdoctoral Studies
The University of Western Ontario
London, Ontario, Canada

THE UNIVERSITY OF WESTERN ONTARIO
SCHOOL OF GRADUATE AND POSTDOCTORAL STUDIES

CERTIFICATE OF EXAMINATION

Chief Advisor:

Dr. Xianbin Wang

Advisory Committee:

Examining Board:

Dr. Liying Jiang

Dr. Abdelkader H. Ouda

Dr. Serguei L. Primak

The thesis by

Cong Wang

entitled:

PIP-OFDM System Design and Application for Cognitive Radio Communications

is accepted in partial fulfillment of the

requirements for the degree of

Master of Engineering Science

Date: _____

Chair of Examining Board
Dr. Robert Sobot

Abstract

This thesis defines a new Orthogonal Frequency Division Multiplexing (OFDM) system with Precoded In-band Pilots (PIP) tailored for cognitive radio (CR) communications. The motivation, principle, system design, implementation architecture, and CR application specific considerations of proposed PIP-OFDM system are investigated in this thesis.

Principles and limitations of existing spectrum sensing techniques for cognitive radio communications are first analyzed and compared, with a focus on implementation challenges of pilot-based spectrum sensing for OFDM signals due to its robust performance in low signal-to-noise ratio (SNR) conditions. Several technical difficulties which haven't been well addressed in previous pilot-based OFDM spectrum sensing studies, including impact of cyclic prefix, frequency offset between transmitter and spectrum sensing device, and noise uncertainty in the sensing threshold design, are taken into consideration in the analysis.

Considering the poor performance of existing spectrum sensing techniques on user identification in cognitive radio network, where multiple secondary users may coexist, a precoded in-band pilots design is proposed in this thesis to enhance the user identification capabilities at low SNRs. The pilots in proposed PIP-OFDM system consist of uniform pilots and identification pilots. Each secondary user is associated with a unique identification pilot signal for identification purpose. Encoding of identification pilots is investigated, which will be used at the spectrum sensing device to identify the active user on the frequency band of interest.

Abstract

To demodulate/decode identification pilots for user identification purpose, synchronization between transmitter and spectrum sensing device needs to be established. The synchronization in PIP-OFDM system, which is different from that in traditional OFDM systems, is subsequently investigated. Coarse time and frequency synchronization are achieved by correlation respectively in time and frequency domain. Through phase shift estimation in time domain, fine frequency synchronization is reached using a modified maximum likelihood estimation algorithm exploiting the redundancy in cyclic prefix. Based on this observation, a fine time synchronization algorithm is proposed in this thesis using redundant information on specifically designed uniform pilots. A multiple OFDM symbols processing strategy is used to improve the synchronization performance of PIP-OFDM system considering the poor performance of synchronization at low SNR.

With the developed synchronization strategies, channel estimation in PIP-OFDM system is achieved using well developed estimation techniques in frequency domain. User identification is subsequently realized through demodulating the identification pilots. Theoretical performance and simulation results of user identification in PIP-OFDM system are provided to further confirm the effectiveness of the proposed design.

Acknowledgements

I present my sincerest appreciation to those who made this thesis possible.

I would like to first thank my supervisor, Dr. Xianbin Wang, whose encouragement and support from the initial to the final level enabled me to develop a solid understanding of this subject. His guidance and freedom encouraged me to endeavor into this new research area. It has been a true fortune and privilege working with him.

I would also like to thank the examination committee chair Dr. Robert Sobot, and examination committee members, including Dr. Liying Jiang, Dr. Abdelkader H. Ouda, and Dr. Serguei L. Primak. Their reviews and comments helped a lot on the final version of this thesis, and also give great assistants on the future work.

I also owe my deepest gratitude to Dr. Serguei L. Primak, Dr. Raveendra K. Rao, and Dr. Lalu Mansinha for those courses greatly improved my work in theoretical analysis, understanding of communication systems, and simulation works.

It's an honor for me to thank my fellows in my research group, including Jahidur, Hao, Imran, Frank, and Sahar, for their help and support. These thanks are also for my other friends, roommates, and those old friends in China, who have helped me a lot remotely.

I also want to thank Graduate Assistant, Sandra, and librarians in Allyn & Betty Taylor Library and The D. B. Weldon Library for their work and help.

I am indebted to my family. Even far away, they have been present and supportive through every step of my study, providing help in difficult times, and enjoying every single accomplishment during my study.

Lastly, I offer my regards and blessings to all of those who supported me in any respect during the completion of this study.

Table of Contents

Certificate of Examination . . . . . **ii**

Abstract . . . . . **iii**

Acknowledgements . . . . . **v**

List of figures . . . . . **x**

Acronyms . . . . . **xi**

1 Overview of The Thesis **1**

1.1 Overview of the Thesis 1

1.2 Thesis Organization 3

1.3 Notations in the Thesis 4

2 Motivation and Background **5**

2.1 Motivation of the Thesis 5

2.2 Review of Related Works 8

2.2.1 Cognitive Radio and Dynamic Spectrum Access 8

2.2.2 Spectrum Sensing Techniques for Cognitive Radio 9

2.2.2.1 General Techniques on Spectrum Sensing 9

2.2.2.2 Pilot-based Spectrum Sensing 10

2.2.3 User Identification 10

2.2.4 Synchronization Technologies in OFDM System 11

2.2.4.1 Frequency Synchronization 11

2.2.4.2 Time Synchronization 12

2.3 Summary 13

3 Spectrum Sensing for Cognitive Radio Communications 14
3.1 Background of Spectrum Sensing 14
3.1.1 Definition of Cognitive Radio 14
3.1.2 Definition of Spectrum Sensing 16
3.1.3 Requirements and Challenges of Spectrum Sensing 16
3.1.3.1 Low SNR Requirement and Synchronization Challenge . 16
3.1.3.2 Sensing Time Requirement 17
3.1.3.3 User Identification Capability of Spectrum Sensing . . . 17
3.2 Spectrum Sensing Techniques Overview 18
3.2.1 Two Hypotheses in Spectrum Sensing 18
3.2.2 Energy Detection and Matched Filter Detection 18
3.2.3 Cyclostationary Detection 21
3.3 Pilot-based Spectrum Sensing for OFDM 25
3.3.1 System Model and Assumptions 25
3.3.1.1 OFDM Signal Generation 25
3.3.1.2 In-band Pilots Insertion 26
3.3.1.3 Received Signal at Spectrum Sensing Device 27
3.3.2 Principle of Pilot-based OFDM Spectrum Sensing 28
3.3.3 Challenges of Pilot-based OFDM Spectrum Sensing 31
3.3.4 Impacts of Timing Offsets and Cyclic Prefix 32
3.3.5 Pilot-based OFDM Spectrum Sensing with SFC 34
3.3.6 Noise Uncertainty and Threshold Design 37
3.3.7 Theoretical Analysis of Pilot-based OFDM Spectrum Sensing . . . 38
3.3.7.1 False Alarm Probability and Threshold Design 38
3.3.7.2 Probability of Mis-detection 41
3.3.7.3 Pilot-based OFDM Spectrum Sensing Time 42
3.3.7.4 Impacts of Interference and Multipath Channel 43
3.3.8 Simulations 44
3.4 Chapter Summary 48

4 Design of PIP-OFDM System 50
4.1 Motivation of PIP-OFDM 50
4.2 Design of PIP-OFDM System 51
4.2.1 Pilot tones in PIP-OFDM System 51
4.2.2 Design and Precoding of the Pilot Tones 53
4.3 Spectrum Sensing in PIP-OFDM System 56
4.4 Chapter Summary 57

5 Synchronization in PIP-OFDM System 58
5.1 Background of Synchronization in PIP-OFDM 58
5.2 Coarse Synchronization Algorithms 59
5.2.1 Coarse Frequency Synchronization 59
5.2.2 Coarse Time Synchronization 61
5.3 Fine Synchronization Algorithms 63
5.3.1 Fine Frequency Synchronization 63
5.3.2 Fine Time Synchronization 65
5.4 Performance Analysis of Synchronization in PIP-OFDM 70
5.4.1 Performance of Fine Frequency Synchronization 70
5.4.2 Performance of Fine Time Synchronization 72
5.5 Simulations 75
5.6 Chapter Summary 75

6 User Identification in PIP-OFDM System 79
6.1 Channel Estimation and Equalization 79
6.2 User Identification Algorithm 80
6.2.1 Demodulation and Identification Process 80
6.2.2 Performance Analysis of User Identification in PIP-OFDM 81
6.2.3 Simulations 83
6.3 Chapter Summary 85

7 Conclusions and Future Works 86
7.1 Contributions of This Thesis 86
7.2 Future Works 87

References 89

Curriculum Vitae 96

List of Figures

2.1 U.S. frequency allocation chart (NTIA). 6
2.2 Spectrum allocation in dynamic spectrum access. 9

3.1 Architecture of cognitive radio network considered in this thesis. 15
3.2 Received signal power at energy detection device. 19
3.3 Performance of the energy detection. 21
3.4 Cyclostationarity of FSK signals. 22
3.5 Cyclostationarity of QPSK signals. 23
3.6 Cyclostationarity of noise signals. 23
3.7 Impact of average processing on signal's power distribution. 29
3.8 Flowchart of pilot-based OFDM spectrum sensing algorithm. 30
3.9 Received OFDM signal with unknown timing offset. 33
3.10 Illustration of sliding frequency correlation processing. 35
3.11 Probability of successful detection of pilot-based spectrum sensing. 45
3.12 Probability of mis-detection of pilot-based spectrum sensing. 46
3.13 Probability of mis-detection of pilot-based spectrum sensing. 46
3.14 Impacts from cyclic prefix on pilot-based spectrum sensing. 47
3.15 Theoretical spectrum sensing time for DVB-T 2K mode signal. 48

4.1 Illustration of pilots in PIP-OFDM signal. 51

5.1 Averaged OFDM symbol's power distribution in frequency domain. 60
5.2 Illustration of received OFDM signal with unknown time delay. 61
5.3 Output of the correlation function with DC method. 62
5.4 Theoretical fine synchronization performances in PIP-OFDM system. . . . 76
5.5 Simulated fine synchronization performances in PIP-OFDM system. 77

6.1 User identification performance in terms of identification error rate. 84

Acronyms

ATSC	*Advanced Television Systems Committee*
AWGN	*Additive White Gaussian Noise*
BER	*Bit Error Rate*
CFO	*Carrier Frequency Offset*
CP	*Cyclic Prefix*
CR	*Cognitive Radio*
DSA	*Dynamic Spectrum Access*
DVB-T	*Digital Video Broadcasting-Terrestrial*
FCC	*Federal Communications Commission*
FSK	*Frequency Shift Keying*
ICI	*Inter-carrier Interference*
IEEE	*Institute of Electrical and Electronics Engineers*
IER	*Identification Error Rate*
ISI	*Intersymbol Interference*
ML	*Maximum Likelihood*
MMSE	*Minimum Mean Squared Error*
OFDM	*Orthogonal Frequency Division Multiplexing*
OSA	*Opportunistic Spectrum Access*
PDA	*Personal Digital Assistant*
PIP-OFDM	*Precoded In-band Pilots OFDM*
PPM	*Parts Per Million*
PRR	*Peak-to-remaining Ratio*
QAM	*Quadrature Amplitude Modulation*
QPSK	*Quadrature Phase Shift Keying*
SFC	*Sliding Frequency Correlator*
SFO	*Sampling Frequency Offset*
SU	*Secondary User*

Chapter 1

Overview of The Thesis

This thesis first analyzes, compares, and summarizes spectrum sensing techniques for cognitive radio communications, with a focus on pilot-based spectrum sensing for Orthogonal Frequency Division Multiplexing (OFDM) system. Considering the poor performances of these spectrum sensing techniques in user identification, an OFDM system with precoded in-band pilots (PIP-OFDM) is proposed to improve user identification capability in low signal-to-noise ratio (SNR) conditions. Related system design and enabling techniques for the proposed PIP-OFDM system, including encoding/modulation, synchronization, channel estimation, and decoding/identification are investigated subsequently.

1.1 Overview of the Thesis

Cognitive radio was proposed as a promising solution to improve spectrum resource utilization efficiency in wireless communications through dynamic spectrum sharing. Spectrum sensing has been regarded as one key enabling technology during the implementation of cognitive radio, which determines the availability of frequency band of interest. A major challenge for spectrum sensing in cognitive radio is the low SNR requirement. Existing spectrum sensing techniques, including energy detection, matched filter detection, cyclostationary detection, and pilot-based detection, are discussed with technique principles and limitations. It is found that pilot-based detection has a relatively better performance at

low SNR environment. Factors that impact the performance of pilot-based spectrum sensing algorithm for OFDM signal, including cyclic prefix impact, frequency offset between transmitter and sensing device, and noise uncertainty in designing the sensing threshold, are subsequently investigated. Specifically, the impact of cyclic prefix during the implementation of pilot-based spectrum sensing for OFDM signal is analyzed and proved to be neglectable with computer simulations. In addition, a sliding frequency correlator is proposed in this thesis to address the difficulties in random frequency offset and noise uncertainty.

It is also observed in the thesis that the existing spectrum sensing techniques perform poorly on user identification in low SNR conditions. In cognitive radio network, with the coexistence of multiple secondary users, user identity is an essential information in determining the spectrum sharing mechanism and managing the wireless network. This thesis consequently proposes a precoded in-band pilots design for OFDM signal, which improves the user identification capability of spectrum sensing device in cognitive radio network. Two groups of pilots, uniform pilots and identification pilots, are multiplexed with information bearing subcarriers in the proposed PIP-OFDM system. The identification pilots built in transmitted signal are specifically designed to carry unique ID information, while uniform pilots are kept identical in every secondary user in one cognitive radio network. The identity of the active secondary user is then estimated through PIP demodulation at spectrum sensing device after synchronization between transmitter and sensing device is achieved.

Synchronization in PIP-OFDM system is very challenging due to the low SNR requirement and the elimination of training symbols. Some relative correlation methods are adopted to implement coarse frequency and coarse time synchronization for PIP-OFDM systems. Fine frequency synchronization is realized by estimating phase shift in time domain using redundant information in cyclic prefix. Using this principle, fine time syn-

chronization is achieved by estimating phase shift in frequency domain considering the redundant information on specially designed uniform pilots. Similar to spectrum sensing, synchronization in PIP-OFDM system is performed at low SNR. Consequently, a multiple OFDM symbols processing strategy is used to improve synchronization performances in proposed PIP-OFDM system.

Channel estimation and equalization techniques used in the proposed PIP-OFDM system are briefly introduced subsequently, followed by the details of user identification algorithm with the decoding/demodulation of identification pilots. The theoretical and simulation results on user identification at low SNR further confirm the effectiveness of the proposed PIP-OFDM design.

1.2 Thesis Organization

The motivation and background of this work are discussed in Chapter 2. Historical background and definition of cognitive radio are presented. As one of the most critical difficulties in cognitive radio communications, spectrum sensing is subsequently introduced with definition and challenges. Overview of related research works are also presented in Chapter 2, including previous spectrum sensing techniques and synchronization methods in OFDM systems.

Chapter 3 discusses spectrum sensing techniques in cognitive radio communications. Existing spectrum sensing techniques are summarized, followed by numerical simulations and performance comparisons. Implementation challenges of pilot-based spectrum sensing for OFDM signal are analyzed in detail in this chapter. A new pilot-based OFDM spectrum sensing algorithm with sliding frequency correlator is proposed subsequently to address these challenges.

The definition and design details of PIP-OFDM system are presented in Chapter 4. Encoding and modulation on identification pilots are discussed; the user capacity of cognitive radio network in the PIP-OFDM design is introduced in this chapter.

Chapter 5 investigates synchronization technologies in PIP-OFDM systems. Principles of coarse and fine synchronization, both in time and frequency domain, are considered in this chapter, followed by theoretical analysis and computer simulations.

Based on the synchronization between transmitter and spectrum sensing device, Chapter 6 develops the identification algorithm by demodulating identification pilots after the equalization process. Decoding theory is also presented and analyzed with theoretical performances and simulations.

Finally, this thesis is concluded in Chapter 7. Research contributions and future works of the thesis are summarized in this chapter.

1.3 Notations in the Thesis

Standard notations are used in this thesis. Capitalized symbols denote signal in frequency domain, and lowercase symbols denote signal in time domain. Vectors and matrices are denoted by boldface characters.

Specifically, x is transmitted signal, h is channel response, y is signal at the receiver side, w is noise (with interference signals), and z is received signal with noise (and timing/frequency offsets if exist); k is used as sample index in frequency domain, n is the sample index in time domain, and m is the OFDM symbol index in time domain; τ is timing offset, and ε is frequency offset; noise's power in this thesis is denoted by δ_n^2, and signal's power is δ_s^2; C represents correlation, while P denotes probability.

Other variables and notations are defined when used in the thesis.

Chapter 2

Motivation and Background

2.1 Motivation of the Thesis

Spectrum resource scarcity has been accompanying the fast development of broadband wireless communications in recent years, creating a lot of challenges for the design and implementation of efficient wireless communication systems. The Federal Communications Commission (FCC) frequency allocation table [1] and the National Telecommunications and Information Administration's (NTIA) frequency allocation chart (Figure 2.1) indicate an exhausted assignment on current prime radio frequency spectrum (i.e., less than 3GHz). At the same time, many studies on the spectrum usage reveal very low utilization efficiency in current spectrum allocations [2]–[6]. Cognitive radio (CR), based on an opportunistic spectrum sharing mechanism, is being proposed as a revolutionary technology to improve the spectrum utilization efficiency [2]. Since then, both academia and industry have been searching for an efficient and practical solution for cognitive radio communications. The IEEE 802.22 working group has been formed to develop the standard for cognitive radio technology in TV bands due to the transition from analog to digital broadcast [7].

As numerous regulation related issues emerged, the recent development of cognitive radio brings significant technical challenges in the design of robust adaptive transmission technique, reliable spectrum sensing, and efficient wireless resource allocation in hostile communication environment [4]. Among the technical difficulties associated with cognitive

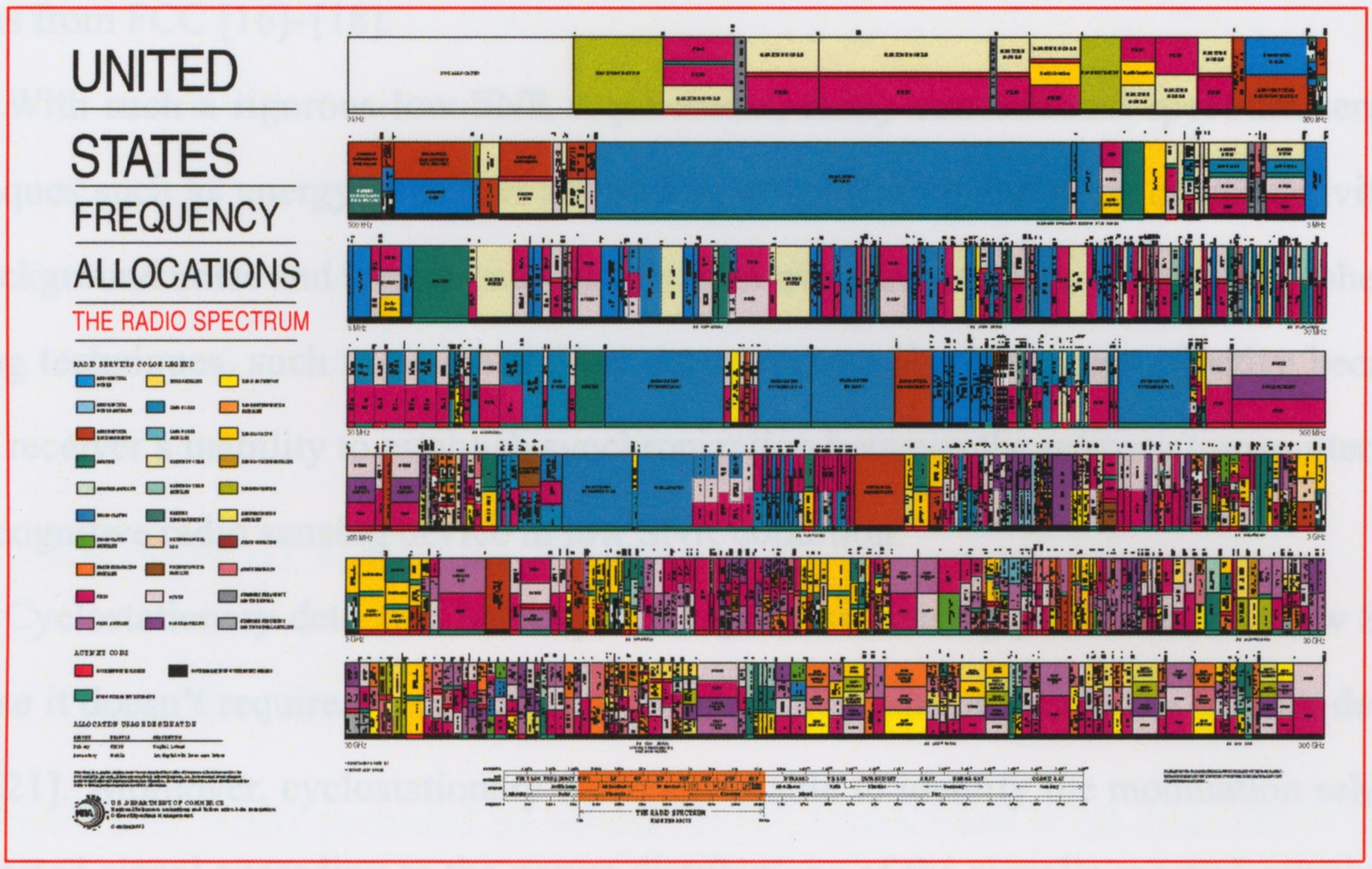

Figure 2.1: U.S. frequency allocation chart (NTIA).
[Available at: http://www.ntia.doc.gov/osmhome/allochrt.PDF.]

radio design, spectrum sensing (or signal sensing, detection) is emerging as one of the fundamental and primary challenges in the implementation of cognitive radio systems [8]–[14].

For the appropriate operation of a CR network, secondary users (SUs) are allowed to use the spectrum resources only when they do not create unacceptable interference to the primary users (licensed users) [4]. This means it's the CR user's responsibility to detect the existence of primary user. In order to ensure the absence of primary user before spectrum sharing and to avoid what is called the *hidden terminal problem* [15], the CR sensing devices must have the capability of performing accurate sensing in very low signal-to-noise ratio (SNR) conditions. In addition, the cognitive user's sensing device should outperform the primary receiver by a large margin to minimize the potential impact to the primary user. Consequently, the SNR of the received primary signal for spectrum sensing can be as low as −25dB to −10dB according to some previous research contributions and the recommen-

dations from FCC [16]–[18].

With such a rigorous low SNR requirement, many conventional spectrum sensing techniques such as energy detection are no longer applicable due to its oversensitivity to the background noise and interference signals from other transmitters. Some other coherent sensing techniques, such as matched filter detection, are also no longer effective because of the receiver's inability to establish synchronization between the primary transmitter and local cognitive radio sensing device in low SNR condition.

Cyclostationary detection has improved spectrum sensing performance at low SNR because it doesn't require synchronization between the transmitter and the sensing device [19]–[21]. Moreover, cyclostationary detection is able to identify the modulation scheme of detected signal according to the power distributions of the signal's spectral correlation [21]. However, the cyclostationary detection requires a high implementation complexity from the spectral correlation function as we will see in Chapter 3. Moreover, cyclostationary detection is also unable to identify the user when several users are using the same modulation scheme.

On the other hand, pilot-based spectrum sensing technique, based on detecting the energy of embedded pilot signals, shows many significant advantages over existing techniques including good performance at low SNR and the low implementation complexity. However, pilot-based spectrum sensing for OFDM signal has its own technical problems, including impact of cyclic prefix in OFDM signal, frequency offset between transmitter and sensing device, and noise uncertainty in the sensing threshold design. This thesis will further discuss these challenges, and propose a new sliding frequency correlator to address the challenges.

In cognitive radio network, spectrum sensing determines the availability of the current frequency band of interest. However, to better manage a cognitive radio network, where many secondary users coexist, another practical problem appears: Who is currently

using this frequency band? The process of identifying the secondary user that is using this frequency band is called *user identification*. Previous spectrum sensing algorithms rarely consider the user identification capabilities of spectrum sensing devices. Consequently, a more effective transmission signal design in cognitive radio network is necessary for reliable spectrum sharing and user identification.

2.2 Review of Related Works

2.2.1 Cognitive Radio and Dynamic Spectrum Access

Cognitive Radio, firstly proposed by Mitola [2] [3], is described in his dissertation [2] as "the point at which wireless personal digital assistants (PDAs) and the related networks are sufficiently computationally intelligent about radio resources and related computer-to-computer communications to: (a) detect user communications needs as a function of use context, and (b) to provide radio resources and wireless services most appropriate to those needs."

In the cognitive radio system initially proposed by Mitola, wireless terminals have full knowledge of every parameter in the current communication network, which is apparently difficult to achieve. Consequently, a more practical idea appears, known as "Dynamic Spectrum Access" (DSA) [22]–[24], which is also called "Opportunistic Spectrum Access" (OSA) [25]–[27]. In DSA systems, wireless terminals try to search for "spectrum holes" to access to available spectrum resource.

Figure 2.2 shows the resource allocation of DSA in frequency domain, where DSA users access to those spectrum holes and at the same time, have no (or limited but acceptable) influence to primary user(s). DSA is also regarded as a narrow sense and example of cognitive radio [22]. However, as a creative and popular definition, cognitive radio is still

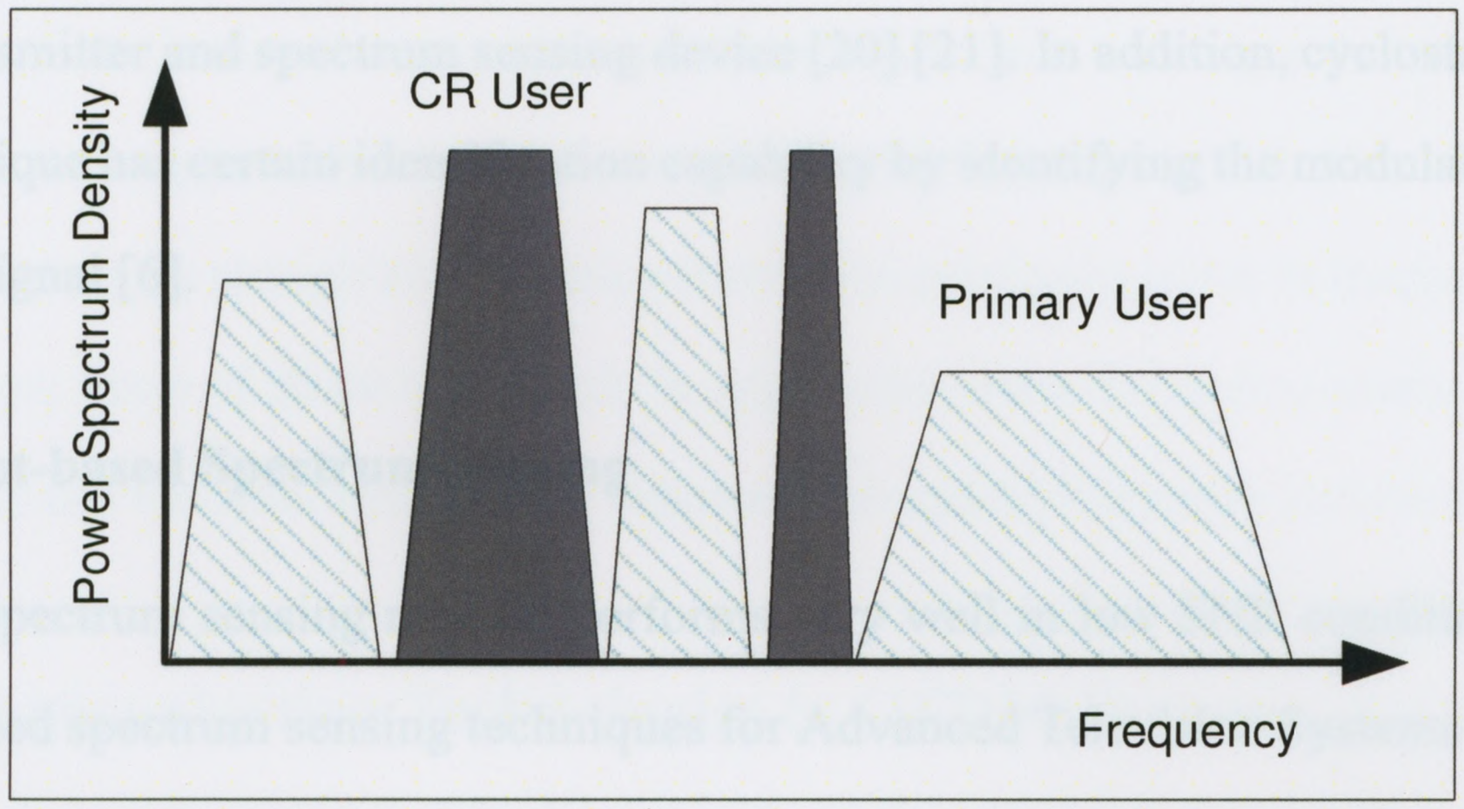

Figure 2.2: Spectrum allocation in dynamic spectrum access.

being widely used to represent DSA and OSA, which is the case in this thesis, as a general representative for communication with intelligence. Spectrum sensing, which is the process that wireless terminals search for spectrum holes, is consequently regarded as one of the most fundamental enabling techniques in cognitive radio communications [8] [9].

2.2.2 Spectrum Sensing Techniques for Cognitive Radio

As an enabling technique in cognitive radio system, spectrum sensing has been attracting much attention from both academia and industry. Low SNR requirement and user identification capability are regarded as two major challenges for spectrum sensing.

2.2.2.1 General Techniques on Spectrum Sensing

Several publications have summarized spectrum sensing techniques, which are normally classified into energy detection, matched filter detection, cyclostationary detection, and pilot-based detection [6] [8] [9]. In these literatures, the latter two sensing techniques are considered to be more effective considering the practicability and performance [8] [9]. Cyclostationary detection works well at low SNR since it doesn't require synchronization

between transmitter and spectrum sensing device [20] [21]. In addition, cyclostationary detection technique has certain identification capability by identifying the modulation scheme of received signal [6].

2.2.2.2 Pilot-based Spectrum Sensing

Pilot-based spectrum sensing method performs very well in low SNR conditions [28]. A few pilot-based spectrum sensing techniques for Advanced Television Systems Committee (ATSC) standard signals have been investigated [28] [29], with some works being proposed for standard in IEEE 802.22 group [30]. Several spectrum sensing algorithms for OFDM signals utilizing in-band pilots have also been proposed [31]–[34]. Nevertheless, some of these works are based on the assumption of perfect synchronization between the OFDM signal transmitter and CR sensing device [31]–[33], which is difficult to achieve in low SNR conditions. Other techniques have sensing performances very sensitive to timing and/or frequency offsets [34]. Moreover, most of these techniques are designed based on a sensing threshold that's sensitive to the unknown noise statistics, which are difficult to estimate [35] [36]. At the same time, noise statistics are usually varying over time, which makes threshold design more difficult.

2.2.3 User Identification

In cognitive radio communications, spectrum sensing determines the availability of the frequency band of interest. However, to better improve environment awareness in cognitive radio network, where many secondary user coexist, it is essential to identify the active user who is using this frequency band. Of those spectrum sensing techniques discussed above, only cyclostationary detection and pilot-based detection have limited identification capabilities. Some previous works identify user by estimating modulation parameters of the signal

[37] [38]. Cyclostationary detection is essentially a detection technique that identifies user through differentiating modulation scheme of the received signal [39]. Pilot-based detection identifies user by recognizing location distributions of pilot tones in frequency domain [40]. However, none of these techniques is applicable when secondary users in cognitive radio network use the same modulation scheme with same pilot tones locations.

2.2.4 Synchronization Technologies in OFDM System

Precoded in-band pilots is proposed in this thesis for user identification purpose. Synchronization issues need to be addressed at the spectrum sensing device side before user identification which is realized by demodulating predesigned identification pilot tones. Since PIP-OFDM system is essentially an OFDM system, synchronization techniques in traditional OFDM system are helpful when performing synchronization in PIP-OFDM system. Synchronization in OFDM system is divided into frequency synchronization (frequency offset estimation) and time synchronization (timing offset estimation).

2.2.4.1 Frequency Synchronization

OFDM system has been proved to be very sensitive to frequency offset since it introduces interference among the multiplicity of carriers in the OFDM signal [41]. An arbitrary frequency offset normally contains an integer frequency offset and an fractional frequency offset, indicating integer subcarrier and fractional subcarrier offsets of OFDM signal in frequency domain.

The easiest and frequently used method for the integer frequency offset estimation method is frequency domain auto-correlation technique [42]–[44], which is based on a correlation between received signal and local reference signal in frequency domain.

Moose [41] first proposed an idea that fractional frequency offset could be estimated through calculating phase shift in time domain. In his method, repeating OFDM symbols designed for synchronization purpose are used. Subsequently, several publications extended this idea in [45]–[48], of which maximum likelihood estimation method [45] contributes the mainstream of fractional frequency offset estimation algorithms. These frequency offset estimation algorithms also require repeating samples in transmitted signal. Some of these algorithms are based on specially designed training symbols [41] [45] [46], and some utilize cyclic prefix as repeating patterns [48]. However, algorithms using cyclic prefix as repeating signal normally have a FFT window length of N (OFDM system subcarriers number) samples [45]–[48], which leads to a large error in the estimation results as discussed in Chapter 5.

2.2.4.2 Time Synchronization

Similar to frequency offset estimation, timing offset estimation also contains integer timing offset estimation (coarse time synchronization) and fractional timing offset estimation (fine time synchronization).

Delay and correlation (DC) method is frequently used in integer timing offset estimation because of the low complexity [49]. DC method is sensitive to the power varyings of received signal and noise [49]. Consequently, more robust algorithms have been proposed, such as maximum likelihood metric [50] and minimum mean squared error (MMSE) metric [51].

After coarse time synchronization algorithm provides a rough timing offset estimation result, fractional timing offset still exists, which will cause phase rotations in frequency domain. A cross-correlation method using matched filter is proposed in [52], where preambles are used in correlation functions to estimate fractional timing offset. However, this is

not achievable for opportunistic communication in cognitive radio, where training symbols for spectrum sensing and identification are not available.

2.3 Summary

This chapter introduces the background of the thesis. Specifically, the motivation and related works of this thesis are presented in details, respectively. Current spectrum sensing techniques for cognitive radio communications are briefly introduced in this chapter, followed by a discussion on the necessity and current development of user identification. In addition, previous synchronization techniques in OFDM system are concluded in this chapter for future usage in the synchronization of proposed PIP-OFDM system.

Chapter 3

Spectrum Sensing for Cognitive Radio Communications

3.1 Background of Spectrum Sensing

3.1.1 Definition of Cognitive Radio

Without any official definition of cognitive radio network's architecture, current understandings of cognitive radio vary among different researchers [3] [4] [8]–[12]. The cognitive radio network in this thesis is defined and illustrated in Figure 3.1, where only one primary user exists and multiple secondary users (cognitive users) coexist, sharing the same frequency band. In the ideal situation, primary user has the priority to use this frequency band (primary user active), and only one secondary user accesses to this resource if primary user is not using it (primary user idle). Consequently, secondary users not only need to detect the existence of primary signal, but also need to detect the existence of secondary signal[1]. Furthermore, to better achieve environment awareness and network management, secondary users need to identify the user who is currently using the resource if necessary.

Figure 3.1 shows two scenes of cognitive radio network. In Figure 3.1(a), primary user is transmitting, while the secondary users are detecting the availability of this fre-

---

1. Here, "existence/absence" is equivalent to "active/idle" or "using/not using the spectrum resource".

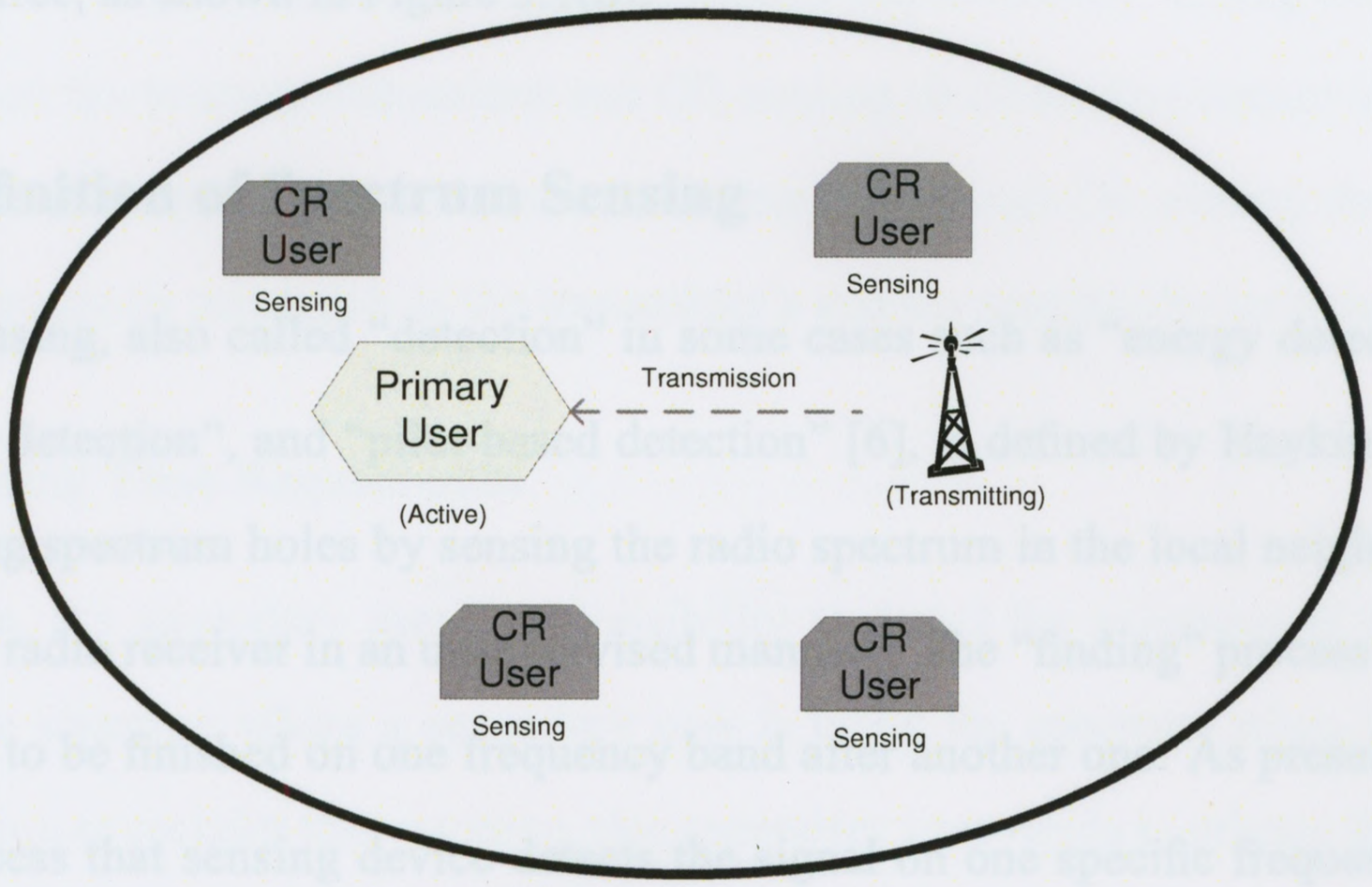

(a)

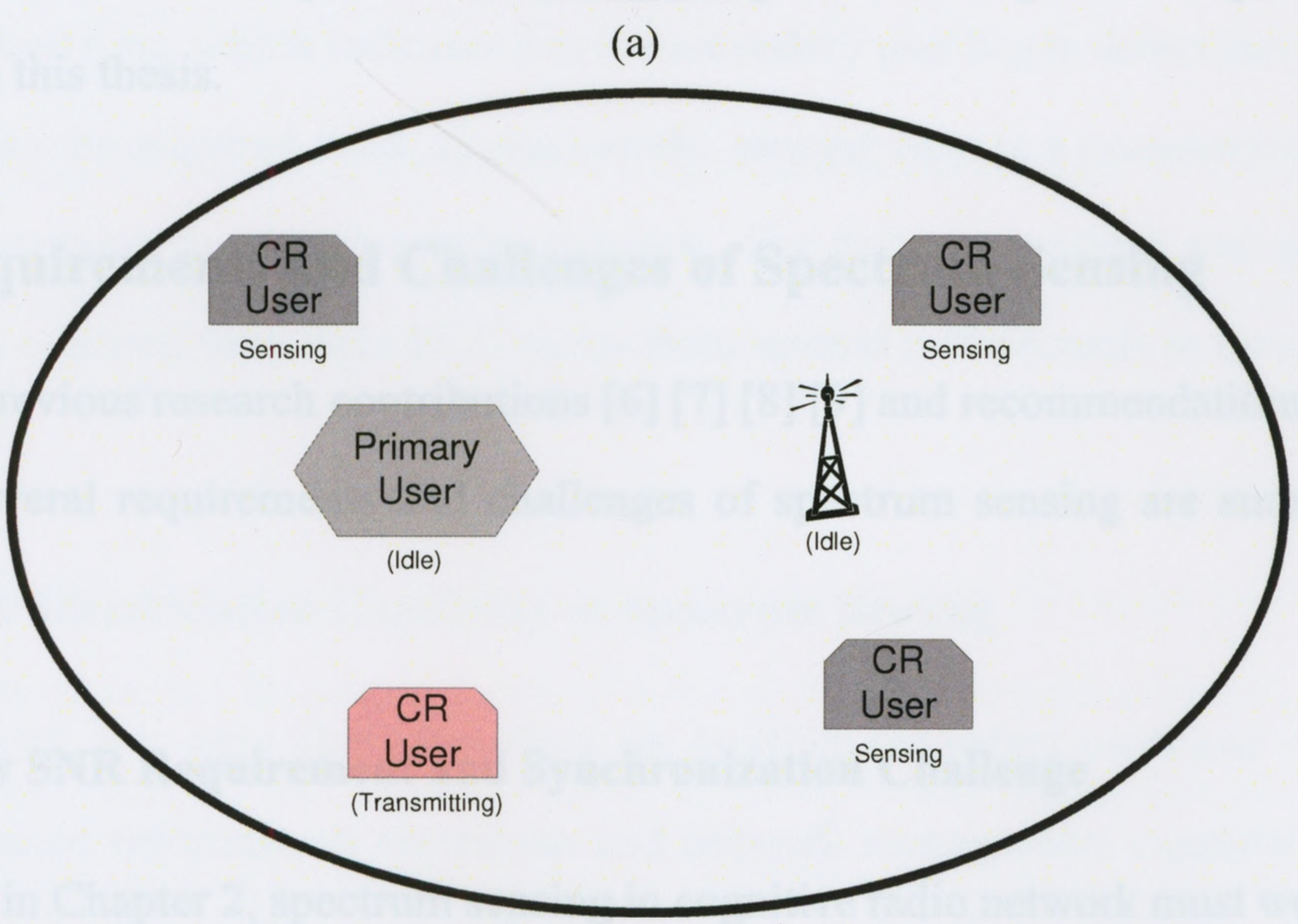

(b)

Figure 3.1: Architecture of cognitive radio network considered in this thesis. (a) Primary user is active, and cognitive users are sensing. (b) Primary user is idle, and one cognitive user is transmitting, while other cognitive users are sensing.

quency band[2]. When primary user is idle, only one secondary user can access to the resource, and other secondary users keep sensing (identification if necessary) until the resource is set free, as shown in Figure 3.1(b).

3.1.2 Definition of Spectrum Sensing

Spectrum sensing, also called "detection" in some cases such as "energy detection", "cyclostationary detection", and "pilot-based detection" [6], is defined by Haykin [9] as "the task of finding spectrum holes by sensing the radio spectrum in the local neighborhood of the cognitive radio receiver in an unsupervised manner". The "finding" process in this definition needs to be finished on one frequency band after another one. As presented above, only the process that sensing device detects the signal on one specific frequency band is considered in this thesis.

3.1.3 Requirements and Challenges of Spectrum Sensing

From some previous research contributions [6] [7] [8] [9] and recommendations from FCC [16]–[18], several requirements and challenges of spectrum sensing are summarized as follows.

3.1.3.1 Low SNR Requirement and Synchronization Challenge

As presented in Chapter 2, spectrum sensing in cognitive radio network must work reliably in very low SNR conditions. According to some previous studies and recommendations from FCC, this thesis considers SNR range of -25dB to -10dB for spectrum sensing.

---

2. In general, secondary users also detect other frequency bands for more spectrum sharing opportunities. However, we only consider one specific frequency band in this thesis without loss of generality.

Low SNR requirement also leads to challenges of synchronization during the spectrum sensing. The actual design and implementation of the spectrum sensing algorithm need to take into consideration of two crucial system imperfections: timing and frequency offsets between the primary transmitter and CR sensing devices. The former is a result of the lack of temporal synchronism between the transmitter and CR sensing devices while the latter is caused by mismatch in the transmitter's and the sensing device's oscillators.

3.1.3.2 Sensing Time Requirement

In CR system, it's secondary user's responsibility to detect the existence of the primary signal. In the situation where a secondary user is using the spectrum when the primary user is returning to reclaim this resource, this secondary user needs to release this resource within a required time, which indicates that the secondary user has to detect the existence of primary user in the required time. Consequently, sensing time is a necessary requirement for spectrum sensing in cognitive radio network. For different systems and applications, the suggested required time from FCC varies from several milliseconds to several seconds [17].

3.1.3.3 User Identification Capability of Spectrum Sensing

In a CR network, it is very likely that there are multiple secondary users and one primary user. To enhance environment awareness and network management capabilities such as interference estimation and resource allocation with priority, the spectrum sensing devices need to identify the user who is using the current spectrum resource, which is called user identification in this thesis. Very few previous works consider user identification capability of spectrum sensing method in cognitive radio communications. This thesis will focus on user identification capability, and propose a precoded in-band pilots design to improve this capability in cognitive radio communications.

3.2 Spectrum Sensing Techniques Overview

3.2.1 Two Hypotheses in Spectrum Sensing

Two hypotheses exist in a general spectrum sensing problem. Specifically, $\mathcal{H}_1$ represents the hypothesis that signal exists in the frequency band of interest, while $\mathcal{H}_0$ represents the absence of any signal in concerned frequency band. Mathematically:

$$\begin{cases} \mathcal{H}_1 : \ z(t) = y(t) + w(t) \\ \mathcal{H}_0 : \ z(t) = w(t) \end{cases}, \tag{3.1}$$

where the $y(t)$ and $w(t)$ represent the received signal and the noise respectively. Spectrum sensing at the CR device side is the process that differentiates these two hypotheses.

3.2.2 Energy Detection and Matched Filter Detection

Based on estimating the power on the frequency band of interest, energy detection is a very easy way to detect the existence of signal. Energy detection requires no more than information about the carried frequency (bandwidth as well if necessary) of the target signal. Ideally, the signal power on the target frequency band will be the noise power δ_n^2 when there is no signal on the frequency band of interest, while it becomes into $\delta_n^2 + \delta_s^2$ when the target signal exists on the frequency band, where δ_s^2 represents the power of the target signal. The energies of received signals (with the SNR from −20dB to 10dB) in both two hypotheses are shown in Figure 3.2, which also indicates the difficulty to differentiate these two hypotheses at low SNR.

Energy detector can estimate the energy of received signal as

$$\epsilon_z = \sum_{n=1}^{N} |z(n)|^2, \tag{3.2}$$

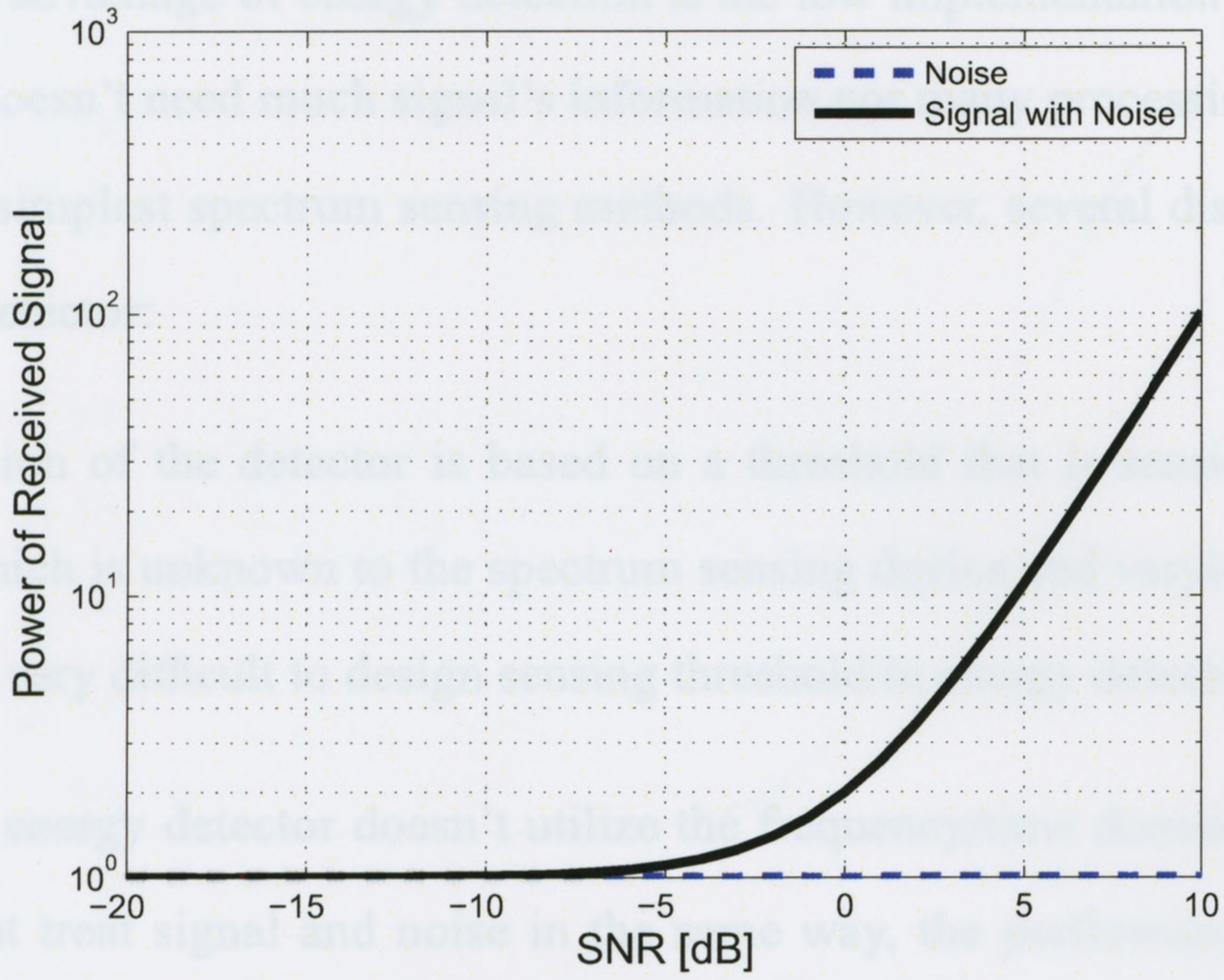

Figure 3.2: Received signal power at energy detection device (the observation points: 1,000,000).

where $z(n)$ is discrete received signal at energy detection device, and N is the number of observation points.

Subsequently, energy detector makes the decision based on the estimated energy as

$$\begin{cases} \mathcal{H}_1 & \text{if } \epsilon_z > \lambda \\ \mathcal{H}_0 & \text{if } \epsilon_z < \lambda \end{cases}, \tag{3.3}$$

where λ is the detection threshold. Normally, the threshold here is set to meet a target *false alarm probability*, P_f. False alarm probability is defined as the probability that sensing device falsely made the sensing decision when signal is absent. Mathematically,

$$P_f = \text{Prob}\left(\epsilon_z > \lambda \,|\, \mathcal{H}_0\right), \tag{3.4}$$

where Prob(X) represents the probability of event X.

The main advantage of energy detection is the low implementation complexity. Energy detection doesn't need much signal's information nor many processing steps, making it as one of the simplest spectrum sensing methods. However, several disadvantages exist for the energy detector:

- The decision of the detector is based on a threshold that is sensitive to the noise power, which is unknown to the spectrum sensing device and varying over time [8], making it very difficult to design sensing threshold in energy detection.

- Since the energy detector doesn't utilize the frequency/time domain features of the signals but treat signal and noise in the same way, the performance of the energy detector is very poor when signal is weak as a simulation example shown in Figure 3.3. Consequently, energy detection requires a long sensing time for the target false alarm probability and successful detection probability [6].

- The energy detector is not able to identify the signal, which means the decision by the detector could be easily influenced by interference signals.

- Frequency offset exists in most wireless communication systems, causing unreliable sensing results for energy detectors.

Similar to energy detection, matched filter detection uses matched filter to get the maximum output of target signal's energy, based on which the detection result is made [8]. However, matched filter requires CR device to demodulate the received signal. Hence, it requires synchronization between primary transmitter and spectrum sensing device, making it very difficult to implement at low SNR [8].

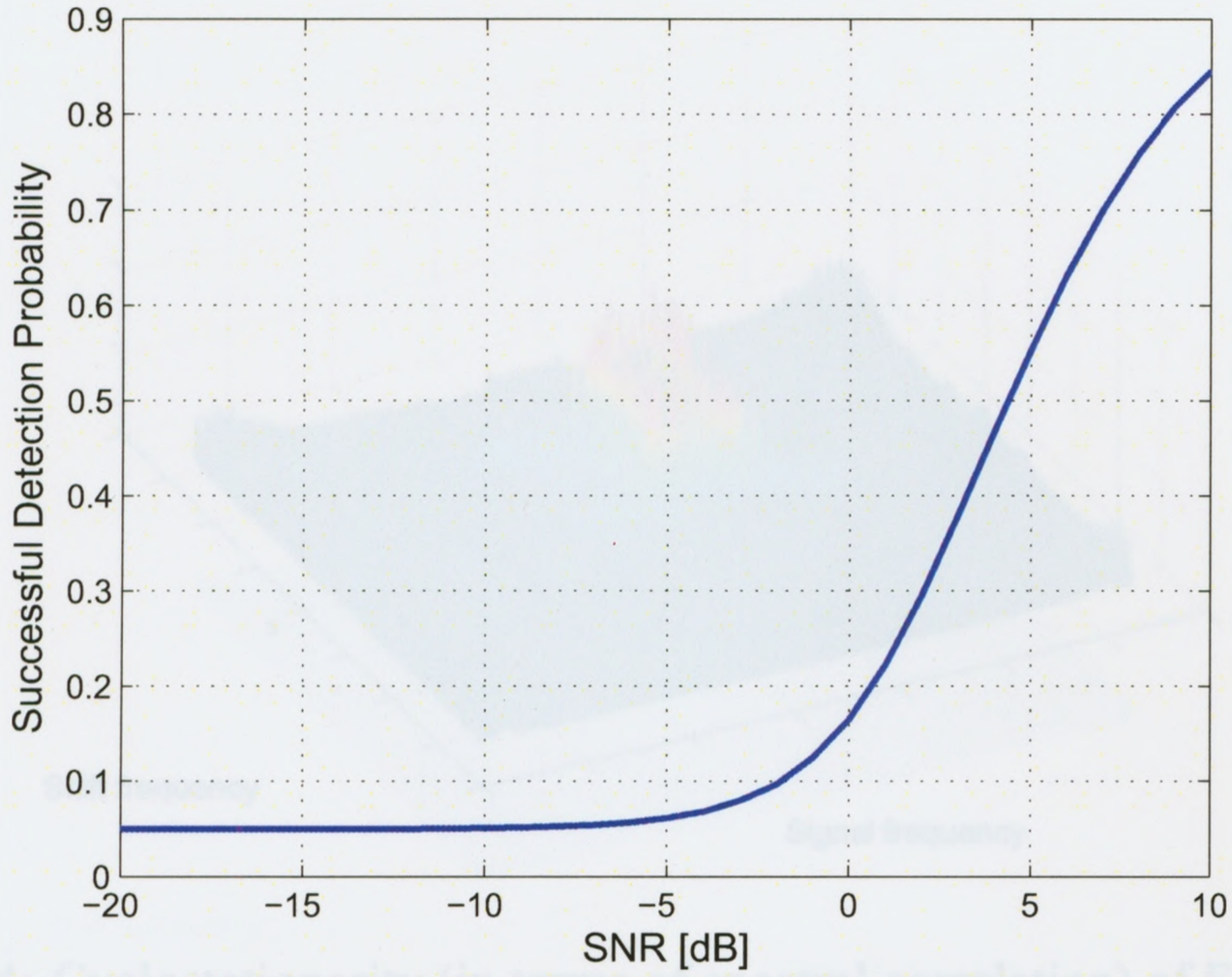

Figure 3.3: Performance of the energy detection (observation points: 1,000,000; false alarm probability: 0.05).

3.2.3 Cyclostationary Detection

Cyclostationary detection techniques utilize the cyclostationary properties of signals for spectrum sensing.

In practical communication systems, modulated signals contain sinusoidal carrier frequencies, pilot tones, cyclic prefix, repeating preambles and some other similar information which result in some stationary properties, which are called "cyclostationarity" in signals [19].

Normally, the cyclostationary detection is based on applying the spectral correlation function (SCF) of the received signal over time [19]:

$$S_z(\upsilon, f) = \lim_{T\to\infty} \lim_{\Delta t\to\infty} \int_{-\Delta t/2}^{\Delta t/2} \frac{1}{T} Z_T(t, f + \upsilon/2) Z_T^*(t, f - \upsilon/2) dt, \tag{3.5}$$

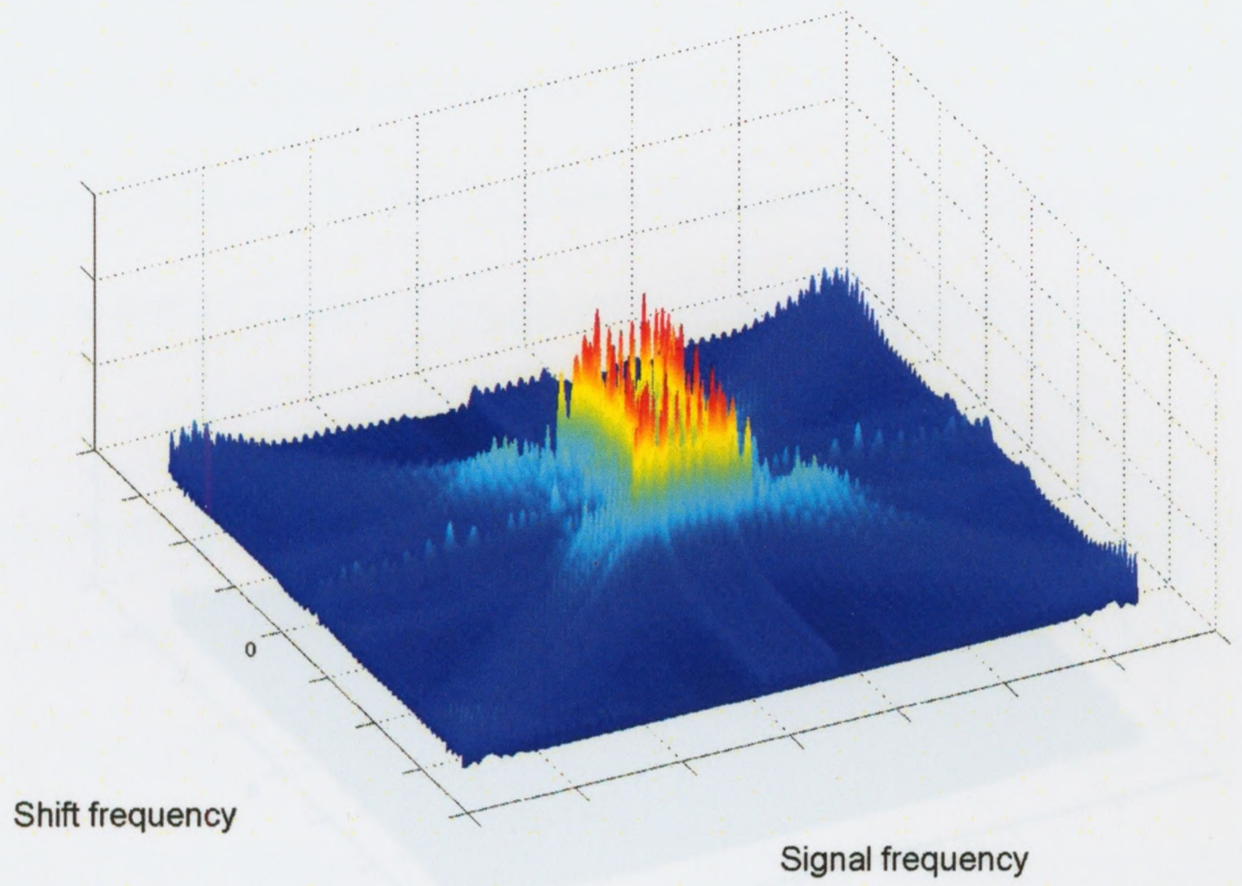

Figure 3.4: Cyclostationarity (in terms of spectral correlation) of FSK signals.

where

$$Z_T(t,f) = \int_{t-T/2}^{t+T/2} z(u)e^{-j2\pi fu}du, \tag{3.6}$$

and υ is the *shifted frequency* (also *cycle frequency* [6] sometimes).

Distribution of spectral correlation varies between signals with different modulation schemes. Figure 3.4 and Figure 3.5 illustrate respectively cyclostationarity of Frequency Shift Keying (FSK) signal and that of Quadrature Phase Shift Keying (QPSK) signal. The spectral correlation function of noise has very distinctive property that it takes non-zero values only when the shifted frequency υ is not zero (see Figure 3.6).

In general, the received signal contains primary signal (if exists) and the noise as shown in (3.1). Therefore, the spectral correlation of the received signal is [6] [19]:

$$\begin{cases} \mathcal{H}_1: & S_z(\upsilon,f) = S_y(\upsilon,f) + S_w(\upsilon,f) \\ \mathcal{H}_0: & S_z(\upsilon,f) = S_w(\upsilon,f) \end{cases}. \tag{3.7}$$

Within the areas that the shifted frequency $\upsilon \neq 0$ in spectral correlation figures, the

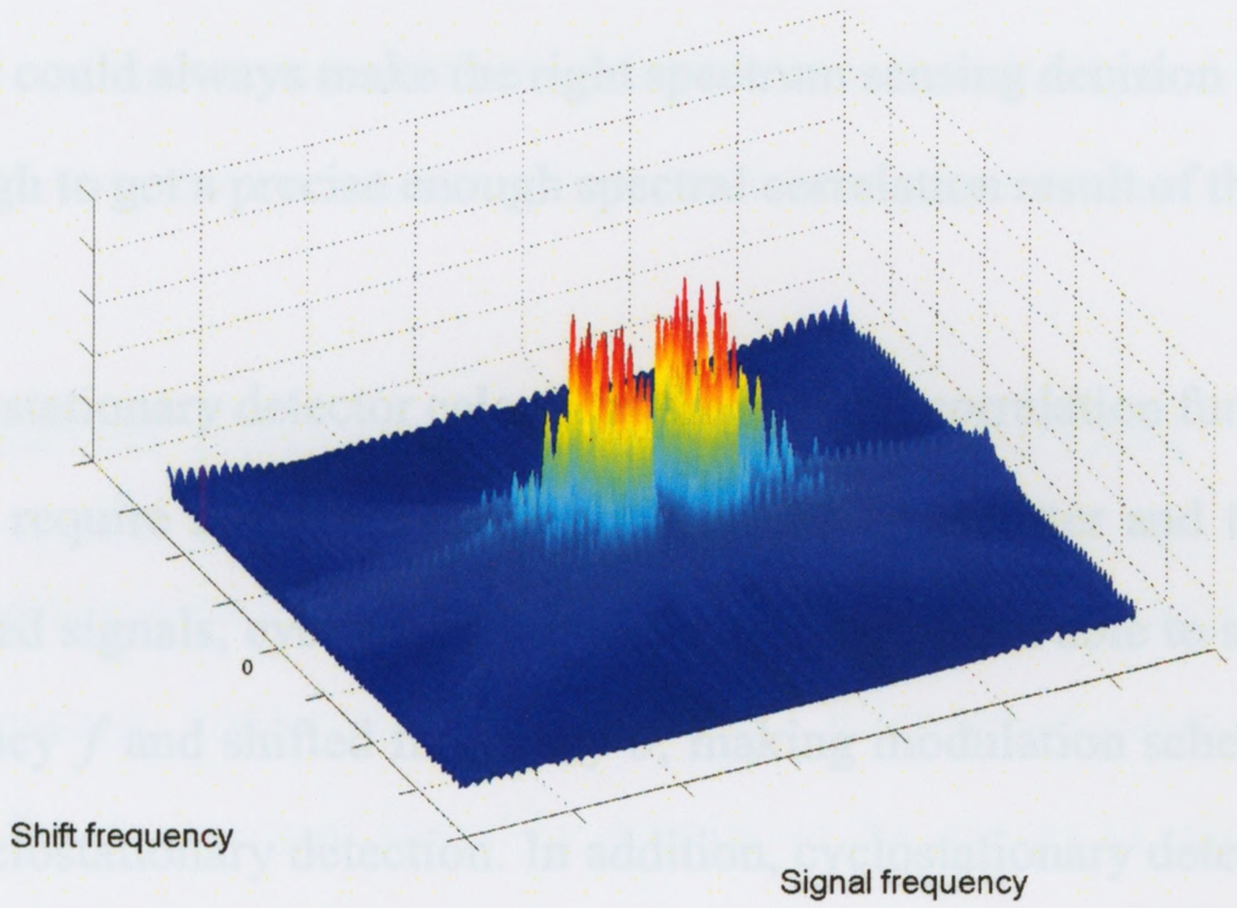

Figure 3.5: Cyclostationarity of (in terms of spectral correlation) QPSK signals.

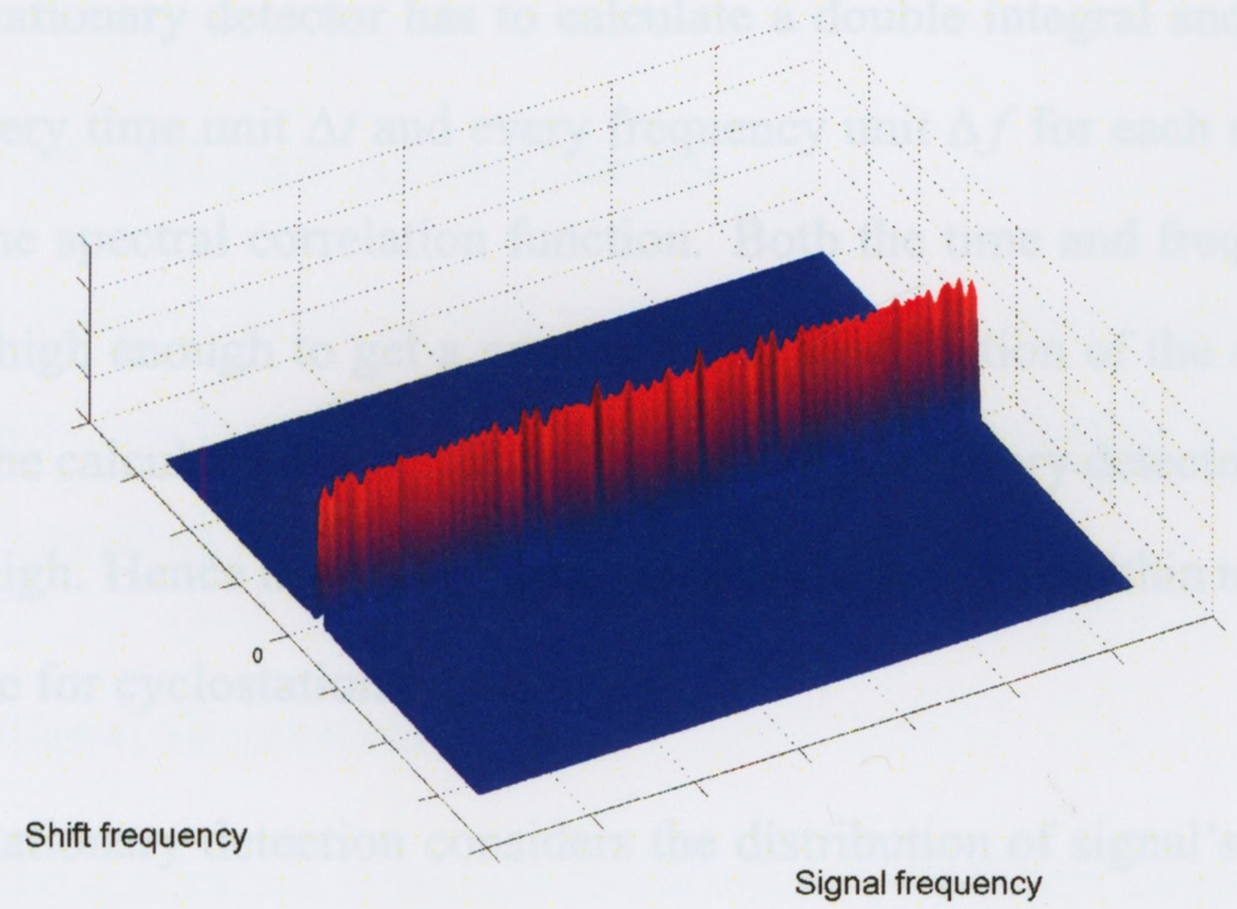

Figure 3.6: Cyclostationarity (in terms of spectral correlation) of noise signals.

spectral correlation of noise is equal to 0 and signals with different modulation schemes have different distinctive distributions (see Figure 3.4–3.6). Ideally, the cyclostationary spectrum detector could always make the right spectrum sensing decision if the observation time is long enough to get a precise enough spectral correlation result of the received signal [20] [21].

Since cyclostationary detector calculates the spectral correlation function of received signal, it doesn't require synchronization between the transmitter and the detector. For different modulated signals, cyclostationary detection method is able to show different results over frequency f and shifted frequency υ, making modulation scheme identification achievable for cyclostationary detection. In addition, cyclostationary detection has a better performance than the energy detector [6] [8] [20] [21], since it utilizes inherent properties of the signals and doesn't treat the noise and signal in the same way as energy detector does.

However, there are still several disadvantages of the cyclostationary detector:

- The cyclostationary detector has to calculate a double integral and a Fourier transform for every time unit Δt and every frequency unit Δf for each shifted frequency $\Delta \upsilon$ to get the spectral correlation function. Both the time and frequency resolution need to be high enough to get a precise enough estimation of the signal's cyclostationarity. The calculation complexity for the cyclostationary detector is consequently extremely high. Hence it is hardly able to make the decision within required spectrum sensing time for cyclostationary detection.

- The cyclostationary detection considers the distribution of signal's energy in statistical way. Therefore, the performance of cyclostationary detector is also poor when the SNR is very low (say -15dB) within the required sensing time [20] [21].

- Although the cyclostationary detection is able to differentiate signals with different cyclostationarities, it can hardly estimate where the signal comes from when many transmitters use the same modulation scheme, which is likely to be true in CR networks considering the system complexity and management convenience.

3.3 Pilot-based Spectrum Sensing for OFDM

Pilot signals are widely used in wireless communication systems for control, synchronization, channel estimation, and/or reference purposes. *Pilot-based spectrum sensing* technique determines the existence of signal by estimating the energy of pilot signals built in transmitted signals. Considering the previous contributions of pilot-based spectrum sensing techniques in signal-carrier signals, and the widely usage of OFDM signals, this thesis only discusses the pilot-based spectrum sensing technique for OFDM signals. Since the pilot signals are referred to be pilot tones in OFDM system in this thesis, pilot signals are also called pilots or pilot tones hereafter.

3.3.1 System Model and Assumptions

The notations and system models as well as the assumptions used in the investigation of *pilot-based spectrum sensing technique for OFDM signal* (also called *pilot-based OFDM spectrum sensing* hereafter) are introduced here for future usage.

3.3.1.1 OFDM Signal Generation

Let $X_m(k)$ denote the quadrature amplitude modulation (QAM) data sample that appears in the k-th subcarrier of the m-th OFDM symbol at the transmitter side. The corresponding

time domain samples of this OFDM symbol are

$$\mathbf{x}_m^{\mathbf{d}} = [x_m(1), x_m(2), x_m(3), \ldots, x_m(N)]^T, \tag{3.8}$$

where

$$x_m(n) = \frac{1}{\sqrt{N}} \sum_{k=0}^{N-1} X_m(k) e^{j2\pi kn/N}, \tag{3.9}$$

and n is the sample index in time domain. The cyclic prefix (guarding interval) with N_g samples,

$$\mathbf{x}_m^{\mathbf{g}} = \left[x_m(N - N_g + 1), x_m(N - N_g + 2), \ldots, x_m(N-1), x_m(N)\right]^T, \tag{3.10}$$

is inserted at the beginning of the N-length data carrying segment $\mathbf{x}_m^{\mathbf{d}}$ to form one complete OFDM symbol in time domain:

$$\mathbf{x}_m = \left[\mathbf{x}_m^{\mathbf{g}}; \mathbf{x}_m^{\mathbf{d}}\right]. \tag{3.11}$$

3.3.1.2 In-band Pilots Insertion

In an OFDM system, carried information on pilot tones is normally multiplexed with the raw data in the frequency domain to form the OFDM symbols $\mathbf{X}_m$. To simplify the analysis, carried information on one specific pilot tone is assumed to be identical over different OFDM symbols.

Let A be the total number of pilot subcarriers in OFDM signal, and $\mathbf{L}$ represent the pilots' locations (subcarrier indices) in the frequency domain. After the multiplexing of the pilot modulating information and data information, the m-th OFDM symbol $\mathbf{X}_m$ in

frequency domain has a structure of

$$X_m(k) = \begin{cases} v(k) & k \in \mathbf{L} \\ \text{data} & \text{otherwise} \end{cases}, \tag{3.12}$$

where $v(k)$ is the carried information on the pilot tone with the frequency domain index of k. This carried information keeps the same over different OFDM symbols, and is known to the receiver. All the pilot tones are assumed to have the same power, i.e., $|v(k)| = v_0$ for any $k \in \mathbf{L}$, where v_0 is a positive real variable. Since the embedded pilots stay on the same subcarriers in every transmitted OFDM symbol, the pilot symbol is simply obtained as

$$R(k) = \begin{cases} v(k) & k \in \mathbf{L} \\ 0 & \text{otherwise} \end{cases}. \tag{3.13}$$

The energy of pilot symbol, $|R(k)|^2$, will be used as a reference to perform correlation in the CR spectrum sensing device to determine the existence of primary signal in later discussions.

3.3.1.3 Received Signal at Spectrum Sensing Device

The received signal in the spectrum sensing device is unavoidably corrupted by noise and interferences. The *noise* in the analysis here is assumed to be complex white Gaussian noise and is denoted by $w \sim \mathcal{N}\left(0, \delta_n^2\right)$. To simplify the analysis, the noise term in this thesis contains all the noises from the internal circuit of the sensing device, the external environment, and interference signals that are not from the primary transmitter.

The structure of the received OFDM symbol ($\mathbf{z}_m$) at the CR sensing device depends

on the existence ($\mathcal{H}_1$) or absence ($\mathcal{H}_0$) of the primary signal. Specifically,

$$\begin{cases} \mathcal{H}_1: & \mathbf{z}_m = \mathbf{y}_m + \mathbf{w}_m \\ \mathcal{H}_0: & \mathbf{z}_m = \mathbf{w}_m \end{cases}, \tag{3.14}$$

where $\mathbf{y}_m$ and $\mathbf{w}_m$ denote the received signal from primary transmitter and the noise, respectively.

3.3.2 Principle of Pilot-based OFDM Spectrum Sensing

The basic principle of pilot-based spectrum sensing technique for OFDM signal is estimating the energy on pilot tones after averaging received signal symbol-by-symbol. Figure 3.7 shows the power changes before and after the average processing in pilot-based spectrum sensing algorithm for OFDM signal, where δ_n^2, δ_s^2, and M represent power of noise, power of signal, and average times, respectively. Shown in these two figures, the impacts from the noise and data subcarriers in the received signal can be effectively mitigated in the average processing. In an ideal situation (AWGN channel, no timing/frequency offset, etc.), the result of a large enough times of symbol-by-symbol averaging,

$$\overline{Z}(k) = \sum_{m=1}^{M} Z_m(k), \tag{3.15}$$

is approaching to zero when there is no signal on the frequency band of interest, and approximately equal to the pilot signal in (3.13) when a signal is present.

After averaging, the correlation between the power spectra of averaged signal and that of local reference signal is performed. The correlation results allow us to differentiate the two spectrum sensing hypotheses. Mathematically, the correlation function could be

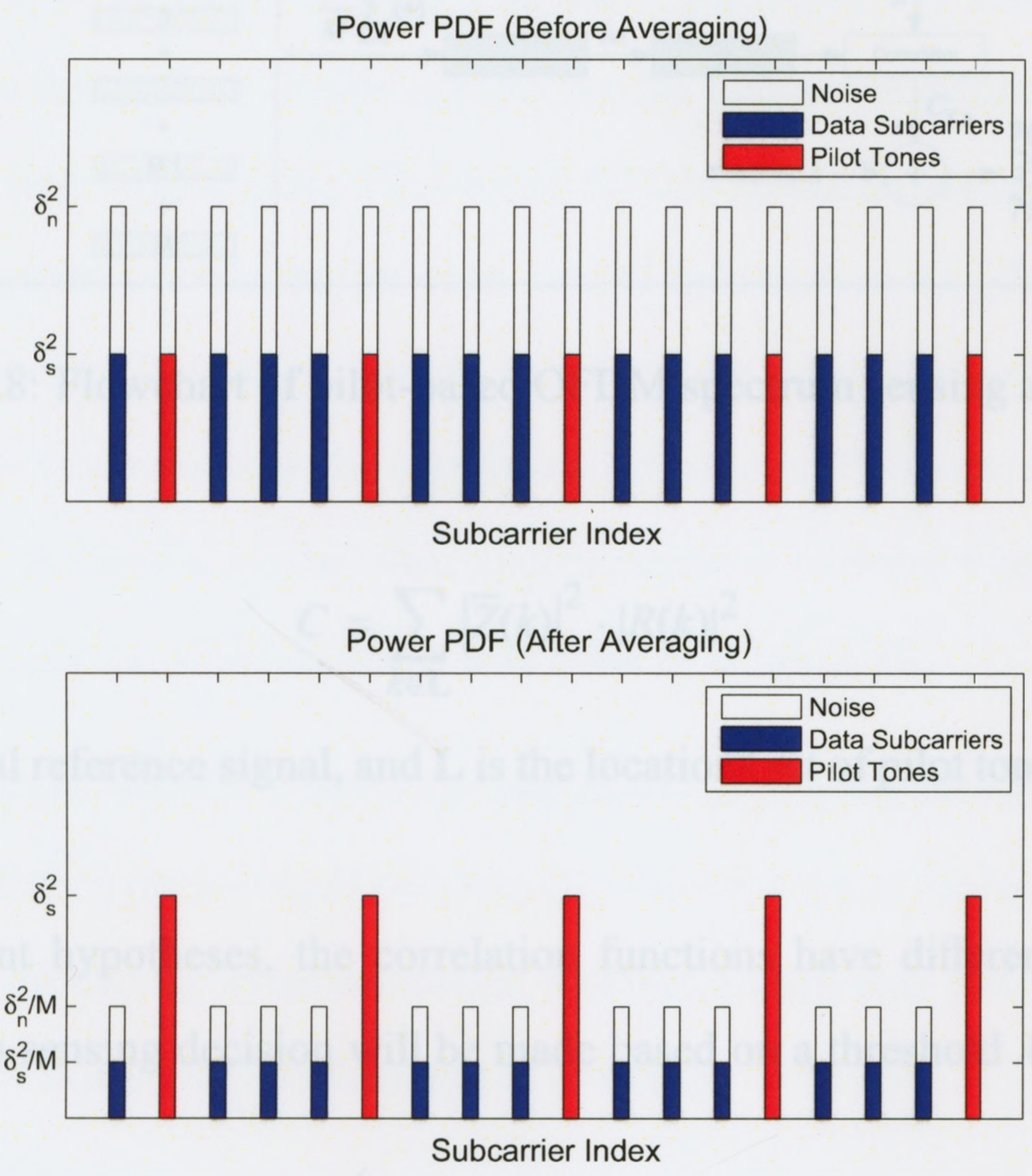

Figure 3.7: Impact of average processing on signal's power distribution in pilot-based OFDM spectrum sensing algorithm. (Shown in frequency domain, and PDF = Probability Distribution Function).

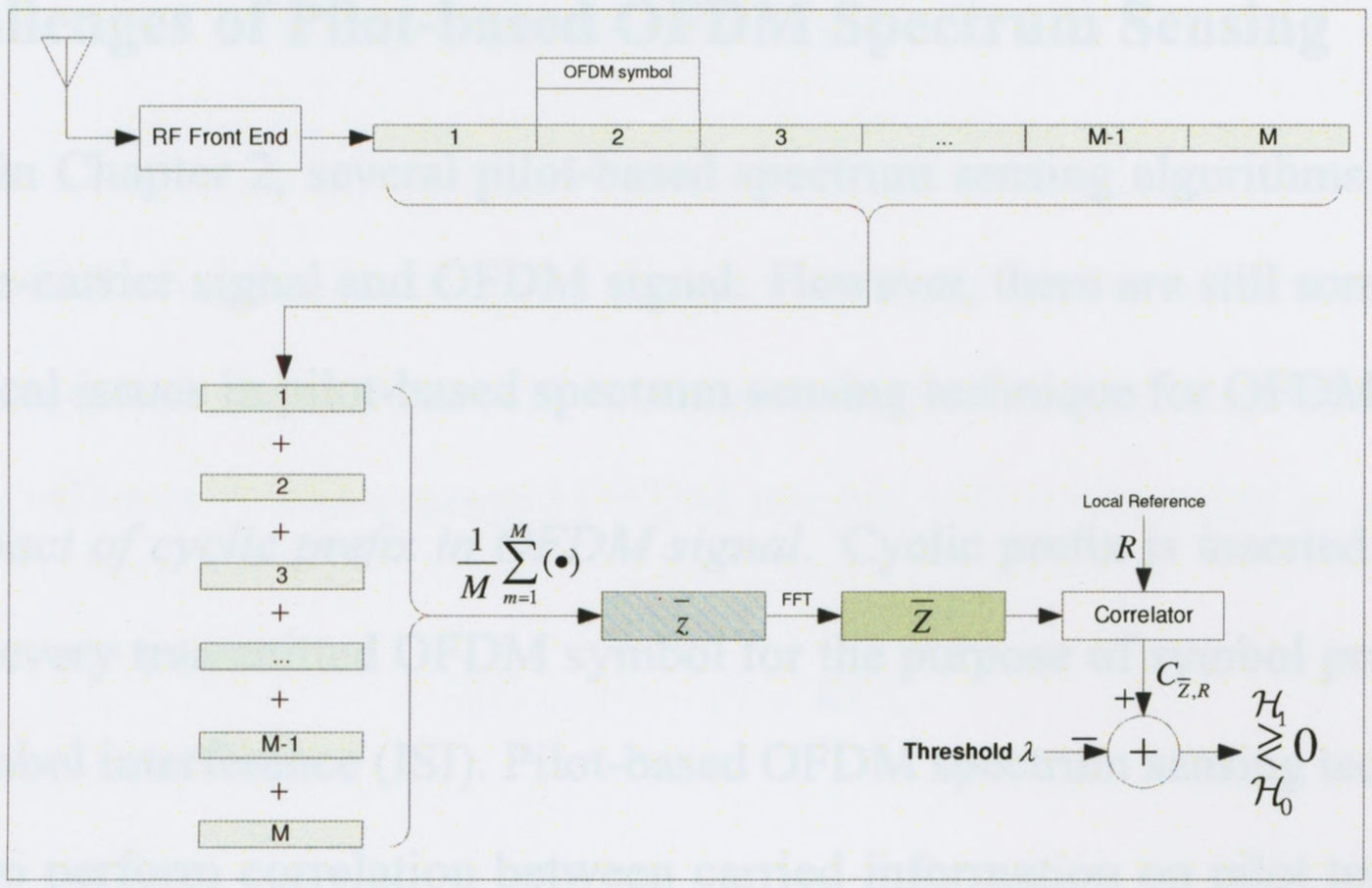

Figure 3.8: Flowchart of pilot-based OFDM spectrum sensing algorithm.

written as

$$C = \sum_{k \in \mathbf{L}} \left|\overline{Z}(k)\right|^2 \cdot |R(k)|^2, \tag{3.16}$$

where $R(k)$ is local reference signal, and $\mathbf{L}$ is the locations set of pilot tones (see Subsection 3.3.1).

For different hypotheses, the correlation functions have different values. Subsequently, spectrum sensing decision will be made based on a threshold λ. Mathematically,

$$\begin{cases} \mathcal{H}_1, & \text{if } C > \lambda \\ \mathcal{H}_0, & \text{if } C < \lambda \end{cases}. \tag{3.17}$$

This completes the basic principle of pilot-based OFDM spectrum sensing algorithm, and Figure 3.8 illustrates the flowchart of this algorithm.

However, the implementation of pilot-based OFDM spectrum sensing algorithm at low SNR needs to consider the impacts of unknown timing and frequency offsets, as well as threshold design difficulties as discussed later.

3.3.3 Challenges of Pilot-based OFDM Spectrum Sensing

As presented in Chapter 2, several pilot-based spectrum sensing algorithms are proposed for both single-carrier signal and OFDM signal. However, there are still some rarely considered technical issues in pilot-based spectrum sensing technique for OFDM signal:

- *The impact of cyclic prefix in OFDM signal.* Cyclic prefix is inserted at the beginning of every transmitted OFDM symbol for the purpose of symbol protection from intersymbol interference (ISI). Pilot-based OFDM spectrum sensing technique is designed to perform correlation between carried information on pilot tones and local reference signal in frequency domain, which means the cyclic prefix needs to be removed before implementing the correlation operations. However, the elimination of cyclic prefix requires a symbol time synchronization between transmitter and spectrum sensing device, which is difficult to achieve at low SNR.

- *Frequency offset between transmitter and spectrum sensing device.* The correlation operation between the averaged received OFDM symbol and the local reference symbol requires frequency synchronization between transmitter and spectrum sensing device, which is also very challenging at low SNR.

- *Unknown noise statistics in sensing threshold design.* The threshold, which is λ in (3.17), is usually designed to meet the requirements of false alarm probability and successful detection probability in spectrum sensing. This makes the threshold in pilot-based OFDM spectrum sensing method always sensitive to noise statistics which are difficult to estimate. In addition, the noise statistics in most situations are varying over the time.

3.3.4 Impacts of Timing Offsets and Cyclic Prefix

As we discussed earlier, received signals are combined with timing offsets in spectrum sensing at low SNR. In pilot-based spectrum sensing algorithm for OFDM signal, the timing offset will cause phase rotations on the received signal in frequency domain. Assume that the timing offset is τ. The averaged OFDM symbol with noise could be written as

$$\bar{z}(t) = \bar{y}(t-\tau) + \bar{w}(t). \tag{3.18}$$

Considering

$$\mathcal{F}\left[\bar{y}(t-\tau)\right] = \bar{Y}(f) \cdot e^{-j2\pi f\tau}, \tag{3.19}$$

the timing offset does not have any impact on the sensing result because only the energy of the signal is considered in the spectrum sensing process. Mathematically,

$$\sum_{k\in\mathbf{L}} \left|\bar{Y}(k)\right|^2 \cdot |R(k)|^2 = \sum_{k\in\mathbf{L}} \left|\bar{Y}(k)e^{-\frac{j2\pi k\tau}{N}}\right|^2 \cdot |R(k)|^2. \tag{3.20}$$

However, due to the lack of time synchronization between the transmitter and the CR sensing device, one received OFDM symbol ($\mathbf{y}_m$) from primary user, in general, comprises of $N_s = (N + N_g)$ samples spanning two adjacent OFDM symbols relative to the timing offset, in terms of τ samples, as shown in Figure 3.9. This unknown timing offset makes it difficult to locate the starting point of one OFDM symbol, hence difficult to eliminate the cyclic prefix before correlation in frequency domain (for the reason of eliminating cyclic prefix, see Subsection 3.3.3).

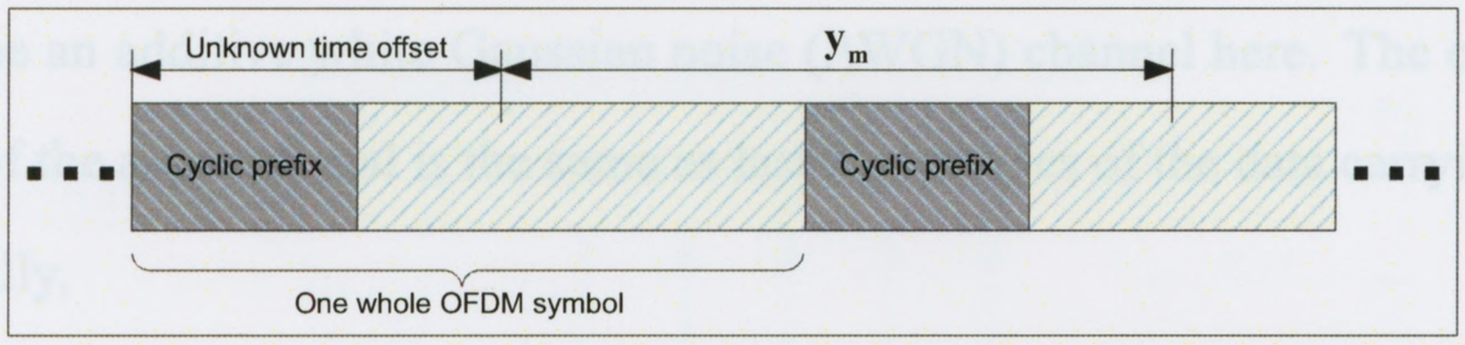

Figure 3.9: Received OFDM signal with unknown timing offset.

The *m*-th received OFDM symbol then can be written as[3]

$$\mathbf{y}_m = \left[\mathbf{y}_m^{\mathbf{d}}; \mathbf{y}_m^{\mathbf{g}}\right], \tag{3.21}$$

where $\mathbf{y}_m^{\mathbf{d}}$ is the data carrying segment, and $\mathbf{y}_m^{\mathbf{g}}$ is the cyclic prefix segment.

After average processing, we have the averaged OFDM symbol as

$$\overline{\mathbf{y}} = \left[\overline{\mathbf{y}^{\mathbf{d}}}; \overline{\mathbf{y}^{\mathbf{g}}}\right]. \tag{3.22}$$

To estimate the energy on the respective subcarriers in the frequency domain, averaged OFDM symbol is performed the *N*-point discrete Fourier transform. Mathematically, we have the averaged OFDM symbol in frequency domain as

$$\begin{aligned} \overline{Y}(k) &= \frac{1}{N}\sum_{n=1}^{N+N_g} \bar{y}(n) e^{\frac{-j2\pi kn}{N}} \\ &= \frac{1}{N}\sum_{n=1}^{N} \overline{y^d}(n) e^{\frac{-j2\pi kn}{N}} + \frac{1}{N}\sum_{n=1}^{N_g} \overline{y^g}(n) e^{\frac{-j2\pi k(n+N)}{N}}. \end{aligned} \tag{3.23}$$

To simplify the analysis, while focusing on the impact of cyclic prefix, the channel is

---

3. Generally, the cyclic prefix segment is not always at the beginning or end of the received symbol due to the unknown timing offset. However, since the shift of received signal in time domain, as proved in (3.19) and (3.19), doesn't have any impact on the pilot energy in frequency domain, it will not lose any generality to put the cyclic prefix segment at the end of the received symbol as one example to simplify the subsequent analysis.

assumed to be an additive white Gaussian noise (AWGN) channel here. The cyclic prefix segment $\overline{\mathbf{y^g}}$ of the above signal is the same as last N_g samples of the data carrying segment $\overline{\mathbf{y^d}}$. Specifically,

$$\overline{\mathbf{y^g}} = \left[\overline{y^d}(N - N_g + 1), \overline{y^d}(N - N_g + 2), \ldots, \overline{y^d}(N)\right]^T. \tag{3.24}$$

From (3.23) and (3.24), we have

$$\begin{aligned} \overline{Y}(k) &= \frac{1}{N}\sum_{n=1}^{N} \overline{y^d}(n) e^{\frac{-j2\pi kn}{N}} + \frac{1}{N}\sum_{n=1}^{N_g} \overline{y^d}(N - N_g + n) e^{\frac{-j2\pi kn}{N}} \\ &= \overline{Y^d}(k) + \overline{Yg}(k). \end{aligned} \tag{3.25}$$

The frequency correlation between the energy of data carrying segment $\left|\overline{Y^d}(k)\right|^2$ and that of the local pilot reference signal $|R(k)|^2$ provides a good spectrum sensing result. While as we can see from (3.25), the cyclic prefix segment will lead to some interference (no matter positive or negative) to the pilot subcarriers and influence the subsequent final decision of spectrum sensing. Some previous spectrum sensing techniques ignore the impact of cyclic prefix by considering perfect synchronization, an assumption difficult to realize in practice because of the low SNR requirement [31]. In this thesis, computer simulations will be used to evaluate the impact of cyclic prefix, as shown in Subsection 3.3.8.

3.3.5 Pilot-based OFDM Spectrum Sensing with SFC

Mismatch between the oscillator of primary transmitter and that of the spectrum sensing device will lead to frequency offsets in spectrum sensing. Considering the low SNR requirement for spectrum sensing in cognitive radio communications, these offsets are very difficult to eliminate. The oscillators used in wireless communications typically have fre-

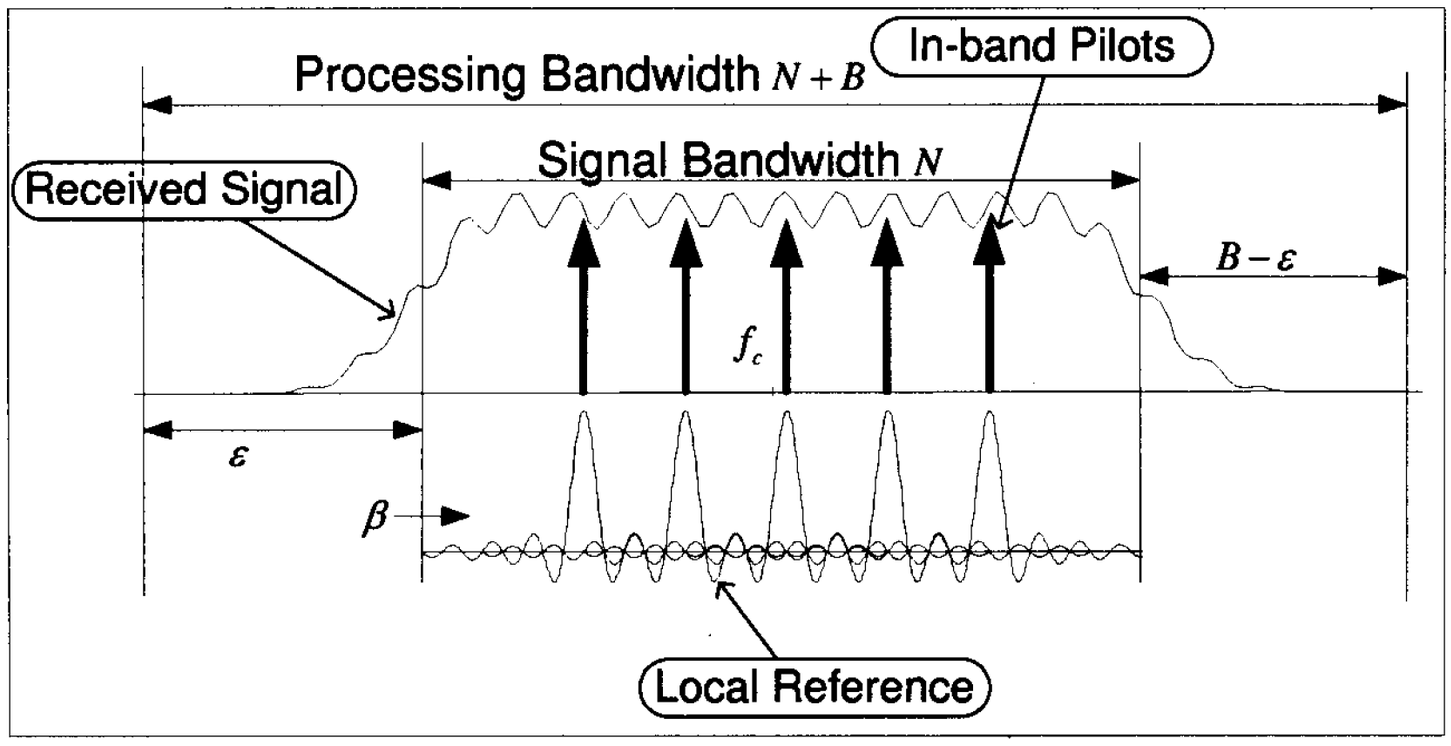

Figure 3.10: Illustration of sliding frequency correlation processing.

quency stability of ±30ppm (parts per million). The corresponding frequency offset could lead to detrimental effect in pilot-based OFDM spectrum sensing systems, since it's realized by frequency correlations. Some previous studies assume the perfect synchronization in frequency domain [31] [32] [33], which is difficult to achieve at low SNR. Other studies rely on accurate control of the local frequency by deploying a set of parallel correlators that address every possible frequency offset within maximum expected range [34]. Even with these complex and expensive designs, residual frequency offset from the hardware, as well the channel-induced Doppler frequency offset are still unavoidable.

To address the impact from frequency offset, a *sliding frequency correlator* (SFC) is proposed in this thesis to achieve a more robust pilot-based OFDM spectrum sensing algorithm. The signal receiver in the proposed spectrum sensing algorithm spans a total of $(N + B)$ subcarriers, where $\pm B/2$ denotes the maximum possible frequency offset in terms of subcarrier spacing.

Figure 3.10 shows the principle of the proposed spectrum sensing algorithm with sliding frequency correlator. Specifically, the algorithm proceeds as follows: The received signal has a bandwidth of $(N + B)$ subcarriers with a central frequency of f_c; the averaged signal $\bar{\mathbf{z}}$ is then converted to the $(N + B)$-length frequency domain symbol $\overline{\mathbf{Z}}$; sliding corre-

lation is performed as shown in Figure 3.10, where ε is frequency offset in terms of OFDM subcarrier spacing. A repeated correlation operation will be implemented by shifting the received signal with different frequency offset tentatively:

$$C(\beta) = \sum_{k=1}^{N} |R(k)|^2 \times \left|\overline{Z}(\beta + k)\right|^2, \qquad \beta = 0, 1, \ldots, B-1, \tag{3.26}$$

where **R** is the pilot symbol in (3.13), and β is the shifted frequency.

After collecting a set of correlation results **C** for different shifted frequency β, the pilot-based OFDM spectrum sensing device with sliding frequency correlator takes the maximum correlation result, $C(\beta^*)$, for further usage. Mathematically,

$$\beta^* = \arg\max_{\beta} C(\beta). \tag{3.27}$$

Subsequently, *peak-to-remaining ratio* (PRR) is defined as

$$\mathcal{R} = \frac{C(\beta^*)}{\overline{C}'}, \tag{3.28}$$

where $\overline{C}'$ is the averaged value of the remaining correlation results Cs, i.e.,

$$\overline{C}' = \frac{1}{B-1}\left(\sum_{\substack{0 \le \beta < B \\ \beta \ne \beta^*}} C(\beta)\right). \tag{3.29}$$

The reason that the peak-to-remaining ratio, rather than peak-to-average ratio, is defined here is that in the ideal situation (ε is correctly located, namely, $\beta^* = \varepsilon$), the remaining correlation results are all noise, and only one result, $C(\beta^*)$, contains signal information. Therefore, potential correlation result from signal component, $C(\beta^*)$, is eliminated to get the distribution of noise term for analysis convenience.

Based on the peak-to-remaining ratio, the spectrum sensing decision will be made as

$$\begin{cases} \mathcal{H}_1, & \text{if } \mathcal{R} > \lambda \\ \mathcal{H}_0, & \text{if } \mathcal{R} < \lambda \end{cases}. \tag{3.30}$$

The threshold λ in this pilot-based OFDM spectrum sensing algorithm with sliding frequency correlator will be later proved to be not sensitive to noise statistics.

3.3.6 Noise Uncertainty and Threshold Design

The performance of spectrum sensing algorithm is normally evaluated by false alarm probability and mis-detection probability. *False alarm* happens when $\mathcal{H}_1$ is determined at the absence of primary signal. Since the threshold in the spectrum sensing is normally designed to meet certain upper limit of false alarm probability, the threshold is always relative to the noise power [35] [36]. Chen [31] gives a sensing threshold in traditional pilot-based OFDM spectrum sensing algorithm as

$$\lambda = \sqrt{-\delta_n^2 \ln P_f}, \tag{3.31}$$

where δ_n^2 is the noise power, and P_f is the target false alarm probability.

However, in the spectrum sensing model where the sensing device doesn't know whether the primary signal is present or not, it is even more difficult to estimate the noise statistics. Furthermore, the noise statistics may actually be varying over time. In the pilot-based OFDM spectrum sensing algorithm with sliding frequency correlator, a ratio threshold, which is not sensitive to the noise power, is derived to eliminate the impact of noise uncertainty. The formulation of the threshold under certain false alarm probability upper limit is analyzed in Subsection 3.3.7.

3.3.7 Theoretical Analysis of Pilot-based OFDM Spectrum Sensing

The performance of the proposed spectrum sensing algorithm is assessed according to the probability of false alarm P_f, and the successful detection probability P_d. A good spectrum sensing device should have a low false alarm probability and a high successful detection probability while meeting the sensing time requirement.

3.3.7.1 False Alarm Probability and Threshold Design

According to the false alarm definition above, false alarm in pilot-based OFDM spectrum sensing algorithm with sliding frequency correlator occurs at

$$\mathcal{R} > \lambda, \qquad \text{when } \mathcal{H}_0, \tag{3.32}$$

where λ is the threshold. For any given false alarm probability (P_f), a larger successful detection probability (P_d) indicates a better sensing performance. To determine the false alarm probability as a function of the threshold λ, we proceed as follows.

Firstly, the false alarm probability P_f for any given threshold λ is determined as

$$\begin{aligned} P_f(\lambda) &= \text{Prob}\left(\mathcal{R} > \lambda \middle| \mathcal{H}_0\right) \\ &= \text{Prob}\left(\frac{C(\beta^*)}{\overline{C}'} > \lambda \middle| \mathcal{H}_0\right) \\ &= 1 - \text{Prob}\left(\frac{C(\beta^*)}{\overline{C}'} < \lambda \middle| \mathcal{H}_0\right). \end{aligned} \tag{3.33}$$

With the absence of the signal from the primary user, the averaged signal in (3.15) is simply noise. This means the averaged symbol in the frequency domain

$$\overline{Z}(k) = \overline{W}(k), \quad \overline{W}(k) \sim \mathcal{N}\left(0, \frac{\delta_n^2}{M}\right) \tag{3.34}$$

is noise as well. Consequently, the correlation result in (3.26) takes the form as

$$C(\beta) = \sum_{k \in \mathbf{L}} v_0^2 \left| \overline{W}(k) \right|^2. \tag{3.35}$$

Split the complex white Gaussian noise $\overline{W}(k)$ into real and imaginary parts, we have

$$\overline{W}(k) = W^R(k) + j \cdot W^I(k), \tag{3.36}$$

where both $W^R(k)$ and $W^I(k)$ are real Gaussian variables, and they have the same distribution as

$$W^R(k) \sim \mathcal{N}\left(0, \frac{\delta_n^2}{2M}\right), W^I(k) \sim \mathcal{N}\left(0, \frac{\delta_n^2}{2M}\right). \tag{3.37}$$

Since there are totally A pilot subcarriers in OFDM symbol, which means the length of $\mathbf{L}$ is A, the correlation result in (3.35) could be written as

$$\begin{aligned} C(\beta) &= \sum_{a=1}^{A} v_0^2 \left(\left| W^R(a) \right|^2 + \left| W^I(a) \right|^2 \right) \\ &= \sum_{a=1}^{2A} \left| W'(a) \right|^2, \end{aligned} \tag{3.38}$$

where

$$W'(a) = \sqrt{v_0^2 \frac{\delta_n^2}{2M}} W_0, \qquad W_0 \sim \mathcal{N}(0,1), \quad a = 1, 2, 3, \ldots, 2A. \tag{3.39}$$

Thus we have

$$C(\beta) = \sum_{a=1}^{2A} \left(\sqrt{v_0^2 \frac{\delta_n^2}{2M}} W_0 \right)^2 = v_0^2 \frac{\delta_n^2}{2M} \chi_{2A}^2, \tag{3.40}$$

where χ_{2A}^2 is a chi-square random variable with $2A$ degrees of freedom. Therefore the

probability density function (PDF) of $C(\beta)$ is

$$f(x) = \begin{cases} \dfrac{\left(\frac{2M}{\delta_n^2 v_0^2}x\right)^{A-1}}{2^A \Gamma(A)} e^{-\left(\frac{M}{\delta_n^2 v_0^2}x\right)} \dfrac{2M}{\delta_n^2 v_0^2} & \text{for} \quad x > 0 \\ 0 & \text{for} \quad x \le 0 \end{cases}, \tag{3.41}$$

with

$$\Gamma(A) = (A-1)! \tag{3.42}$$

being the Gamma function with integer arguments.

The false alarm probability P_f in (3.33) is difficult to evaluate because the probability density function (pdf) of the term $\mathcal{R} = \frac{C(\beta^*)}{\overline{C}'}$ is not easy to derive. To simplify the analysis, we proceed the averaged value of remaining correlation results Cs, which is the square average of $(B-1)$ number of Gaussian noise, as a constant. Mathematically,

$$\overline{C}' \approx v_0^2 \frac{A\delta_n^2}{M}, \qquad \text{for } \mathcal{H}_0. \tag{3.43}$$

Substituting (3.43) into (3.33) allows us to approximate the false alarm probability as

$$\begin{aligned} P_f(\lambda) &= 1 - \text{Prob}\left(C(\beta^*) < v_0^2 \frac{A\delta_n^2}{M}\lambda \middle| \mathcal{H}_0 \right) \\ &= 1 - \left(\int_0^{v_0^2 \frac{A\delta_n^2}{M}\lambda} \frac{\frac{2M}{\delta_n^2 v_0^2}\left(\frac{2M}{\delta_n^2 v_0^2}x\right)^{A-1}}{2^A \Gamma(A)} e^{-\frac{M}{\delta_n^2 v_0^2}x} \, dx \right)^B \\ &= 1 - \left(1 - \sum_{a=0}^{A-1} \frac{(A\lambda)^a}{a!} e^{-A\lambda} \right)^B . \end{aligned} \tag{3.44}$$

To find the threshold that meets a given false alarm probability requirement, we rewrite the

last equation as

$$\sum_{a=0}^{A-1} \frac{(A\lambda)^a}{a!} e^{-A\lambda} = 1 - \left(1 - P_f\right)^{\frac{1}{B}}. \tag{3.45}$$

This is actually a A-degree inverse Poisson equation of the form

$$\sum_{a=0}^{A-1} \frac{x^a}{a!} e^{-x} = y, \tag{3.46}$$

whose implicit solution, in this thesis, is expressed as

$$x = h_P(y, A). \tag{3.47}$$

Although the inverse Poisson process equation does not have a close-form solution, a numerical or table look-up approach can be used to search for the sensing threshold. In any event, the spectrum sensing threshold is expressed as

$$\lambda(P_f) = \frac{1}{A} h_P\left(1 - \left(1 - P_f\right)^{\frac{1}{B}}, A\right), \tag{3.48}$$

which also indicates pilot-based OFDM spectrum sensing algorithm with sliding frequency correlator has a threshold not sensitive to unknown noise statistics.

3.3.7.2 Probability of Mis-detection

Mis-detection means the spectrum sensing device fails to detect the existence of the primary signal. It happens at

$$\mathcal{R} < \lambda, \qquad \text{when } \mathcal{H}_1. \tag{3.49}$$

According to the definition of successful detection probability, the mis-detection probability

$$P_m = 1 - P_d. \tag{3.50}$$

For a certain threshold λ, the mis-detection probability could be formulated as

$$\begin{aligned} P_m(\lambda) &= \text{Prob}\left(\mathcal{R} < \lambda \,|\mathcal{H}_1\right) \\ &= \text{Prob}\left(\frac{\sum_{a=1}^{A}\left(v_0\sqrt{\gamma\delta_n^2}\right)^2 + \sum_{a=1}^{A}|W(a)|^2}{\sum_{a=1}^{A}|W(a)|^2} < \lambda\right) \\ &= \text{Prob}\left(\sum_{a=1}^{2A}\left|W'(a)\right|^2 > \frac{A\gamma\delta_n^2}{\lambda-1}\right). \end{aligned} \tag{3.51}$$

From (3.41), we have

$$\begin{aligned} P_m(\lambda) &= \int_{\frac{A\gamma\delta_n^2}{\lambda-1}}^{+\infty} \frac{\frac{2M}{\delta_n^2}\left(\frac{2M}{\delta_n^2}x\right)^{A-1}}{2^A\Gamma(A)} e^{-\frac{M}{\delta_n^2}x}\,\mathrm{d}x \\ &= \sum_{a=0}^{A-1}\frac{\left(\frac{\gamma AM}{\lambda-1}\right)^a}{a!}e^{-\frac{\gamma AM}{\lambda-1}}, \end{aligned} \tag{3.52}$$

where γ denotes the SNR.

3.3.7.3 Pilot-based OFDM Spectrum Sensing Time

In addition to the false alarm probability P_f and the successful detection probability P_d, the *spectrum sensing time* represents another important performance index of a spectrum sensing algorithm. The recommendations from FCC [16]–[18] suggest that when CR users are sharing the spectrum resource, they need to release the resource within a required time

if the primary user comes back to use the resource. For different systems and standards, this suggestion leads to different required spectrum sensing time, varying from several milliseconds to several seconds [17] [18].

Comparing to the cyclostationary detection, where the spectral correlation function needs a long computation time [6], the proposed sensing algorithm in this thesis has moderate calculation complexity from the average processing, a FFT calculation, and several correlation functions. These simple calculations will only cost very short processing time considering the fast processing speeds of today's electronic devices. Consequently, the sensing time is actually the time we receive the signal when we neglect the signal processing time. The sensing time for the proposed sensing algorithm then can be approximated by M, which is the number of OFDM symbols in average processing. Specifically, the processing time M for any combination of $\{P_m, P_f, \gamma\}$ can be obtained from (3.48) and (3.52) as

$$M = \frac{h_P\left(1-\left(1-P_f\right)^{\frac{1}{B}}, A\right) - A}{A^2\gamma} h_P(P_m, A). \tag{3.53}$$

3.3.7.4 Impacts of Interference and Multipath Channel

The proposed spectrum sensing algorithm is based on the detection of the unique pilots' energy in target signal. The probability that the interferences have the same modulation scheme, the same symbol period, and the same pilots on the same frequency would be extremely low. As a result, all the interferences could be regarded as noise and will be significantly mitigated after the average processing and the correlation processing in this algorithm. Thus, interference signal will not have much impact on the proposed pilot-based OFDM spectrum sensing algorithm.

On the other hand, frequency selective multipath channel can only change the energy distribution of received signal and consequently has very limited impact to the proposed

sensing algorithm which only considers the energy on pilot tones. This is because the in-band pilots for OFDM system are distributed evenly across the whole channel bandwidth and the combined pilot energy won't be significantly influenced by the frequency selectivity from the multipath channel.

3.3.8 Simulations

To verify the effectiveness of the proposed spectrum sensing algorithm, several simulations have been run and presented in this section.

In the spectrum sensing simulations, an OFDM system with 1024 subcarriers, 4MHz bandwidth, and 32 pilot subcarriers is adopted. The simulated OFDM system has a carrier frequency of 1GHz and oscillator stability of ±30ppm. Therefore, the maximum frequency offset from the ±30ppm oscillator is ±30kHz. To overcome the potential impact of the frequency offset on spectrum sensing, a 64kHz of extra processing bandwidth is used in the sensing devices, which is equivalent to $B = 32$ subcarriers. This means the system in this simulation has a maximum tolerable frequency offset of ±32kHz. Random timing offset and frequency offset (less than the maximum tolerable frequency offset) are included in every round of the simulations. Considering some previous research contributions and the recommendations from FCC [17] [18], the upper limit of the false alarm probability is set as $P_f = 0.05$ in the simulations. The SNR range in the simulation is set from −25dB to −15dB to meet the low SNR recommendations from FCC [16]–[18]. The corresponding spectrum sensing threshold is calculated via (3.48).

Figure 3.11 shows the simulation result of the successful detection probability over different sensing time M and different SNRs of the received signal from the primary user. The simulation results indicate that the proposed spectrum sensing algorithm exhibits a very good performance at SNR as low as −20dB, while most existing algorithms can only

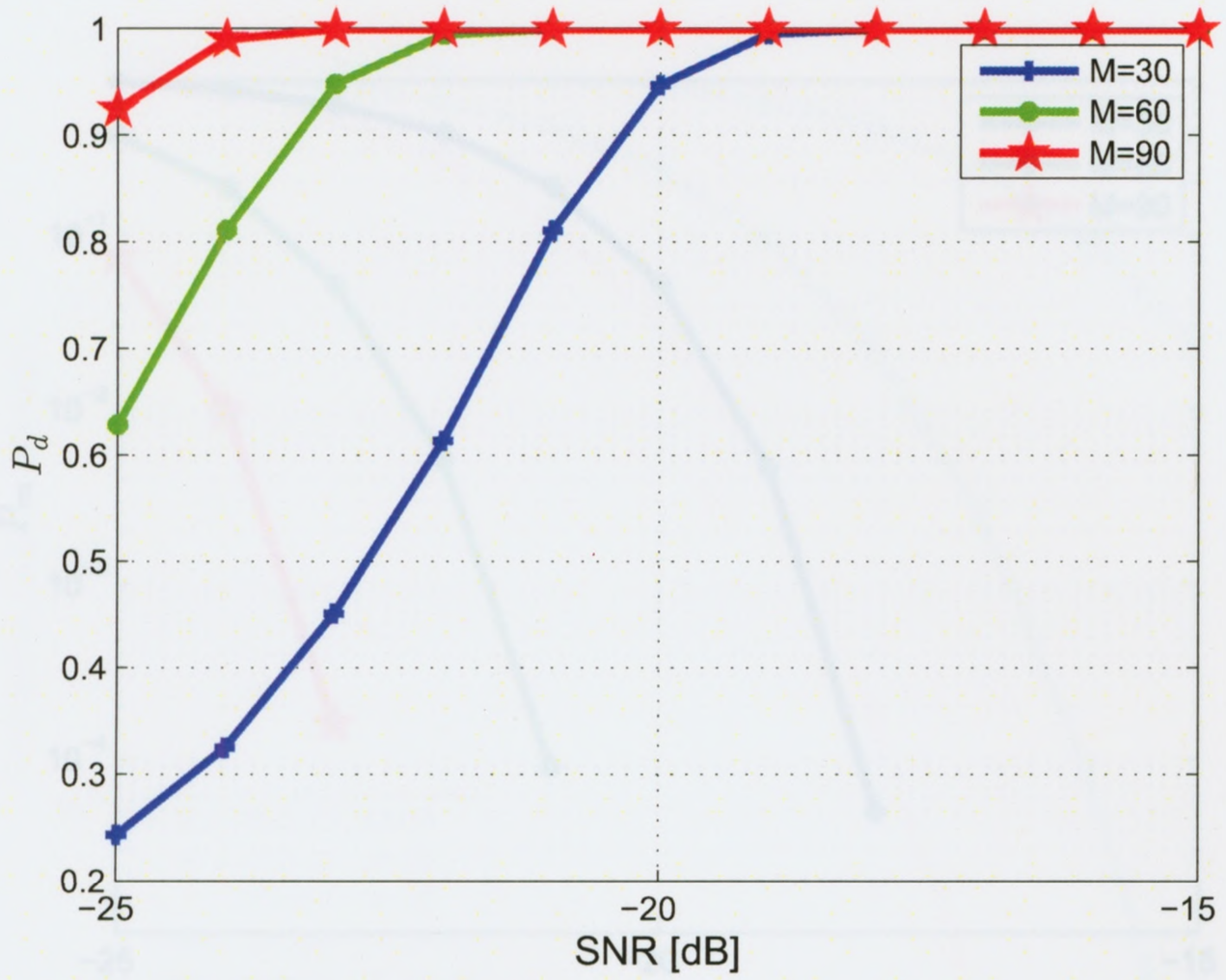

Figure 3.11: Probability of successful detection of pilot-based OFDM spectrum sensing, P_d (1,024 subcarriers, 32 pilot subcarriers per OFDM symbol, $P_f = 0.05$).

detect signal with the SNR of minus few dB [20]–[34]. It is also observed from this figure that an increase of spectrum sensing time (in terms of the number of OFDM symbols M) improves the performance of the algorithm. The mis-detection probability, which is equal to $1 - P_d$, is also shown in Figure 3.12.

The proposed algorithm is based on detecting the energy on in-band pilots, which means an increasing of the power of pilot subcarriers in OFDM symbols will effectively improve the performance of the spectrum sensing algorithm. Figure 3.13 shows the performance of the spectrum sensing when an OFDM system with 8096 subcarriers and 512 pilot tones is adopted. Comparison between these two figures indicates that an increase of the pilot subcarriers comes with a better performance in the spectrum sensing.

Also, the impact of cyclic prefix is simulated, and the result is shown in Figure 3.14. As we can see from the result, the interference signal from cyclic prefix, which is randomly distributed in frequency domain, does not have much impact on the spectrum sensing based

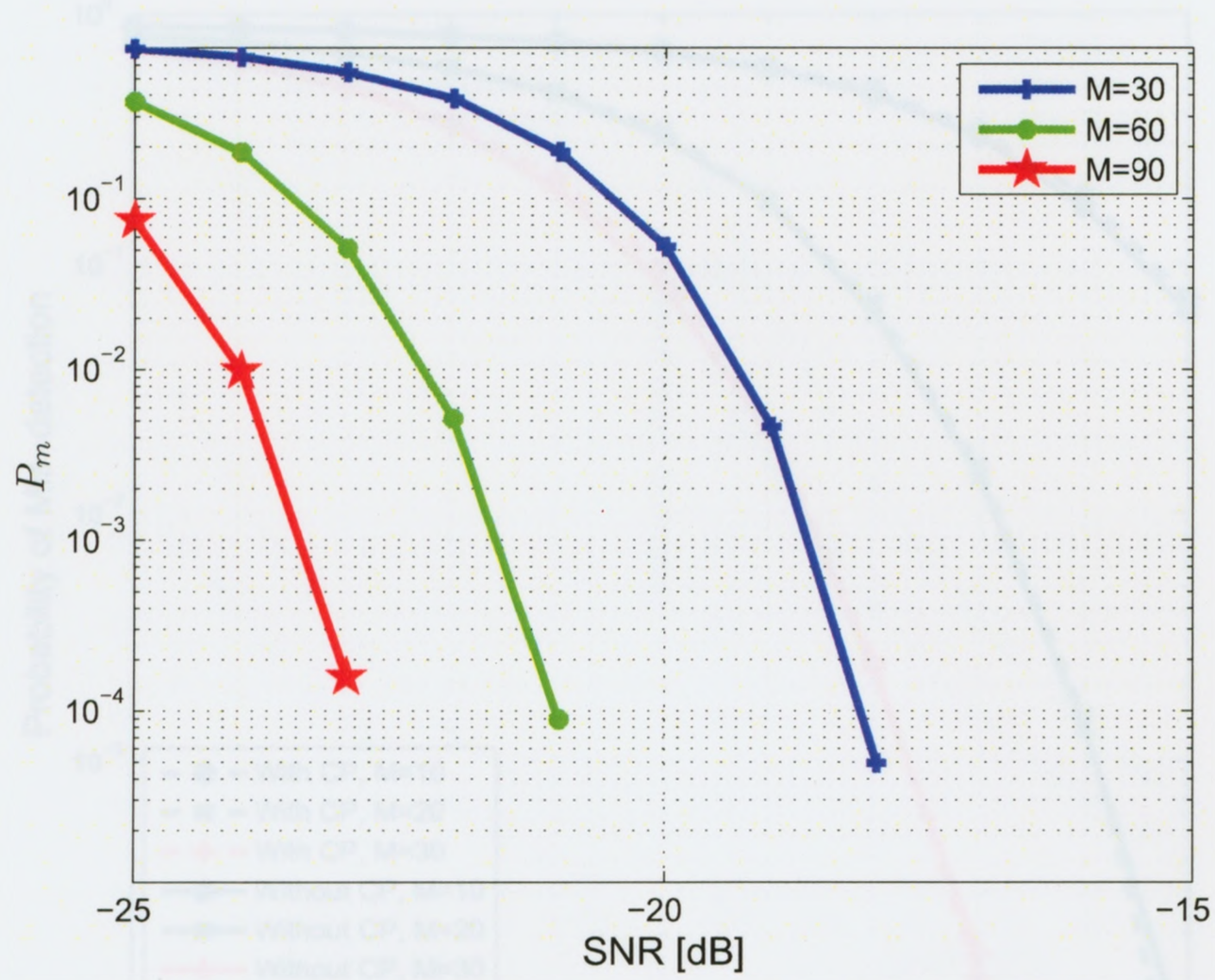

Figure 3.12: Probability of mis-detection of pilot-based OFDM spectrum sensing, P_m (1,024 subcarriers, 32 pilot subcarriers per OFDM symbol, $P_f = 0.05$).

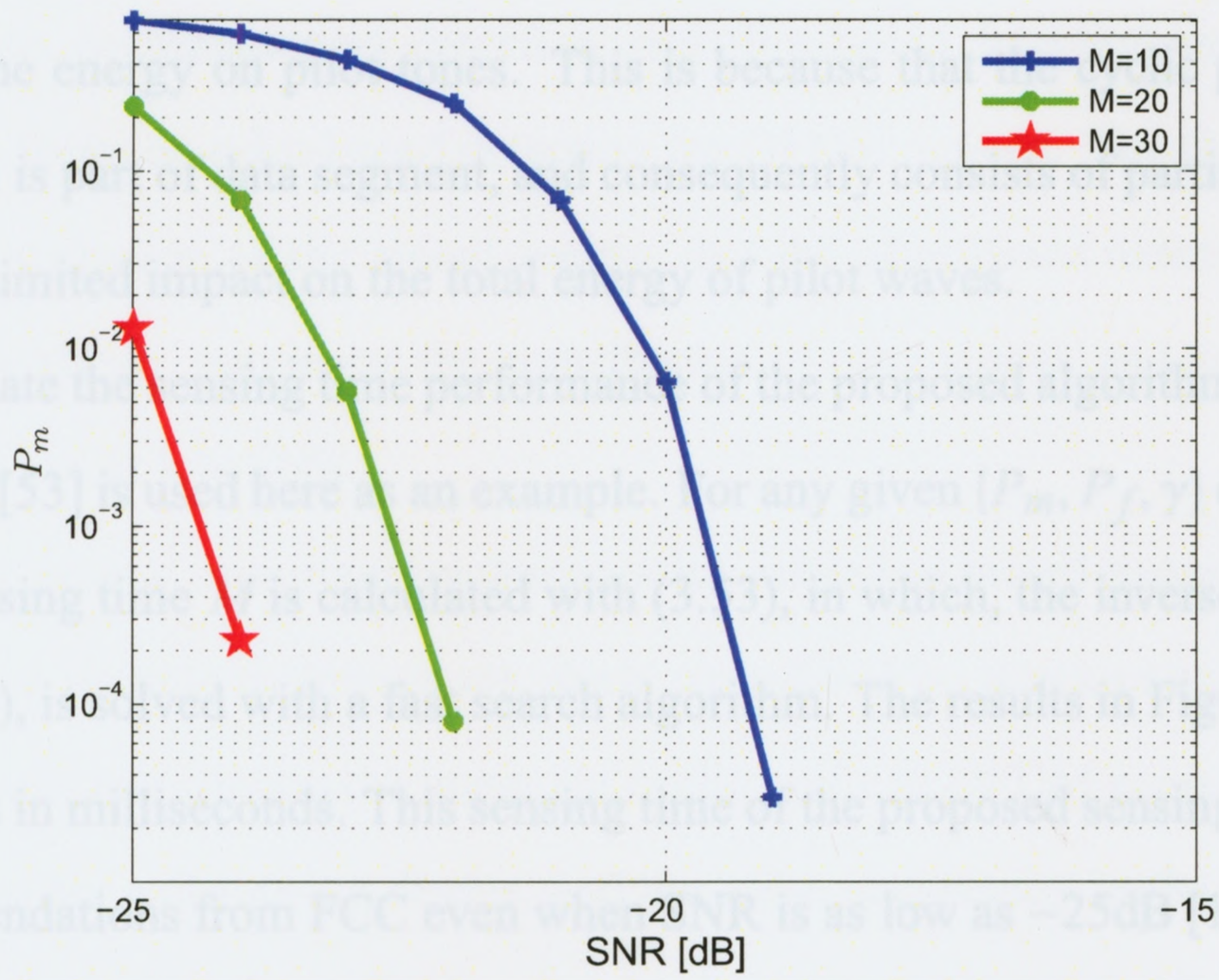

Figure 3.13: Probability of mis-detection of pilot-based OFDM spectrum sensing, P_m (8,096 subcarriers, 512 pilot subcarriers per OFDM symbol, $P_f = 0.05$).

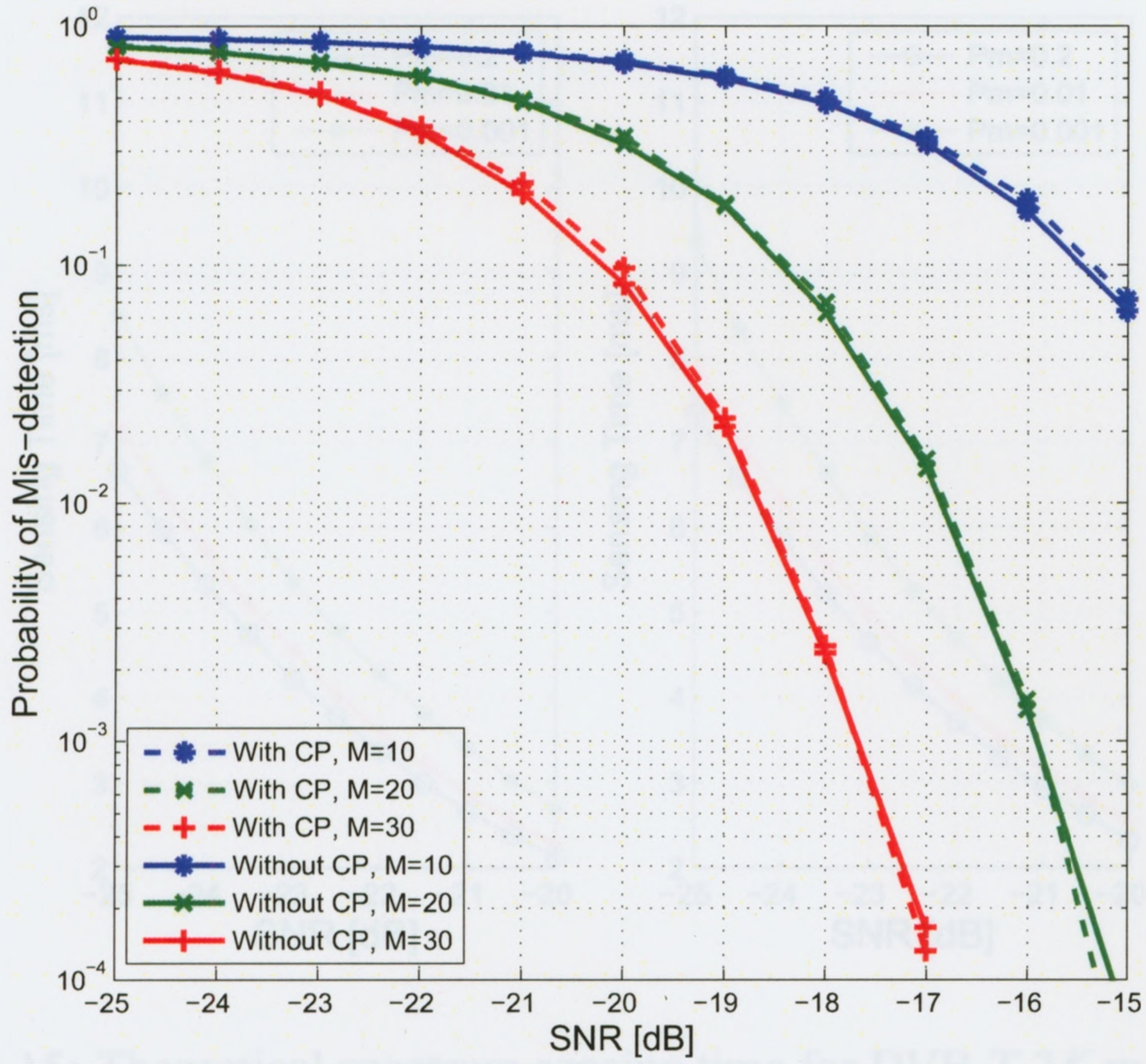

Figure 3.14: Pilot-based OFDM spectrum sensing performance, illustration of impacts from cyclic prefix ($2K$ subcarriers, 128 in-band pilots, 5% false alarm probability).

on detecting the energy on pilot tones. This is because that the cyclic prefix segment in OFDM system is part of data segment, and consequently consists of partial pilot wave, and then has very limited impact on the total energy of pilot waves.

To evaluate the sensing time performance of the proposed algorithm, the $2K$ mode of DVB-T signal [53] is used here as an example. For any given $\{P_m, P_f, \gamma\}$ combinations, the theoretical sensing time M is calculated with (3.53), in which, the inverse Poisson process equation, $h_P(x)$, is solved with a fast search algorithm. The results in Figure 3.15 show the sensing time is in milliseconds. This sensing time of the proposed sensing algorithm meets most recommendations from FCC even when SNR is as low as -25dB [16]–[18].

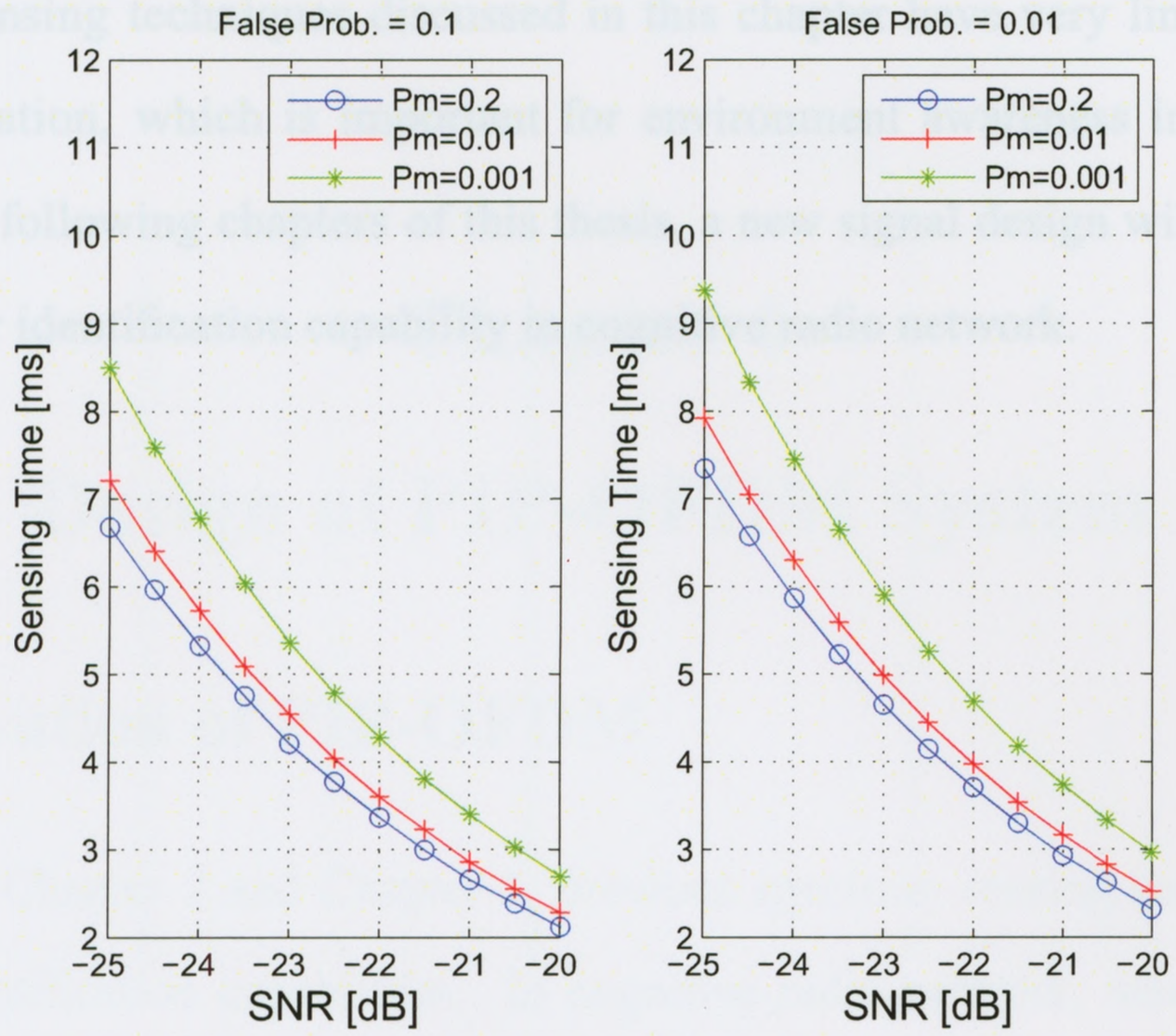

Figure 3.15: Theoretical spectrum sensing time for DVB-T 2K mode signal.

3.4 Chapter Summary

Energy detection, cyclostationary detection, and pilot-based detection are discussed in this chapter, with a focus on pilot-based detection for OFDM signals. The first two techniques consider the distribution of the signal energy, and the pilot-based detection use the characteristic of the signal, maximize the contribution of pilot signal, and consequently has a better performance at low SNR.

However, several important implementation related technical issues for the pilot-based OFDM spectrum sensing technique are rarely considered by previous researchers. Consequently, this thesis investigates the impact of cyclic prefix in OFDM signal, frequency offset between transmitter and sensing device, and the noise uncertainty in the sensing threshold design. The impact of cyclic prefix is proved to be neglectable in pilot-based OFDM spectrum sensing. A new pilot-based OFDM spectrum sensing algorithm with sliding frequency correlator is proposed in this Chapter to address the later two issues.

All the sensing techniques discussed in this chapter have very limited capabilities in user identification, which is important for environment awareness in cognitive radio network. In the following chapters of this thesis, a new signal design will be proposed to enhance the user identification capability in cognitive radio network.

Chapter 4

Design of PIP-OFDM System

4.1 Motivation of PIP-OFDM

As discussed in Chapter 2 and Chapter 3, previous spectrum sensing methods have very limited user identification capabilities. In cognitive radio network, where multiple secondary users coexist, a reliable user identification technique is needed to achieve a better network management. Previous techniques, including cyclostationary detection method, identify signal by estimating modulation parameters of received signal. Pilot-based sensing method is able to identify some special OFDM signals by differentiating location distributions of pilot tones in frequency domain [40]. Nevertheless, none of these methods are still effective to identify the active secondary user when the secondary users in one cognitive radio network use the same modulation method.

Demodulation is an effective solution for identification purpose in some wireless systems. However, demodulation is very difficult to achieve for spectrum sensing in cognitive radio network where the SNRs are very low. Considering the averaging theory gained from pilot-based OFDM spectrum sensing technique in Chapter 3, a solution that utilizes pilot tones, i.e., PIP-OFDM system, is proposed in this thesis for user identification purpose in cognitive radio network. Proposed PIP-OFDM system encodes the pilot tones so that they carry ID information of the transmitter. The PIP-OFDM system doesn't lose any bandwidth efficiency because all those precoded in-band pilot tones could be used as traditional pilot

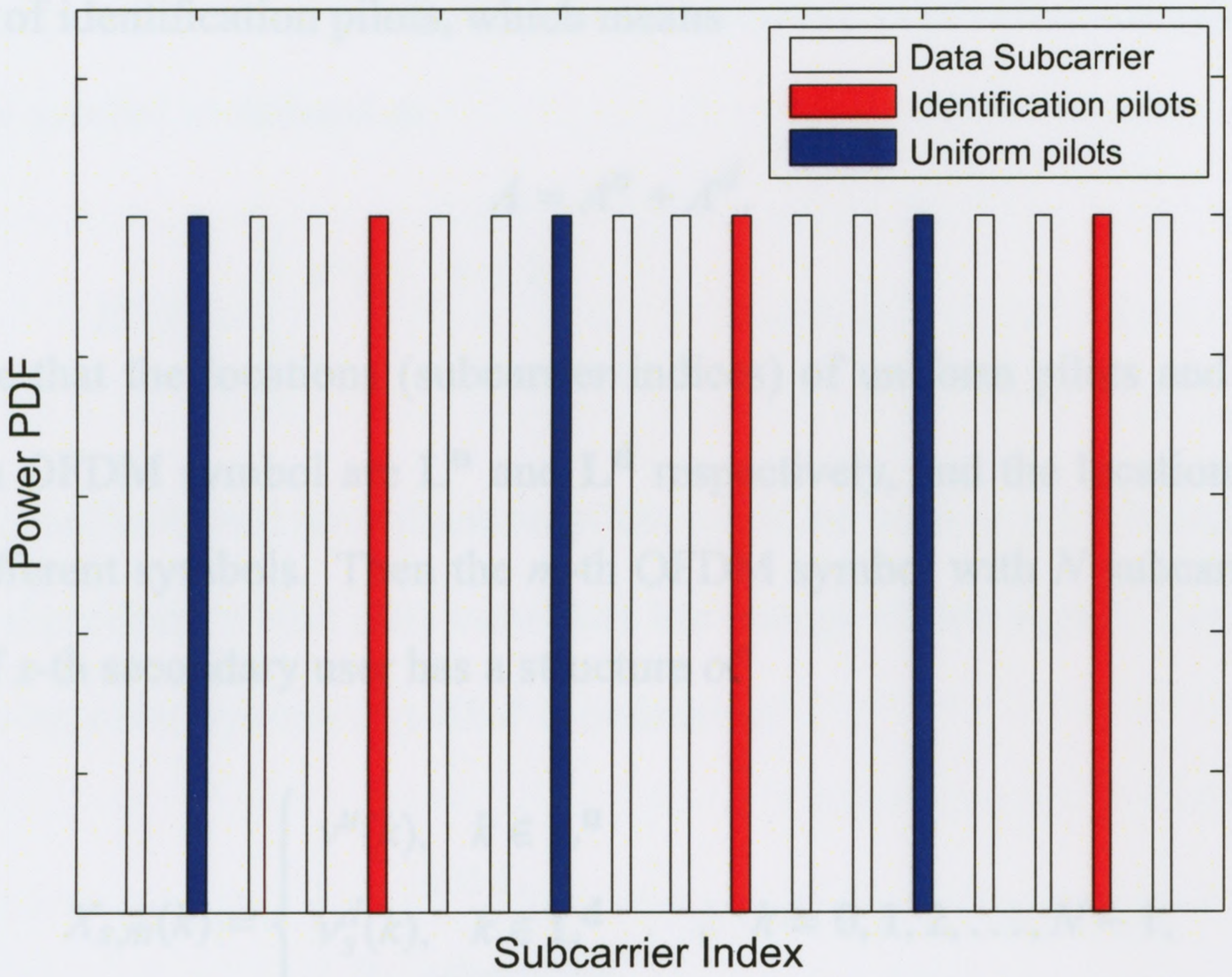

Figure 4.1: Illustration of pilots in PIP-OFDM signal (frequency domain).

tones in regular communications; at the same time, they could be used for user identification during spectrum sensing at low SNR as discussed later.

4.2 Design of PIP-OFDM System

4.2.1 Pilot tones in PIP-OFDM System

In the proposed PIP-OFDM system, two groups of pilot tones, *uniform pilots* and *identification pilots*, are multiplexed with the data-carrying subcarriers in frequency domain. All secondary users in one cognitive radio network use the same uniform pilot signal, while each secondary user is assigned a unique identification pilot signal. A brief illustration of pilot architecture in PIP-OFDM system is shown in Figure 4.1.

Let A be the total number of pilots in the PIP-OFDM signal, including A^u of uniform

pilots and A^d of identification pilots, which means

$$A = A^u + A^d. \tag{4.1}$$

Assume that the locations (subcarrier indices) of uniform pilots and identification pilots in each OFDM symbol are $\mathbf{L^u}$ and $\mathbf{L^d}$ respectively, and the locations are kept the same over different symbols. Then the m-th OFDM symbol with N subcarriers from the transmitter of s-th secondary user has a structure of

$$X_{s,m}(k) = \begin{cases} v^u(k), & k \in \mathbf{L^u} \\ v_s^d(k), & k \in \mathbf{L^d} \\ \text{data}, & \text{otherwise} \end{cases}, \quad k = 0, 1, 2, \ldots, N-1, \tag{4.2}$$

where $\mathbf{v^u}$ are the carried information on the uniform pilots, and $\mathbf{v_s^d}$ are the identity information built in identification pilots, which are also called *identification pilot code word*. Uniform pilots in all transmitters use the same modulating information $\mathbf{v^u}$ in one CR network for reference purpose, and each transmitter has a unique identification pilot code word, $\mathbf{v_s^d}$, with s corresponding to the transmitter ID. To simplify the analysis, the power on all pilots is assumed to be the same in this thesis. Mathematically,

$$\left|v^u(k_1)\right|^2 = \left|v_s^d(k_2)\right|^2 = v_0^2, \quad \text{for any } k_1, k_2, \text{ and } s. \tag{4.3}$$

The corresponding time version of the m-th OFDM symbol in (4.2) could be written as

$$x_{s,m}(n) = \frac{1}{\sqrt{N}} \sum_{k=0}^{N-1} X_{s,m}(k) e^{j2\pi kn/N}, \quad n = 0, 1, 2, \ldots, N-1. \tag{4.4}$$

Two pilot reference symbols in frequency domain are introduced here for future use,

i.e., uniform pilot reference symbol and spectrum sensing pilot reference symbol. *Uniform pilot reference symbol* is defined as

$$R^u(k) = \begin{cases} v^u(k) & k \in \mathbf{L^u} \\ 0 & \text{otherwise} \end{cases}, \quad k = 0, 1, 2, \ldots, N-1. \tag{4.5}$$

Both the uniform and identification pilots could be used in pilot-based OFDM spectrum sensing algorithm, which only considers the energy of one signal. Consequently, the *spectrum sensing pilot reference symbol* is defined as

$$|R(k)|^2 = \begin{cases} 1 & k \in \mathbf{L} \\ 0 & \text{otherwise} \end{cases}, \quad k = 0, 1, 2, \ldots, N-1, \tag{4.6}$$

where $\mathbf{L} = \left\{\mathbf{L^u}, \mathbf{L^d}\right\}$ are the locations of all pilots.

This completes the architecture of OFDM system with precoded in-band pilots. In the PIP-OFDM system, uniform pilots are known to every user in this network, and hence could be used for synchronization and channel estimation during the demodulation of identification pilots. Since the identification pilots are designed to be unique from each secondary user in one cognitive radio network, user identification is then achievable by identifying the received signal. Consequently, *signal identification*, *user identification*, and *identification pilots demodulation* are equivalent to each other in PIP-OFDM systems.

4.2.2 Design and Precoding of the Pilot Tones

The design of pilot tones in PIP-OFDM system includes the design of uniform pilots and that of identification pilots. The design of uniform pilots is similar to traditional pilots design in OFDM system, which is a tradeoff between system performances (such as channel estimation) and bandwidth cost [54]. At the same time, to avoid any direct current

(DC) component in the transmitted signal, polarity modulated pseudo random sequences are frequently used in the design of pilot tones. Details of uniform pilots design, similar to traditional pilots design, are not included in this thesis, and could be found in [54].

To facilitate CR receivers (or spectrum sensing device) identify the active secondary user through signal identification, it's apparent to minimize the cross-correlation coefficient among identification pilots from different transmitters, which is to maximize the geometric distance between identification pilot signals from different transmitters in signal space. Thereby, the design of identification pilots is similar to channel coding design in digital communications (see [55] for channel coding design). Each transmitter has a unique identification pilot code word $\mathbf{v}_s^{\mathbf{d}}$, and the combination of all the code words make up of a code, $\mathbf{V}^{\mathbf{d}}$, which is the complete identification pilot signals set. With a certain length of identification pilot code word, an increase of supported users in this network will decrease the geometric distance of a code and hence degrade the performance of the user identification. Consequently, the design of identification pilot tones is actually a tradeoff between user capacity of the network and performance of the user identification.

To design an identification pilot code $\mathbf{V}^{\mathbf{d}}$, a set of orthogonal discrete signals is introduced here:

$$O = \{\mathbf{o}_1, \mathbf{o}_2, \ldots, \mathbf{o}_\varphi, \ldots, \mathbf{o}_\psi\}. \tag{4.7}$$

Each of the signal $\mathbf{o}_\varphi$ in this set has the same dimension of identification pilot code word, which is the number of subcarriers of identification pilots, A^d. There are all together $\frac{A^d}{\psi}$ non-zero elements in each signal $\mathbf{o}_\varphi$, and they only take values with the amplitude of v_0. By orthogonal, it means

$$\sum_{k=1}^{A^d} o_i(k) \cdot o_j^*(k) \begin{cases} \neq 0, & \text{if } i = j \\ = 0, & \text{if } i \neq j \end{cases}. \tag{4.8}$$

Specifically, since there are $\frac{A^d}{\Psi}$ non-zero elements in signal $\mathbf{o}_\varphi$ and they only take values with the amplitude of v_0, then,

$$\sum_{k=1}^{A^d} o_i(k) \cdot o_j^*(k) = \begin{cases} \frac{A^d}{\Psi} v_0^2, & \text{if } i = j \\ 0, & \text{if } i \neq j \end{cases}. \tag{4.9}$$

For the transmitter with the ID of s, the identification pilot code word is expressed as

$$\mathbf{v}_s^{\mathbf{d}} = \sum_{\varphi=1}^{\Psi} c_s(\varphi) \cdot \mathbf{o}_\varphi, \tag{4.10}$$

where $\mathbf{c}_s$ is the unique ID for transmitter s, and $c_s(\varphi)$ only takes value of '+1' or '−1'. Therefore the total number of the active transmitters supported by the proposed identification pilots, also called the user capacity of this cognitive radio network, is

$$\mathcal{S} = 2^{\Psi}, \quad \Psi \leq A^d. \tag{4.11}$$

The distance of the code $\mathbf{V}^{\mathbf{d}}$, which is defined as the minimum geometric distance between any two code words in this code, could be expressed as

$$\mathcal{D} = \frac{A^d}{\Psi} = \frac{A^d}{log_2 \mathcal{S}}. \tag{4.12}$$

From (4.11), the maximum user capacity ($\mathcal{S}$) of the network with A^d identification pilots is 2^{A^d}. However, having a design with the user capacity of 2^{A^d} will make the distance of the code as $\mathcal{D} = 1$, which would lead to a poor performance for the user identification because of the low SNR condition and the strong correlations between identification pilot signals from different transmitters. It is therefore necessary to increase the geometric distance of the designed code to improve the performance of user identification. Fortunately,

this is achievable because the number of pilots in a practical system is usually large enough to support a large number of identification pilots, and the user capacity of the system does not need to be very high in one cognitive radio network. The effectiveness of this design will be verified with the user identification theoretical analysis and simulation in Chapter 6.

This completes the design of PIP-OFDM system. As we presented above, each transmitter has a unique identification pilot code word, and carried information on both the uniform pilots and identification pilots for one certain transmitter do not change over time. These two important properties of PIP-OFDM signal allow us to identify the active secondary user using the procedures in the following discussions.

4.3 Spectrum Sensing in PIP-OFDM System

Pilot-based OFDM spectrum sensing algorithm with sliding frequency correlator, as presented in Chapter 3, could be used in the proposed PIP-OFDM system in cognitive radio network for spectrum sensing purpose. The basic principle of pilot-based OFDM spectrum sensing is to estimate the energy on the pilot tones of averaged OFDM symbol. The only difference between the spectrum sensing in the PIP-OFDM system and that in Chapter 3 is that the former one needs to detect the existence of secondary signal, while the later one only detects the existence of primary signal. However, the principles of spectrum sensing algorithms in these two conditions are identical. More details of pilot-based spectrum sensing for OFDM signal can be found in Chapter 3.

4.4 Chapter Summary

Since previous signal and system designs for cognitive radio communications perform poorly on user identification, an OFDM system with new precoded in-band pilots is proposed in this chapter. Identification pilots in proposed PIP-OFDM system carry unique user identity information, and will be used to identify the active user in one cognitive radio network shown later in Chapter 6. Uniform pilots are also included in the design of PIP system, which will be used as reference signal during the synchronization and channel estimation in the following discussions.

Chapter 5

Synchronization in PIP-OFDM System

5.1 Background of Synchronization in PIP-OFDM

In the proposed PIP-OFDM system, each secondary user is assigned with a unique identification pilot signal. Consequently, user identification could be achieved through the demodulation of identification pilots in PIP-OFDM systems, which is based on synchronization between transmitter and spectrum sensing device. This Chapter discusses synchronization issues in PIP-OFDM systems.

Synchronization in PIP-OFDM systems is different from that in traditional OFDM systems mainly in two aspects. First, training symbols are difficult to be utilized for the synchronization of PIP-OFDM system considering the lack of handshaking between the transmitter and spectrum sensing device. Consequently, some well developed synchronization techniques exploiting redundant information in specially designed repeating training symbols are not applicable in PIP-OFDM synchronization [41]–[48]. Secondly, since user identification is part of spectrum sensing process, the SNR at the receiver side could be very low as well. According to some previous research and suggestions [16]–[18], we consider the SNR for user identification in CR network from −5dB to 5dB. SNR in synchronization is relatively higher than that in spectrum sensing because synchronization is implemented to identify the signals from secondary users, which consequently has lower priority and lower requirements.

Repeating signal samples in time domain could be utilized to estimate frequency offset by calculating time domain phase shift. This idea was firstly proposed by Moose in [41] and has been extended and upgraded in [45]–[48]. Without training symbols or specially designed repeating segments, PIP-OFDM systems have another option to realize the frequency offset estimation, which is exploiting the redundant information in cyclic prefix. Using similar approach, fractional timing offset can be estimated, in this thesis, through estimating the phase shift of predesigned uniform pilot tones in frequency domain. Considering low SNR requirement in synchronization, a multiple OFDM symbol processing strategy is used in this thesis to improve the synchronization performance.

5.2 Coarse Synchronization Algorithms

An arbitrary timing and frequency offset in OFDM systems include an integer and a fractional parts. Coarse synchronization is also called integer offset estimation. Considering the distinctive energy distribution of averaged OFDM signal in frequency domain (see Chapter 3), coarse frequency synchronization is realized with frequency cross correlation method [40]; using the time-domain redundancy in the cyclic prefix of OFDM signal, coarse time synchronization is achieved with delay and correlation (DC) method in time domain [49].

5.2.1 Coarse Frequency Synchronization

As discussed in Chapter 3, the power of symbol-by-symbol averaged OFDM symbol has a distinctive distribution in frequency domain. As shown in Figure 5.1, noise and data subcarriers are mitigated by average processing, while the power on pilot tones keep the same. The averaged OFDM symbol $\overline{\mathbf{Z}}$ has a correlation coefficient with local reference

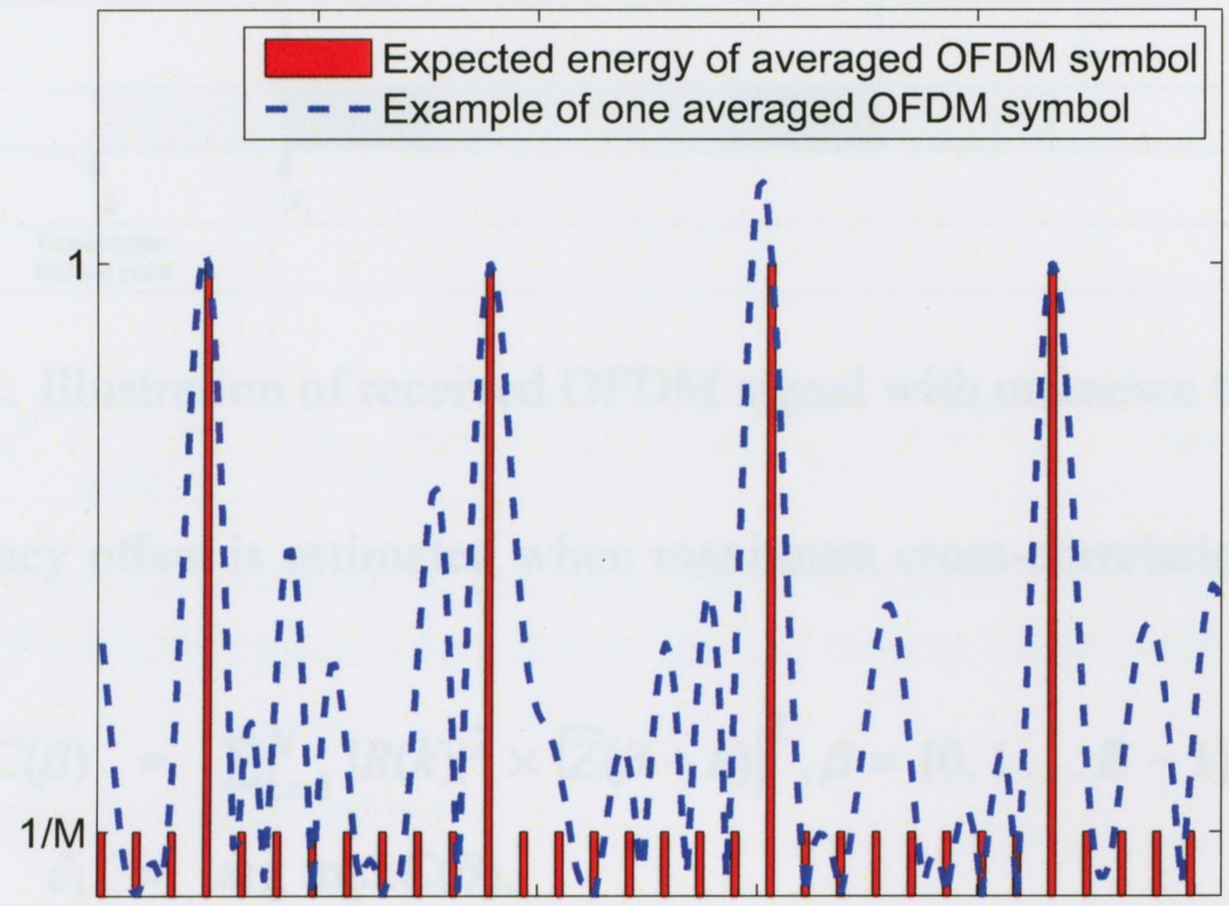

Figure 5.1: Comparison between the ideal power distribution of an averaged OFDM symbol in frequency domain and a simulated example.
(M is the averaged times during the process.)

OFDM symbol in frequency domain as:

$$E\left(\sum_{k=1}^{N}|R(k)|^2\times\left|\overline{Z}(\beta+k)\right|^2\right)=\begin{cases}A\delta_s^2+A\,\delta_n^2/\,M & \beta=\varepsilon_{\mathrm{i}}\\ A\left(\delta_s^2+\delta_n^2\right)/\,M & \text{otherwise}\end{cases}, \tag{5.1}$$

where $R(k)$ is the reference pilot symbol in (3.13), β is the shifted frequency, ε_{i} is the integer part of frequency offset, and local reference is assumed to be normalized with the power of 1 unit.

After the average processing, a coarse frequency synchronization can be achieved with the cross correlation results between the averaged PIP-OFDM symbol and local reference. During the coarse frequency synchronization, sliding frequency correlator in Chapter 3 is used. Similar to the discussion in spectrum sensing, synchronization in PIP-OFDM systems also considers M OFDM symbols. A repeating correlation calculation operation is implemented by tentatively shifting the averaged received PIP-OFDM symbol, through

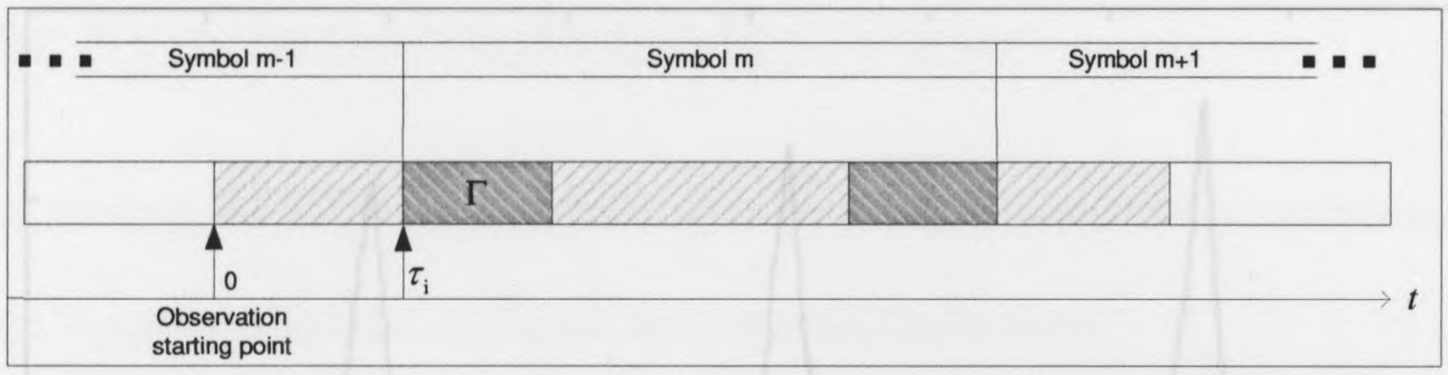

Figure 5.2: Illustration of received OFDM signal with unknown time delay.

which the frequency offset is estimated when maximum cross-correlation is met. Mathematically,

$$\begin{aligned} C(\beta) &= \sum_{k=1}^{N} |R(k)|^2 \times \left|\overline{Z}(\beta+k)\right|^2, \beta = \{0, 1 \ldots B-1\}, \\ \hat{\varepsilon}_i &= \arg\max_{\beta} C(\beta), \end{aligned} \tag{5.2}$$

where B is the additional processing bandwidth in terms of subcarriers number, similar to sliding frequency correlator in Chapter 3.

5.2.2 Coarse Time Synchronization

Due to the unknown timing offset, the received OFDM samples contain an unknown delay τ_i, as shown in Figure 5.2.

Modified delay and correlation (DC) method [49] is proposed to estimate coarse timing offset. We first define the index set (see Figure 5.2)

$$\Gamma = \{\tau_i, \tau_i + 1, \ldots, \tau_i + N_g - 1\}. \tag{5.3}$$

Denote the received time-domain baseband OFDM samples as $z(n)$. The cyclic prefix and it's copies in OFDM signal have a correlation as

$$E\left(z(n)z^*(n+\alpha)\right) = \begin{cases} \delta_s^2 + \delta_n^2 & \alpha = 0 \\ \delta_s^2 e^{-j2\pi\varepsilon} & \alpha = N \\ 0 & \text{otherwise} \end{cases}, \quad n \in \Gamma, \tag{5.4}$$

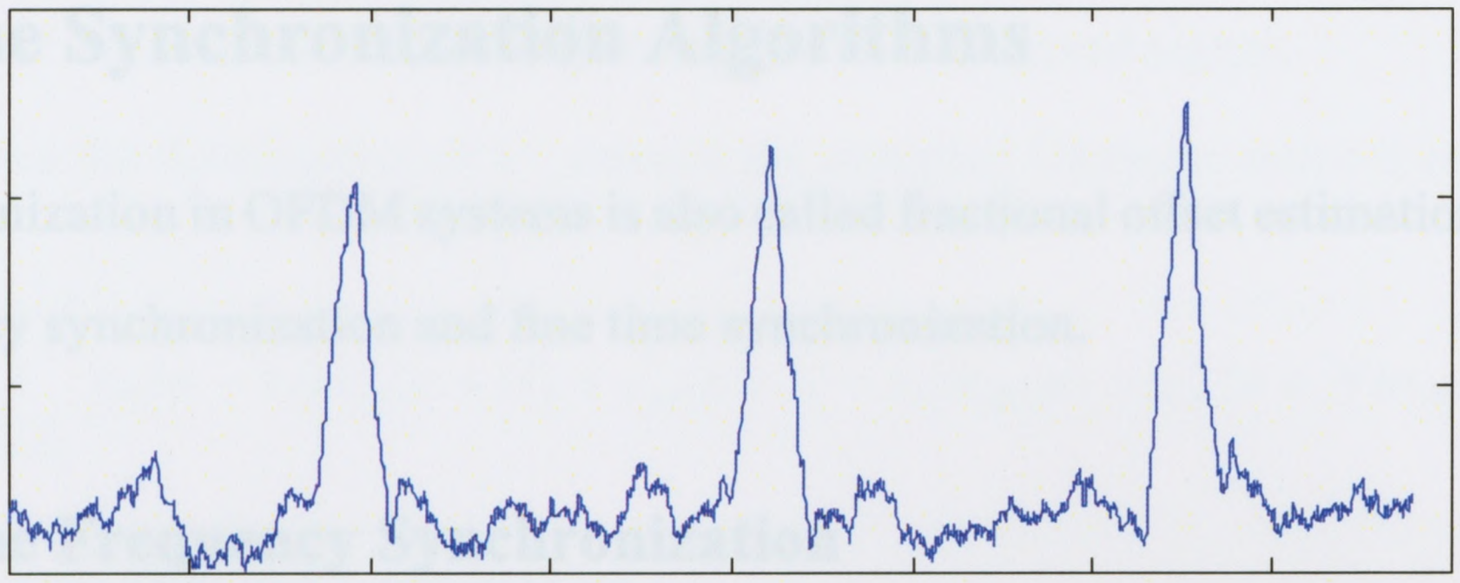

Figure 5.3: Output of the correlation function with DC method. This method can be used in PIP-OFDM systems to achieve integer timing offset estimation.

where ε is unknown frequency offset.

Figure 5.3 shows an example of DC method correlation function in time domain. Using delay and correlation method in time domain, the index of the sample with the maximum auto-correlation coefficient of the received OFDM signal is found by [47]:

$$\begin{aligned} C(\alpha) &= \left|\sum_{n=1}^{Ng} z(n+\alpha)z^*(n+N+\alpha)\right|, \\ \hat{\tau}_{\mathrm{i}} &= \arg\max_{\alpha} C(\alpha). \end{aligned} \tag{5.5}$$

Considering the low SNR requirement, the performance of the time-domain delay and correlation method is very poor. Consequently, similar to coarse frequency synchronization method, performance of coarse time synchronization algorithm can also be improved by processing multiple OFDM symbols. The modified delay and correlation timing offset estimation method with multiple processing symbols in the PIP-OFDM system becomes to

$$\begin{aligned} C(\alpha) &= \sum_{m=1}^{M}\left|\sum_{n=1}^{Ng} z_m(n+\alpha)z_m^*(n+N+\alpha)\right|, \\ \hat{\tau}_{\mathrm{i}} &= \arg\max_{\alpha} C(\alpha). \end{aligned} \tag{5.6}$$

5.3 Fine Synchronization Algorithms

Fine synchronization in OFDM systems is also called fractional offset estimation, including fine frequency synchronization and fine time synchronization.

5.3.1 Fine Frequency Synchronization

Fractional frequency offset can be estimated through phase shift estimation in time domain with the help of repeating segments or samples [41].

With the assumption that integer offsets have been perfectly estimated, we could define the *m*-th received OFDM symbol with normalized fractional frequency offset of ε_f and normalized fractional timing offset of τ_f as

$$z_m(n) = y_m(n - \tau_f)e^{-j2\pi\varepsilon_f n/N_s} + w_m(n), n = 0, 1, 2, \ldots, N_s - 1, \tag{5.7}$$

where $y_m(n)$ is the signal part, and $w_m(n)$ is the noise part. $N_s = N + N_g$ is the length of complete OFDM symbol with cyclic prefix, in which N_g is the length of cyclic prefix.

Considering the coherence between cyclic prefix and ending segment of OFDM symbol,

$$y_m(n) = y_m(n + N), \quad n = 0, 1, 2, \ldots, N_g - 1, \tag{5.8}$$

a correlation function could be written as

$$\begin{aligned}
\Phi^T &= \sum_{m=0}^{M-1}\sum_{n=0}^{N_g-1} z_m(n)z_m^*(n+N) \\
&= e^{j2\pi\varepsilon_f N/N_s}\sum_{m=0}^{M-1}\sum_{n=0}^{N_g-1}\left|y_m(n-\tau_f)\right|^2 + \tilde{w} \\
&\approx N_g M\delta_s^2\left(e^{j2\pi\varepsilon_f N/N_s} + w'\right),
\end{aligned} \tag{5.9}$$

where $\tilde{w}$ and w' are noise terms, and δ_s^2 is the power of received signal.

To derive the distribution of w', rewrite the complex Gaussian noise $\tilde{w}$ in (5.9) as

$$\tilde{w} = \sum_{m=0}^{M-1} \sum_{n=0}^{N_g-1} y_m(n-\tau_f) w_m^*(n+N) + y_m^*(n+N-\tau_f) w_m(n) + w_m^*(n+N) w_m(n), \quad (5.10)$$

which has a mean of 0, and a variation of

$$Var(\tilde{w}) = N_g M\left(2\delta_s^2 \cdot \delta_n^2 + \delta_n^4\right), \quad (5.11)$$

in which δ_n^2 represents the power of noise.

Let $\gamma = \delta_s^2 / \delta_n^2$ denote the SNR of received signal, then

$$w' \sim \mathcal{N}\left(0, \frac{1+2\gamma}{N_g M \gamma^2}\right). \quad (5.12)$$

From (5.9), the fractional frequency offset could be estimated through the correlation function:

$$\begin{aligned} \hat{\varepsilon}_f &= \frac{N_s}{2\pi N} \angle \Phi^T \\ &= \frac{N_s}{2\pi N} \tan^{-1}\left[\frac{Im\left(\Phi^T\right)}{Re\left(\Phi^T\right)}\right], \end{aligned} \quad (5.13)$$

where $Re(\cdot)$ and $Im(\cdot)$ represent the functions of getting the real and imaginary part of the variable respectively.

Since the phase can only be resolved in the $[-\pi, \pi]$ range, the algorithm above can only estimate the frequency offset within $\left[-\frac{N_s}{2N^2} f_s, \frac{N_s}{2N^2} f_s\right]$, where $f_s = 1/T_s$ is the sampling frequency. This range is acceptable after the coarse synchronization, which restricts the frequency offset in a fractional value.

5.3.2 Fine Time Synchronization

The OFDM system is not very sensitive to fractional timing offset since the phase rotation caused by fractional timing offset could be corrected in equalization after channel estimation in frequency domain. Fine time synchronization is then seldom considered by previous researchers. However, subcarriers (uniform pilots) used for channel estimation in PIP-OFDM systems are very limited to achieve precise enough channel estimation results. Consequently, fine time synchronization is necessary for user identification in PIP-OFDM systems.

Some fractional timing offset estimation techniques were proposed in [56]–[59] by calculating cross-correlation with the help of preambles or training symbols. Nevertheless, as presented above, the absence of training symbols during the synchronization of PIP-OFDM systems makes these methods not applicable. A cyclic prefix auto-correlation technique was proposed by Sandell [50] to achieve fine time synchronization, while having limited performance in multipath channel where cyclic prefix correlation coefficient is relatively weak.

In PIP-OFDM systems, carried information on uniform pilots are known to every user in this cognitive radio network. This information could be regarded as repeating information in frequency domain, and consequently used for fractional timing offset estimation similar to fractional frequency offset estimation algorithm.

Two assumptions about the channel need to be made before introducing the fractional timing offset estimation algorithm. Firstly, the channel is assumed to be slow varying, which means the channel impulse response keep the same during the process of user identification, which lasts for M OFDM symbol time. Secondly, the channel is assumed to be slow fading, which means channel response is assumed to be the same on two adjacent uniform pilots subcarriers in frequency domain.

Assume that integer timing offset, integer frequency offset, and fractional frequency offset have been perfectly estimated through discussions above, the signal in frequency domain could actually be written as

$$Z_m(k) = H(k)X_m(k)e^{-j2\pi k\tau_f/N} + W(k), k = 0, 1, 2, \ldots, N-1, \tag{5.14}$$

where, $H(k)$ is the frequency domain channel response (channel transfer function) on the k-th subcarrier, and $W(k)$ is the noise in frequency domain.

Fractional timing offset estimation is achieved based on coherence information on uniform pilots. This leads us to average the received OFDM signal symbol-by-symbol to mitigate the influences from data subcarriers and noise. The averaged OFDM symbol with fractional timing offset can be expressed as

$$\begin{aligned}\overline{Z}(k) &= \frac{1}{M}\sum_{m=0}^{M-1} Z_m(k) \\ &= \frac{1}{M}\sum_{m=0}^{M-1}\left[H(k)X(k)e^{-j2\pi\tau_f/N} + W(k)\right] \\ &= H(k)X(k)e^{-j2\pi k\tau_f/N} + \overline{W}(k), \quad k \in \mathbf{L}^{\mathbf{u}},\end{aligned} \tag{5.15}$$

where,

$$\overline{W}(k) \sim \mathcal{N}\left(0, \delta_n^2/M\right), \quad k \in \mathbf{L}^{\mathbf{u}}, \tag{5.16}$$

is averaged complex Gaussian noise.

Without loss of generality, we assume transmitted signal has a power of 1, then the power of channel response is identical to received signal's power, δ_s^2. Considering the coherence of channel response between adjacent uniform pilot tones,

$$H(L^u(l)) \approx H(L^u(l+1)), l = 0, 1, 2, \ldots, A^u - 2, \tag{5.17}$$

a correlation function could be defined and calculated as

$$\begin{aligned}\Phi^F &= \sum_{l=0}^{A^u-2} \frac{\overline{Z}\,[L^u(l)]}{X\,[L^u(l)]} \cdot \frac{\overline{Z}^*\,[L^u(l+1)]}{X^*\,[L^u(l+1)]} \\ &\approx \sum_{l=0}^{A^u-2} \left|H\,[L^u(l)]\right|^2 e^{j2\pi\tau_f[L^u(l+1)-L^u(l)]/N} + \tilde{W}. \end{aligned} \tag{5.18}$$

Assume that the uniform pilots are evenly distributed in frequency domain, or mathematically:

$$L^u(l+1) - L^u(l) = \frac{N}{A^u}, \text{ for } \quad l = 0, 1, 2, \ldots, A^u - 2. \tag{5.19}$$

Therefore the correlation function in (5.18) could be written as

$$\begin{aligned}\Phi^F &= \sum_{l=0}^{A^u-2} \left|H\,[L^u(l)]\right|^2 e^{j2\pi\tau_f/A^u} + \tilde{W} \\ &\approx (A^u - 1)\delta_s^2 e^{j2\pi\tau_f/A^u} + \tilde{W}, \end{aligned} \tag{5.20}$$

where $\tilde{W}$ is noise term.

For future usage, rewrite the noise $\tilde{W}$ in (5.20) as

$$\begin{aligned}
\tilde{W} &= \sum_{l=0}^{A^u-2} \Big[H^*(L^u(l+1))\,\overline{W}(L^u(l)) + H(L^u(l))\,\overline{W}^*(L^u(l+1)) \\
&\quad + \overline{W}^*(L^u(l+1))\,\overline{W}(L^u(l)) \Big] \\
&\approx \sum_{l=0}^{A^u-2} \Big[H^*(L^u(l))\,\overline{W}(L^u(l)) + H(L^u(l+1))\,\overline{W}^*(L^u(l+1)) \\
&\quad + \overline{W}^*(L^u(l+1))\,\overline{W}(L^u(l)) \Big] \\
&= H^*(L^u(0))\,\overline{W}(L^u(0)) + H(L^u(Au-1))\,\overline{W}^*(L^u(Au-1)) \\
&\quad + \sum_{l=1}^{A^u-2} \Big[H^*(L^u(l))\,\overline{W}(L^u(l)) + H(L^u(l))\,\overline{W}^*(L^u(l)) \Big] \\
&\quad + \sum_{l=o}^{A^u-2} \overline{W}^*(L^u(l+1))\,\overline{W}(L^u(l)) \\
&= H^*(L^u(0))\,\overline{W}(L^u(0)) + H(L^u(Au-1))\,\overline{W}^*(L^u(Au-1)) \\
&\quad + 2\sum_{l=1}^{A^u-2} Re\Big[H^*(L^u(l))\,\overline{W}(L^u(l)) \Big] + \sum_{l=o}^{A^u-2} \overline{W}^*(L^u(l+1))\,\overline{W}(L^u(l)) \\
&= W_1' + W_2', \qquad (5.21)
\end{aligned}$$

where

$$W_1' = 2\sum_{l=1}^{A^u-2} Re\Big[H^*(L^u(l))\,\overline{W}(L^u(l)) \Big] \qquad (5.22)$$

is a zero-mean real Gaussian noise, and

$$W_1' \sim \mathcal{N}\left(0, \frac{2\delta_n^2\delta_s^2(A^u-2)}{M}\right). \qquad (5.23)$$

The noise term

$$W_2' = H^*(L^u(0))\overline{W}(L^u(0)) + H(L^u(Au-1))\overline{W}^*(L^u(Au-1)) + \sum_{l=o}^{A^u-2}\overline{W}^*(L^u(l+1))\overline{W}(L^u(l)) \quad (5.24)$$

is a zero-mean complex Gaussian noise, and

$$W_2' \sim \mathcal{N}\left(0, \frac{\delta_n^4(A^u-1)+2M\delta_n^2\delta_s^2}{M^2}\right). \quad (5.25)$$

From (5.20), fractional timing offset could be estimated using the phase correlation function in frequency domain as

$$\hat{\tau}_f = \frac{A^u}{2\pi}\angle\Phi^F = \frac{A^u}{2\pi}\tan^{-1}\left[\frac{Im\left(\Phi^F\right)}{Re\left(\Phi^F\right)}\right]. \quad (5.26)$$

According to the estimation function from (5.26), this algorithm can only be used to estimate timing offset within the range of $[-A^uT_s/2, A^uT_s/2]$. However, this is usually larger than a sample period. Since a timing offset larger than half sample period time will lead to integer sample timing offsets, and consequently introduce intersymbol interference (ISI), the timing offset estimation range of proposed fractional timing frequency offset estimation algorithm is $[-T_s/2, T_s/2]$, where T_s is sampling interval. The integer part of timing offset could be corrected by the coarse time synchronization in previous discussions.

5.4 Performance Analysis of Synchronization in PIP-OFDM

Mean square error (MSE) is frequently used to evaluate the performance of synchronization in communication systems. We only consider the performance analysis of fine synchronization in this thesis. Some relative research results about coarse synchronization performances could be found in [47] and [49].

5.4.1 Performance of Fine Frequency Synchronization

To formulate the MSE of fractional frequency offset estimator presented above, we firstly introduce a formula

$$\begin{aligned}\tan\left[\frac{2\pi N}{N_s}(\hat{\varepsilon}_{\mathrm{f}}-\varepsilon_{\mathrm{f}})\right] &= \frac{\tan\left(\frac{2\pi N}{N_s}\hat{\varepsilon}_{\mathrm{f}}\right)-\tan\left(\frac{2\pi N}{N_s}\varepsilon_{\mathrm{f}}\right)}{1+\tan\left(\frac{2\pi N}{N_s}\hat{\varepsilon}_{\mathrm{f}}\right)\tan\left(\frac{2\pi N}{N_s}\varepsilon_{\mathrm{f}}\right)} \\ &= \frac{\frac{Im\left(\Phi^T\right)}{Re\left(\Phi^T\right)}-\tan\left(\frac{2\pi N}{N_s}\varepsilon_{\mathrm{f}}\right)}{1+\frac{Im\left(\Phi^T\right)}{Re\left(\Phi^T\right)}\tan\left(\frac{2\pi N}{N_s}\varepsilon_{\mathrm{f}}\right)}. \end{aligned} \tag{5.27}$$

Assume that the observation time is long enough, which means M is large enough, making $|\hat{\varepsilon}_{\mathrm{f}}-\varepsilon_{\mathrm{f}}| \ll \frac{N_s}{2\pi N}$. This leads to

$$\tan\left[\frac{2\pi N}{N_s}(\hat{\varepsilon}_{\mathrm{f}}-\varepsilon_{\mathrm{f}})\right] \approx \frac{2\pi N}{N_s}(\hat{\varepsilon}_{\mathrm{f}}-\varepsilon_{\mathrm{f}}). \tag{5.28}$$

Split the complex white Gaussian noise w' in (5.12) into real and imaginary part, we have

$$w' = w^R + j\cdot w^I, \tag{5.29}$$

where both w^R and w^I are real Gaussian variables, and they have the same distribution as

$$w^R \sim \mathcal{N}\left(0, \frac{1+2\gamma}{2N_g M\gamma^2}\right), \quad w^I \sim \mathcal{N}\left(0, \frac{1+2\gamma}{2N_g M\gamma^2}\right). \tag{5.30}$$

According to (5.28) and (5.29), formula of (5.27) could be written as

$$\begin{aligned}
\hat{\varepsilon}_{\mathrm{f}} - \varepsilon_{\mathrm{f}} &\approx \frac{N_s}{2\pi N}\tan\left[\frac{2\pi N}{N_s}(\hat{\varepsilon}_{\mathrm{f}} - \varepsilon_{\mathrm{f}})\right] \\
&= \frac{N_s}{2\pi N}\frac{\frac{\sin(2\pi\varepsilon_{\mathrm{f}}N/N_s)+w^I}{\cos(2\pi\varepsilon_{\mathrm{f}}N/N_s)+w^R} - \frac{\sin(2\pi\varepsilon_{\mathrm{f}}N/N_s)}{\cos(2\pi\varepsilon_{\mathrm{f}}N/N_s)}}{1+\frac{\sin(2\pi\varepsilon_{\mathrm{f}}N/N_s)+w^I}{\cos(2\pi\varepsilon_{\mathrm{f}}N/N_s)+w^R}\cdot\frac{\sin(2\pi\varepsilon_{\mathrm{f}}N/N_s)}{\cos(2\pi\varepsilon_{\mathrm{f}}N/N_s)}} \\
&= \frac{N_s}{2\pi N}\frac{w^I\cos\frac{2\pi\varepsilon_{\mathrm{f}}N}{N_s} - w^R\sin\frac{2\pi\varepsilon_{\mathrm{f}}N}{N_s}}{1+w^R\cos\frac{2\pi\varepsilon_{\mathrm{f}}N}{N_s} + w^I\sin\frac{2\pi\varepsilon_{\mathrm{f}}N}{N_s}}.
\end{aligned} \tag{5.31}$$

Since M is large enough, making $N_g M$ is large enough to have $|w'| \ll 1$. Consequently,

$$\hat{\varepsilon}_{\mathrm{f}} - \varepsilon_{\mathrm{f}} \approx \frac{N_s}{2\pi N}\left[w^I\cos\frac{2\pi\varepsilon_{\mathrm{f}}N}{N_s} - w^R\sin\frac{2\pi\varepsilon_{\mathrm{f}}N}{N_s}\right]. \tag{5.32}$$

Assuming that ε_{f} is uniformly distributed:

$$\varepsilon_{\mathrm{f}} \sim U\left(-\frac{N_s}{2N^2}f_s, \frac{N_s}{2N^2}f_s\right), \tag{5.33}$$

we have the expected fractional frequency offset estimation error as

$$E(\hat{\varepsilon}_{\mathrm{f}} - \varepsilon_{\mathrm{f}}) = 0, \tag{5.34}$$

and its variance as

$$Var(\hat{\varepsilon}_{\mathrm{f}} - \varepsilon_{\mathrm{f}}) = \left(\frac{N_s}{2\pi N}\right)^2 \cdot \frac{1+2\gamma}{2N_g M\gamma^2}, \tag{5.35}$$

which is the mean square error of fractional frequency offset estimation.

5.4.2 Performance of Fine Time Synchronization

The analysis of performance of fine time synchronization is similar to that of fine frequency synchronization, but slightly different in noise term distribution.

To formulate the MSE of fractional timing offset estimator presented above, we firstly introduce a formula

$$\begin{aligned}\tan\left[\frac{2\pi}{A^u}(\hat{\tau}_{\mathrm{f}}-\tau_{\mathrm{f}})\right] &= \frac{\tan\left(\frac{2\pi}{A^u}\hat{\tau}_{\mathrm{f}}\right)-\tan\left(\frac{2\pi}{A^u}\tau_{\mathrm{f}}\right)}{1+\tan\left(\frac{2\pi}{A^u}\hat{\tau}_{\mathrm{f}}\right)\tan\left(\frac{2\pi}{A^u}\tau_{\mathrm{f}}\right)} \\ &= \frac{\frac{Im\left(\Phi^F\right)}{Re\left(\Phi^F\right)}-\tan\left(\frac{2\pi}{A^u}\tau_{\mathrm{f}}\right)}{1+\frac{Im\left(\Phi^F\right)}{Re\left(\Phi^F\right)}\tan\left(\frac{2\pi}{A^u}\tau_{\mathrm{f}}\right)}. \end{aligned} \tag{5.36}$$

From (5.20) and (5.21), the real and image parts of the correlation coefficient Φ^F could be respectively written as

$$\begin{aligned} Re\left(\Phi^F\right) &= (A^u-1)\delta_s^2\cos\left(2\pi\tau_{\mathrm{f}}/A^u\right)+Re\left(\tilde{W}\right) \\ &= (A^u-1)\delta_s^2\cos\left(2\pi\tau_{\mathrm{f}}/A^u\right)+W_1'+Re\left(W_2'\right), \end{aligned} \tag{5.37}$$

and,

$$\begin{aligned} Im\left(\Phi^F\right) &= (A^u-1)\delta_s^2\sin\left(2\pi\tau_{\mathrm{f}}/A^u\right)+Im\left(\tilde{W}\right) \\ &= (A^u-1)\delta_s^2\sin\left(2\pi\tau_{\mathrm{f}}/A^u\right)+Im\left(W_2'\right). \end{aligned} \tag{5.38}$$

Consequently,

$$\begin{aligned}\frac{Im\left(\Phi^F\right)}{Re\left(\Phi^F\right)} &= \frac{\sin\left(2\pi\tau_{\mathrm{f}}/A^u\right)+\dfrac{Im\left(\tilde{W}\right)}{(A^u-1)\delta_s^2}}{\cos\left(2\pi\tau_{\mathrm{f}}/A^u\right)+\dfrac{Re\left(\tilde{W}\right)}{(A^u-1)\delta_s^2}} \\ &= \frac{\sin\left(2\pi\tau_{\mathrm{f}}/A^u\right)+\dfrac{Im\left(W_2'\right)}{(A^u-1)\delta_s^2}}{\cos\left(2\pi\tau_{\mathrm{f}}/A^u\right)+\dfrac{W_1'+Re\left(W_2'\right)}{(A^u-1)\delta_s^2}} \\ &= \frac{\sin\left(2\pi\tau_{\mathrm{f}}/A^u\right)+W^I}{\cos\left(2\pi\tau_{\mathrm{f}}/A^u\right)+W^R},\end{aligned} \tag{5.39}$$

where,

$$\begin{cases} W^R = \dfrac{W_1'+Re\left(W_2'\right)}{(A^u-1)\delta_s^2} \\ W^I = \dfrac{Im\left(W_2'\right)}{(A^u-1)\delta_s^2} \end{cases} \tag{5.40}$$

are zero-mean real Gaussian noise terms. It is easy to get, from (5.23) and (5.25), the distributions of W^R and W^I as

$$\begin{cases} W^R \sim \mathcal{N}\left(0, \dfrac{4MA^u\gamma-6M\gamma+(A^u-1)}{2M^2\gamma^2(A^u-1)^2}\right) \\ W^I \sim \mathcal{N}\left(0, \dfrac{2M\gamma+(A^u-1)}{2M^2\gamma^2(A^u-1)^2}\right). \end{cases} \tag{5.41}$$

Assume that the observation time is long enough, which means M is large enough, making $|\hat{\tau}_{\mathrm{f}}-\tau_{\mathrm{f}}| \ll \frac{A^u}{2\pi}$. This leads to

$$\tan\left[\frac{2\pi}{A^u}\left(\hat{\tau}_{\mathrm{f}}-\tau_{\mathrm{f}}\right)\right] \approx \frac{2\pi}{A^u}\left(\hat{\tau}_{\mathrm{f}}-\tau_{\mathrm{f}}\right). \tag{5.42}$$

Consequently,

$$\begin{aligned}\hat{\tau}_{\mathrm{f}}-\tau_{\mathrm{f}} &\approx \frac{A^u}{2\pi}\tan\left[\frac{2\pi}{A^u}(\hat{\tau}_{\mathrm{f}}-\tau_{\mathrm{f}})\right] \\ &= \frac{A^u}{2\pi}\frac{\frac{\sin(2\pi\tau_{\mathrm{f}}/A^u)+W^I}{\cos(2\pi\tau_{\mathrm{f}}/A^u)+W^R}-\frac{\sin(2\pi\tau_{\mathrm{f}}/A^u)}{\cos(2\pi\tau_{\mathrm{f}}/A^u)}}{1+\frac{\sin(2\pi\tau_{\mathrm{f}}/A^u)+W^I}{\cos(2\pi\tau_{\mathrm{f}}/A^u)+W^R}\cdot\frac{\sin(2\pi\tau_{\mathrm{f}}/A^u)}{\cos(2\pi\tau_{\mathrm{f}}/A^u)}} \\ &= \frac{A^u}{2\pi}\frac{W^I\cos\frac{2\pi\tau_{\mathrm{f}}}{A^u}-W^R\sin\frac{2\pi\tau_{\mathrm{f}}}{A^u}}{1+W^I\sin\frac{2\pi\tau_{\mathrm{f}}}{A^u}+W^R\sin\frac{2\pi\tau_{\mathrm{f}}}{A^u}}. \end{aligned} \tag{5.43}$$

Considering M is large enough, making both W^R and W^I much smaller than 1,

$$\hat{\tau}_{\mathrm{f}}-\tau_{\mathrm{f}} \approx \frac{A^u}{2\pi}\left(W^I\cos\frac{2\pi\tau_{\mathrm{f}}}{A^u}-W^R\sin\frac{2\pi\tau_{\mathrm{f}}}{A^u}\right). \tag{5.44}$$

For a special case, to get an example of theoretical performance of timing offset estimation algorithm, assume that after the coarse time synchronization, the fractional timing offset is small enough to make

$$\cos\frac{2\pi\tau_{\mathrm{f}}}{A^u}\approx 1, \text{ and } \sin\frac{2\pi\tau_{\mathrm{f}}}{A^u}\approx 0. \tag{5.45}$$

Consequently, the variance of fractional timing offset estimation error is

$$Var(\hat{\tau}_{\mathrm{f}}-\tau_{\mathrm{f}}) = \left(\frac{A^u}{2\pi}\right)^2\cdot\frac{2M\gamma+(A^u-1)}{2M^2\gamma^2(A^u-1)^2}, \tag{5.46}$$

which is the mean square error of fractional timing offset estimation.

5.5 Simulations

Theoretical performances of fractional frequency and timing offset estimation algorithms in (5.35) and (5.46) are demonstrated in Figure 5.4. In these two figures, the number of subcarriers in OFDM signal is set to be $N = 256$. A cyclic prefix with length of $N_g = 32$ is inserted in front of each OFDM symbol before transmission. $A = 16$ pilots are multiplexed with data subcarriers in each OFDM symbol, including $A^u = 8$ uniform pilots and $A^d = 8$ identification pilots. Though the OFDM system is very sensitive to frequency offset, it's shown in this figure that MSE of frequency offset estimation is very small even at very low SNR around −5dB. The timing offset estimation has a relatively worse performance. However, since the OFDM system is not very sensitive to timing offset, and equalization will correct the phase shift caused by timing offset, MSE of timing offset around 10^{-3} degree is acceptable for most OFDM systems.

To simulate the synchronization algorithms for PIP-OFDM systems proposed above, Monte Carlo simulations are performed. Same parameters as theoretical performances in Figure 5.5 are used in these simulations. Random timing offset and frequency offset are included in every simulation round. Figure 5.5(a) and Figure 5.5(b) illustrate simulation results of fractional frequency offset estimation and fractional timing offset estimation respectively. Theoretical performances are also drawn in these two figures, which are slightly different from simulation results when SNRs are lower. This is because approximations in theoretical analysis are not precise when SNR is relatively lower.

5.6 Chapter Summary

This chapter discusses synchronization issues of OFDM systems with precoded in-band pilots (PIP-OFDM), with a focus on fractional timing and frequency offset estimations,

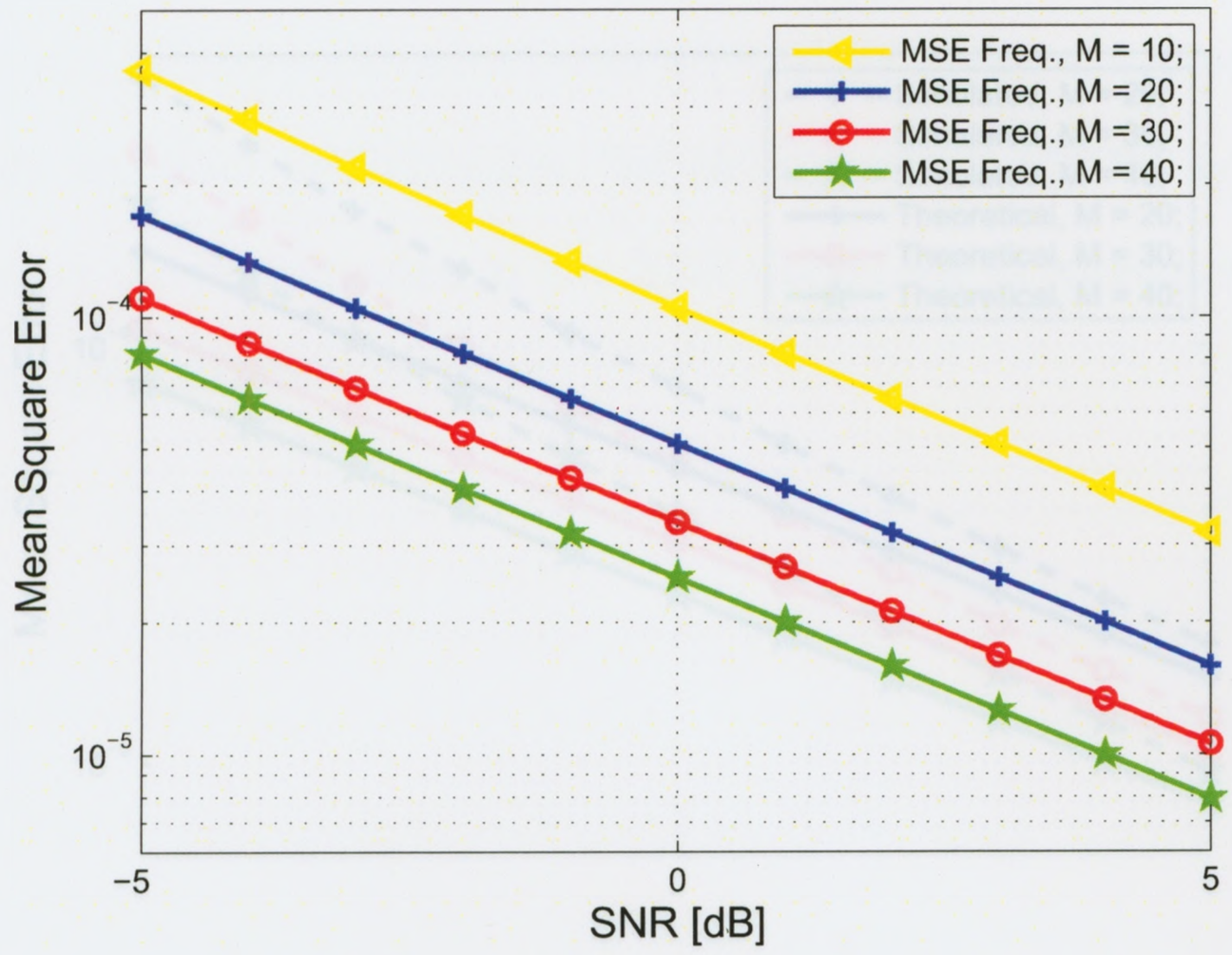

(a)

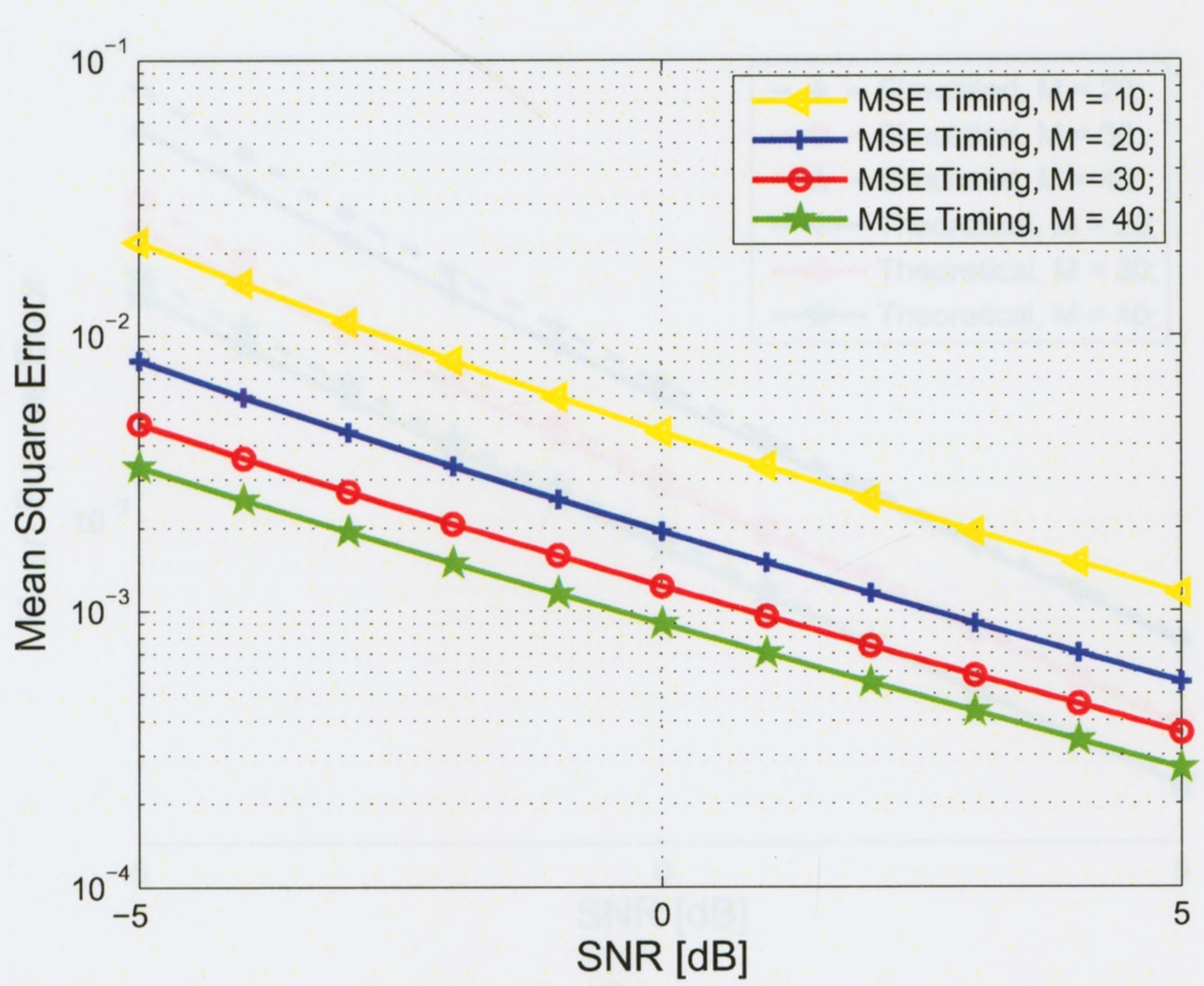

(b)

Figure 5.4: Theoretical fine synchronization performances in PIP-OFDM system (256 subcarriers system with 8 uniform pilots, and 8 identification pilots). (a) Theoretical MSE of frequency offset estimation. (b) Theoretical MSE of timing offset estimation.

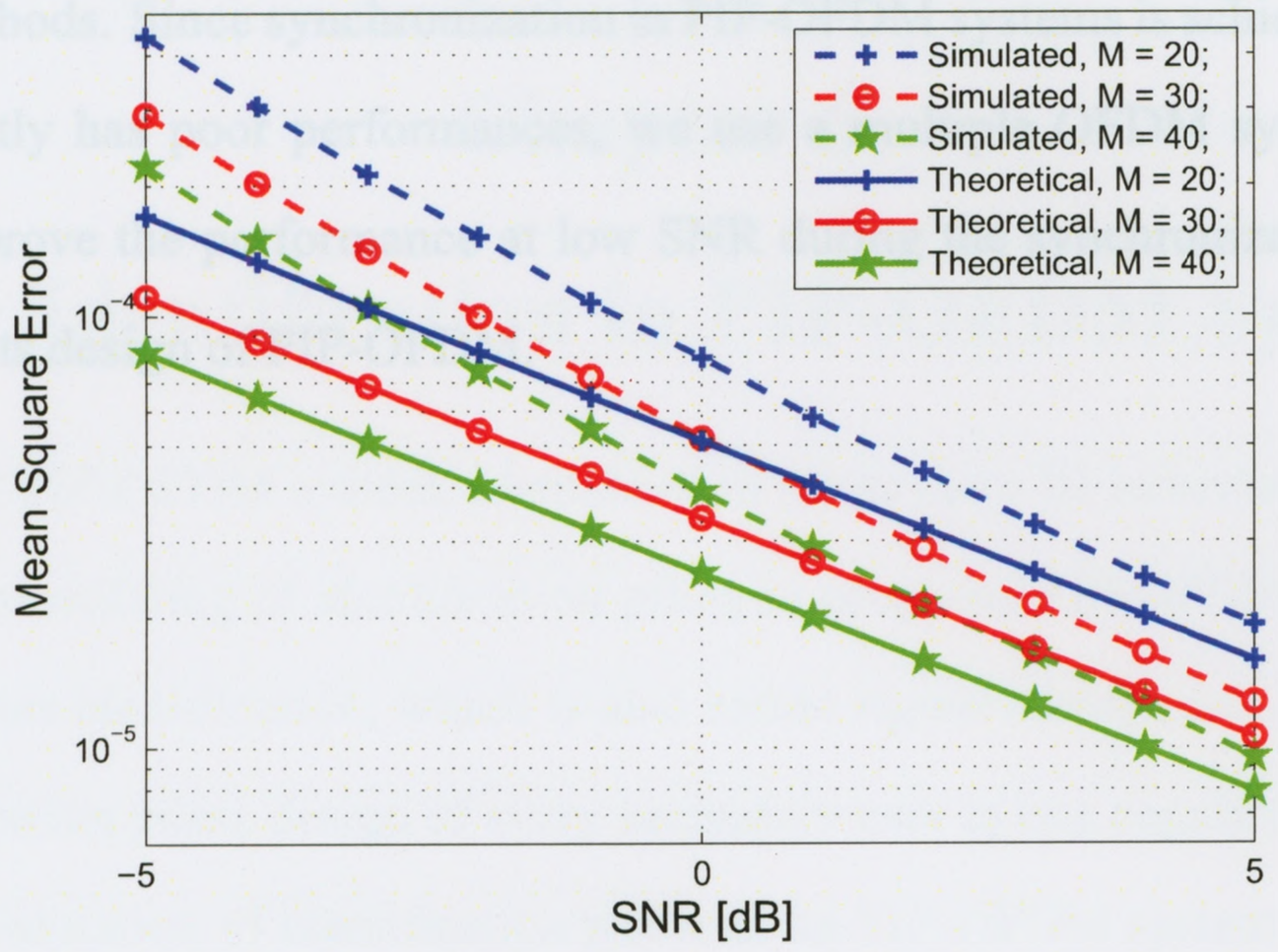

(a)

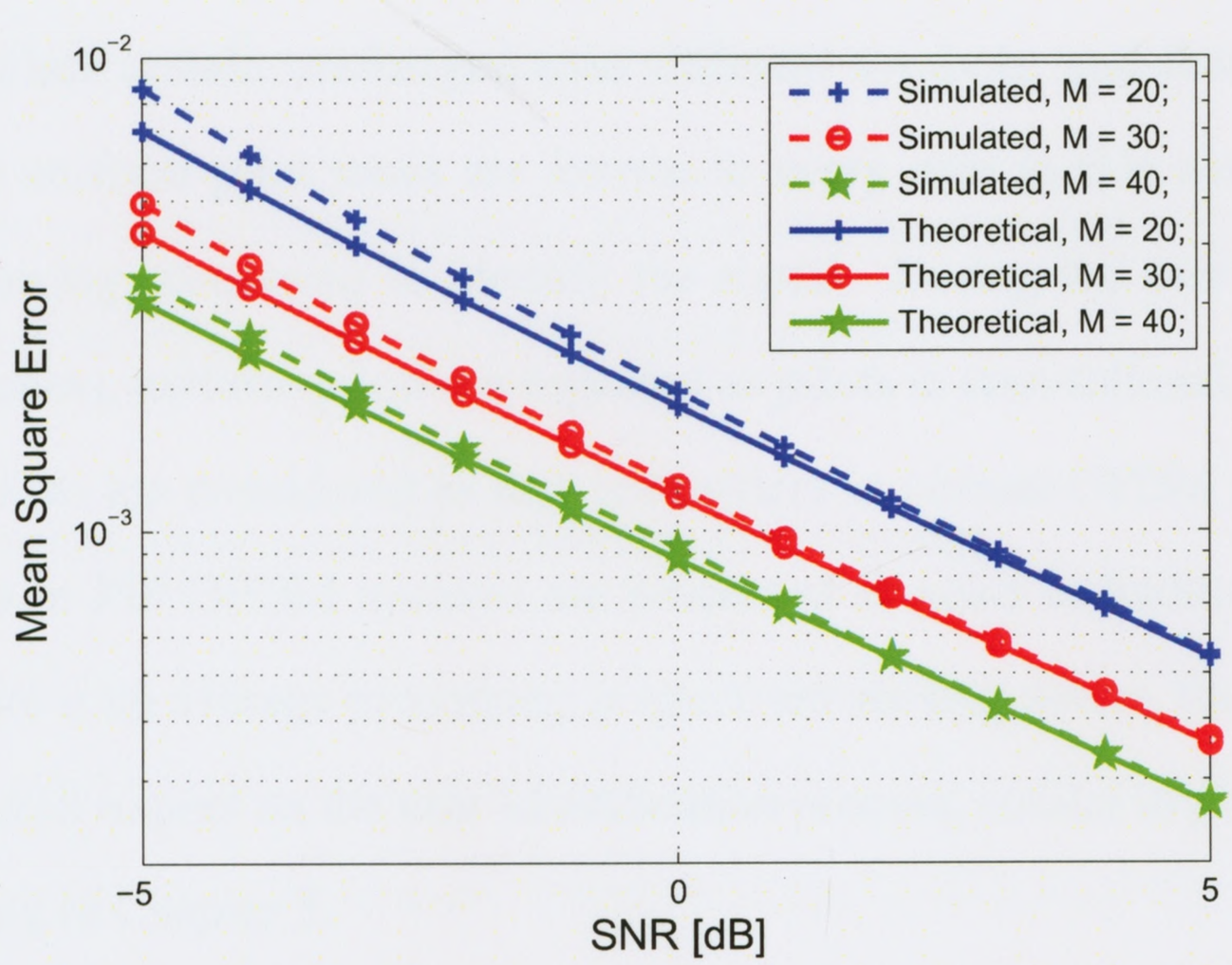

(b)

Figure 5.5: Simulated fine synchronization performances in PIP-OFDM system (256 subcarriers system with 16 identification pilot tones is used). (a) MSE of frequency offset estimation. (b) MSE of timing offset estimation.

which are realized by estimating phase shift in frequency and time domain, respectively. Coarse timing and frequency synchronization algorithms are also briefly discussed with correlation methods. Since synchronization in PIP-OFDM systems is achieved at low SNR, and consequently has poor performances, we use a multiple OFDM symbol processing strategy to improve the performance at low SNR during the synchronization considering the special pilots design of PIP-OFDM.

Chapter 6

User Identification in PIP-OFDM System

In the proposed PIP-OFDM system, identification pilots carry ID information of the transmitter. The demodulating of identification pilots in proposed PIP-OFDM systems is then equivalent to user identification, which is also called *signal identification* considering the unique identification pilots design of every secondary user in one cognitive radio network.

The demodulation of identification pilots in the PIP-OFDM system is different from data demodulation in traditional OFDM systems. The properties that the modulated information on pilots remain unchanged over different symbols, and that the modulating information on uniform pilot tones are known to every user in this network, enable us to explore following processing to identify the signal. During the user identification in PIP-OFDM systems, uniform pilots are regarded as pilots in conventional OFDM systems; identification pilots are considered as data subcarriers in normal OFDM systems; and the data subcarriers in PIP-OFDM systems are processed as noise in traditional OFDM systems. Since there is an average processing in spectrum sensing device, the data subcarriers will not have much impact on the user identification process, similar to pilot-based OFDM spectrum sensing in Chapter 3.

6.1 Channel Estimation and Equalization

In order to mitigate channel effects on the received signal, channel estimation is required to provide information for further processing of the received signal. Channel estimation

is achievable for synchronized OFDM signal with known uniform pilots. In PIP-OFDM system, carried information on uniform pilots are known to each user in current cognitive radio network, therefore channel estimation can be achieved with *Comb-type Pilot Symbol* [60]–[61]. Consequently, MMSE estimator [62], low-rank approximation of MMSE estimator [63], reduced-order ML [64] estimator are all applicable in the PIP-OFDM system for channel estimation purpose. Note that in PIP-OFDM system, the ML estimator and the low rank approach can be derived only if the number of pilot subcarrier, meaning uniform pilots here (A^u), is greater than the number of channel taps or the length of the guard interval (cyclic prefix). Subsequently, equalization can be achieved with channel estimation results easily using traditional equalization methods [65]. Details of channel estimation and equalization are not included in this thesis.

6.2 User Identification Algorithm

According to the insertion of identification pilots as discussed in Chapter 4, user identification could be realized by demodulating identification pilots.

6.2.1 Demodulation and Identification Process

Since the channel has been estimated, and for the convenience of discussion, channel is assumed to be additive white Gaussian noise (AWGN) channel in the demodulation and decoding discussions, with the channel response of $|H_0|$ in frequency domain.

From the PIP-OFDM architecture presented in Chapter 4, the identity of the received signal is estimated by

$$\hat{c}(\varphi) = sgn\left\{Re\left[\sum_{k\in\mathbf{L^d}} \overline{Z}(k)o_{\varphi}^{*}(k)\right]\right\}, \quad \varphi = 1, 2, \ldots, \psi, \tag{6.1}$$

where,

$$sgn(x) = \begin{cases} 1 & \text{if } x \geq 0 \\ -1 & \text{if } x < 0 \end{cases}. \tag{6.2}$$

Since each transmitter has a unique ID $\mathbf{c}_s$, the signal is then identified by the estimated ID $\hat{\mathbf{c}}$.

6.2.2 Performance Analysis of User Identification in PIP-OFDM

Lower bound of the Identification Error Rate (IER) is provided in this thesis to evaluate the theoretical performance of user identification in PIP-OFDM system. *Identification Error Rate* means the probability that the receiver side falsely identified the active user. By lower bound, it means the IER is calculated in ideal situation where OFDM symbol is perfectly synchronized using algorithms in Chapter 5, and channel frequency response is perfectly estimated using channel estimation method above. In this situation, the ID of received signal is estimated as

$$\begin{aligned} \hat{c}(\varphi) &= sgn\left\{Re\left[\sum_{k\in\mathbf{L}^{\mathbf{d}}} \overline{Z}(k)o_{\varphi}^{*}(k)\right]\right\} \\ &= sgn\left\{Re\left[\sum_{k\in\mathbf{L}^{\mathbf{d}}}\left(\frac{1}{M}\sum_{m=1}^{M}(X_m(k)H(k)+W_m(k))o_{\varphi}^{*}(k)\right)\right]\right\} \\ &= sgn\left\{Re\left[\sum_{k\in\mathbf{L}^{\mathbf{d}}}\left(\frac{1}{M}|H_0|\sum_{m=1}^{M}\left(X_m(k)\,o_{\varphi}^{*}(k)\right)+\overline{W}(k)o_{\varphi}^{*}(k)\right)\right]\right\}, \end{aligned} \tag{6.3}$$

in which, $\varphi = 1, 2, \ldots, \psi$, and the averaged noise $\overline{W}(k)$ has a variance of $\frac{\delta_n^2}{M}$. Function $Re(\cdot)$ means getting the real part of the variable.

Since carried information on pilots keep the same on every transmitted OFDM symbol, and from the structure of transmitted signal $\mathbf{X}_m$ in (4.2), the estimated ID in (6.3) could

be written as

$$\hat{c}(\varphi) = sgn\left\{Re\left[\sum_{k\in\mathbf{L^d}} |H_0| v_s^d(k)\, o_\varphi^*(k) + \overline{W}(k) o_\varphi^*(k)\right]\right\}. \tag{6.4}$$

From (4.10), where

$$v_s^d(k) = \sum_{\varphi=1}^{\Psi} c_s(\varphi)\cdot o_\varphi(k), \quad k \in \mathbf{L^d}, \tag{6.5}$$

the estimation of ID can be written as

$$\begin{aligned}
\hat{c}(\varphi) &= sgn\left\{Re\left[\sum_{k\in\mathbf{L^d}} |H_0| c_s(\varphi)\cdot o_\varphi(k) o_\varphi^*(k) + \overline{W}(k) o_\varphi^*(k)\right]\right\} \\
&= sgn\left\{Re\left[\sum_{k\in\mathbf{L^d}} |H_0| c_s(\varphi)\cdot \left|o_\varphi(k)\right|^2 + \overline{W}(k) o_\varphi^*(k)\right]\right\} \\
&= c_s(\varphi) + W'(\varphi),
\end{aligned} \tag{6.6}$$

where W' is an equivalent noise term.

Since $\mathbf{o}_\varphi$ has only $\frac{A^d}{\Psi}$ non-zero points (see Chapter 4), and each takes value with the amplitude of v_0, consequently,

$$W' \sim N\left(0, \frac{\delta_n^2 \Psi}{2Mv_0^2|H_0|^2 A^d}\right). \tag{6.7}$$

Assume that pilot tones have the same power with data subcarriers. Then the received OFDM signal has the power of $v_0^2|H_0|^2$. Consequently, the SNR of the received signal could be written as

$$\gamma = \frac{v_0^2|H_0|^2}{\delta_n^2}. \tag{6.8}$$

Therefore,

$$W' \sim N\left(0, \frac{\Psi}{2M\gamma A^d}\right). \tag{6.9}$$

The bit error rate (BER) of the ID estimation is

$$P_b = Q\left(\sqrt{\frac{2M\gamma A^d}{\psi}}\right), \tag{6.10}$$

where the Q-function is defined as

$$Q(x) = \frac{1}{\sqrt{2\pi}}\int_x^{\infty} \exp\left(-\frac{u^2}{2}\right)du. \tag{6.11}$$

Any bit error in ID $\hat{\mathbf{c}}$ will lead to an identification error. Therefore, the lower bound of identification error rate (IER) is formulated as

$$\begin{aligned} P_i &= 1-(1-P_b)^{\psi} \\ &= 1-\left[1-Q\left(\sqrt{\frac{2M\gamma A^d}{\psi}}\right)\right]^{\psi}. \end{aligned} \tag{6.12}$$

6.2.3 Simulations

Simulation results are provided in this section to verify the effectiveness of the proposed PIP-OFDM design. An OFDM system with $2K$ subcarriers is adopted in these simulations. There are altogether $A = 128$ pilot tones in the designed OFDM signal, which includes $A^u = 64$ uniform pilots and $A^d = 64$ identification pilots. To simulate the performance of user identification, two scenarios are considered in this simulation, i.e., $\psi = 8$ in Figure 6.1(a), and $\psi = 16$ in Figure 6.1(b), representing cognitive radio networks with the user capacity of $\mathcal{S} = 2^8$ and $\mathcal{S} = 2^{16}$, respectively. For comparison purpose, the theoretical lower bound of IER is also calculated through (6.12), and plotted in the figures. It is shown in both figures that the simulated IERs are slightly higher than the corresponding lower bounds of IERs, which are caused by the synchronization errors. Comparing Figure 6.1(a)

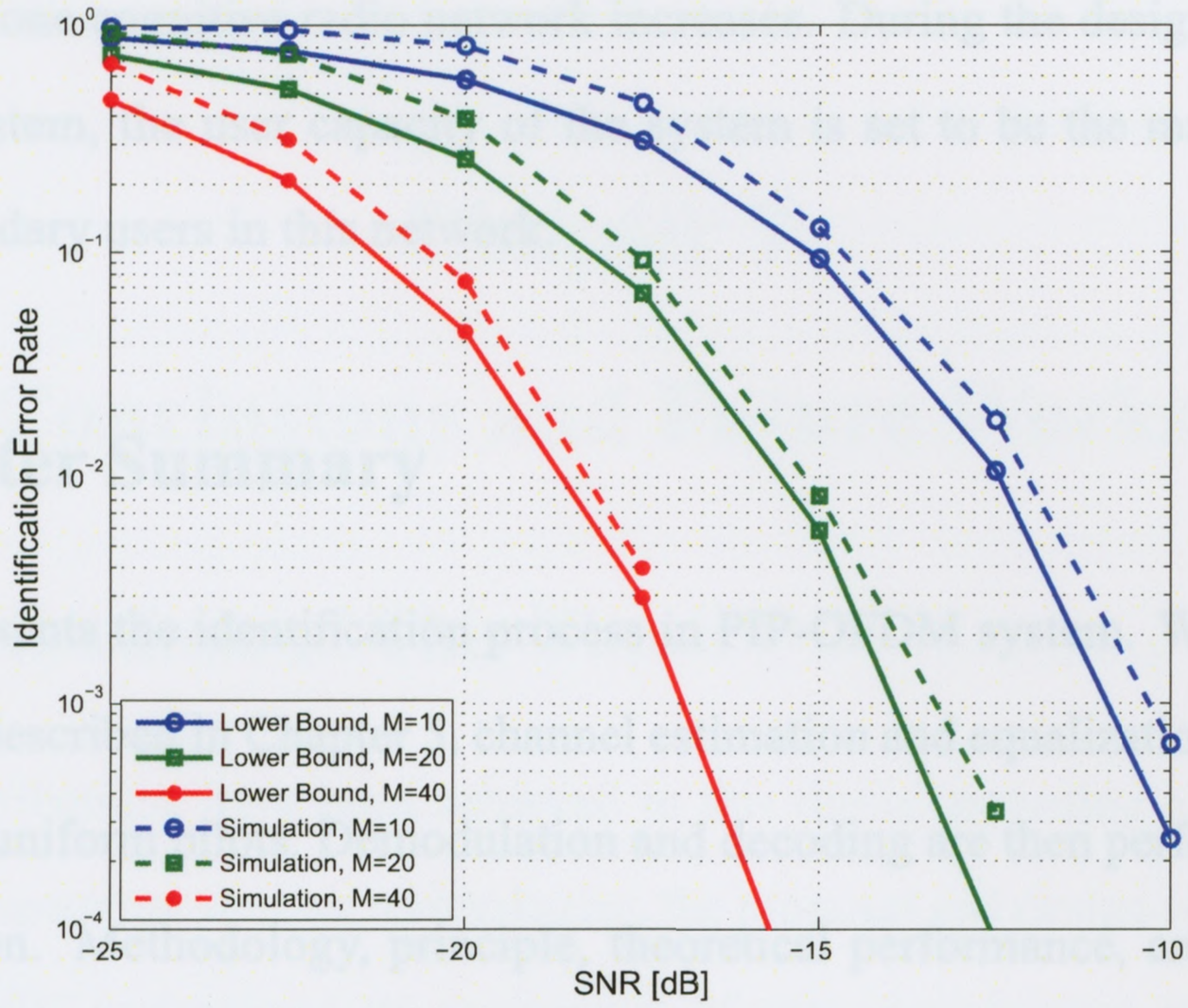

(a)

(b)

Figure 6.1: User identification performance in terms of identification error rate ($2K$ subcarriers system with 64 identification pilot tones is used). (a) $\psi = 8$. (b) $\psi = 16$.

and Figure 6.1(b), it is anticipated that the identification performance degrades when the user capacity of one cognitive radio network increases. During the design and implementation of this system, the user capacity of the system is set to be the maximum possible number of secondary users in this network.

6.3 Chapter Summary

This chapter presents the identification process in PIP-OFDM system. With synchronization algorithms described in Chapter 5, channel estimation and equalization can be realized with the help of uniform pilots. Demodulation and decoding are then performed to achieve user identification. Methodology, principle, theoretical performance, and simulations of identification algorithm in PIP-OFDM system are presented in this chapter.

Chapter 7

Conclusions and Future Works

7.1 Contributions of This Thesis

Three main contributions have been achieved in this thesis, including a comparison and improvement on spectrum sensing technologies, the proposal and design of a new Precoded In-band Pilots (PIP) system and its application of user identification in cognitive radio communications, and the development of enabling techniques for the proposed PIP-OFDM system.

Major spectrum sensing techniques for cognitive radio communications are discussed and compared with the essential principle of energy acquisition during the sensing process, with a focus on pilot-based spectrum sensing for OFDM signals. A new pilot-based OFDM spectrum sensing algorithm with sliding frequency correlator is proposed to address technical difficulties caused by frequency offset and noise uncertainty.

Considering the poor user identification performances of current spectrum sensing techniques, this thesis proposes a new OFDM system design with precoded in-band pilots (PIP-OFDM), which embeds uniform pilots and identification pilots in transmitted signal, and carries user ID information on identification pilots. By demodulating identification pilots in PIP-OFDM system, user identification in cognitive radio network can be realized in low SNR conditions.

Enabling techniques for the implementation of PIP-OFDM system are investigated in this thesis, with a focus on synchronization algorithms at low SNR. Without specifically designed training symbols, coarse synchronization in PIP-OFDM system is realized with correlation methods; fractional frequency offset estimation in PIP-OFDM system is realized by a modified maximum likelihood algorithm in this thesis; a new fractional timing offset estimation algorithm is proposed by estimating phase shift in frequency domain using predesigned uniform pilots. To meet the low SNR requirement, synchronization performance is improved using a multiple OFDM symbols processing strategy in these algorithms.

7.2 Future Works

Due to the existence of unknown sampling frequency offset, the maximum number of averaging times during the spectrum sensing has its limit. This is also one of the technical problems for pilot-based spectrum sensing method at low SNR. A practical sampling frequency offset estimation method is needed for the implementation of pilot-based spectrum sensing and PIP-OFDM system. Alternatively, a maximum number of averaging times should be determined for different maximum sampling frequency offset during the implementation of PIP-OFDM system.

The average processing time in the proposed pilot-based spectrum sensing technique and implementation of PIP-OFDM system has yet one requirement on the stability of the transmission channel, i.e., channel coherence time requirement. Channels used in this thesis are assumed to be either static or slow varying. Similar to the difficulty caused by sampling frequency offset, channel variation also limits the maximum number of average times in the investigations of this thesis.

Precoded in-band pilots, in this thesis, are used to carry ID information of transmitter. Actually, as a general design, precoded in-band pilot technique can be used in other areas, such as bandwidth efficiency improvement and controlling information transmission.

The encoding method in this thesis is based on a simple orthogonal encoding theory. However, in practical systems, other encoding techniques, such as pseudo random sequence, can be used in precoded in-band pilots design for a better efficiency and robustness.

References

[1] Federal Communications Commission, "FCC Online Table of Frequency Allocations," Jan. 2010.

[2] J. Mitola, "Cognitive radio an integrated agent architecture for software defined radio," Ph.D. dissertation, KTH Royal Institute of Technology, Stockholm, 2000.

[3] J. Mitola, *Software Radios: Wireless Architecture for the 21st Century*, John Wiley & Sons Inc, 2000.

[4] S. Haykin, "Cognitive Radio: Brain-Empowered Wireless Communications," *IEEE J. Selected Areas in Commun.*, vol. 23, no. 2, pp. 201–220, Feb. 2005.

[5] J. Yang, "Spatial channel characterization for cognitive radios," Master's thesis, EECS Department, University of California, Berkeley, CA, USA, 2004.

[6] D. B. Cabric and R. W. Brodersen, "Cognitive radios: System design perspective," Ph.D. dissertation, EECS Department, University of California, Berkeley, Berkeley, CA, USA, Dec. 2007.

[7] IEEE 802.22, IEEE 802 LAN/MAN Standards Committee 802.22 WG on WRANs (Wireless Regional Area Networks). [Online]. http://grouper.ieee.org/groups/802/22.

[8] T. Yucek and H. Arslan, "A survey of spectrum sensing algorithms for cognitive radio applications," *IEEE Commun. Survers & Turorials*, vol. 11, no. 1, pp. 116–130, First Quarter 2009.

[9] S. Haykin, D. J. Thomson, and J. H. Reed, "Spectrum Sensing for Cognitive Radio," *Proceedings of the IEEE*, vol. 97, no. 5, pp. 849–877, May 2009.

[10] D. Cabric, S. Mishra, and R. Brodersen, "Implementation issues in spectrum sensing for cognitive radios," in *Proc. Conference Record of the Thirty-Eighth Asilomar*

Conference on Signals, Systems and Computers (ACSSC'04), Nov. 2004, pp. 772–776.

[11] Y. D. Alemseged and H. Harada, "Spectrum sensing for cognitive radio," in *Proc. IEEE Radio and Wireless Symposium (RAWCON'08)*, Jan. 2008, pp. 356–359.

[12] A. Ghasemi and E. Sousa, "Spectrum sensing in cognitive radio networks: requirements, challenges and design trade-offs," *IEEE Commun. Mag.*, vol. 46, no. 4, pp. 32–39, April 2008.

[13] R. Chen, J. Park, and J. Reed, "Defense against Primary User Emulation Attacks in Cognitive Radio Networks," *IEEE J. Select. Areas Commun.*, vol. 26, no. 1, pp. 25–37, Jan. 2008.

[14] Z. Quan, S. Cui, A. Sayed, and H. Poor , "Optimal Multiband Joint Detection for Spectrum Sensing in Cognitive Radio Networks," *IEEE T. Signal Process.*, vol. 57, no. 3, pp. 1128–1140, March 2009.

[15] Z. Han and H. Jiang, "Replacement of spectrum sensing and avoidance of hidden terminal for cognitive radio," in *Proc. IEEE Wireless Communications and Networking Conference (WCNC'08)*, March-April 2008, pp. 1448–1452.

[16] Advanced Television Systems Committee, "ATSC Recommended Practice: Receiver Performance Guidelines," June 2004.

[17] G. Chouinard, D. Cabric, and M. Ghosh, "Sensing thresholds," IEEE 802.22 (IEEE 802.22-06/0051r3), May 2006.

[18] FCC, "FCC OET Bulletin No. 69: Longley-Rice methodology for Evaluating TV Coverage and Interference," Feb. 2004.

[19] W. A. Gardner, A. Napolitano, and L. Paura, "Cyclostationarity: half a century of research," *Signal Process.*, vol. 86, no. 4, pp. 639–697, 2006.

[20] A. Fehske, J. Gaeddert, and J. Reed, "A new approach to signal classification using spectral correlation and neural networks," in *Proc. First IEEE International Symposium on New Frontiers in Dynamic Spectrum Access Networks (DySPAN'05)*, Nov. 2005, vol. 1, pp. 144–150.

[21] P. Sutton, K. Nolan, L. Doyle, "Cyclostationary Signatures in Practical Cognitive Radio Applications," *IEEE J. Select. Areas Commun.*, vol. 26, no. 1, pp. 13–24, Jan. 2008.

[22] Q. Zhao and B. M. Sadler, "A Survey of Dynamic Spectrum Access," *IEEE Signal Processing Magazine*, vol. 24, no. 3 pp. 79–89, May 2007.

[23] Y. Xing, R. Chandramouli, S. Mangold, and S. Shankar, "Dynamic spectrum access in open spectrum wireless networks," *IEEE J. Selected Areas Commun.*, vol. 24, no. 3, pp. 626–637, March 2006.

[24] I. Akyildiz, W. Lee, M. Vuran, and S. Mohanty, "Next generation/ dynamic spectrum access/cognitive radio wireless networks: a survey," *Elsevier Computer Networks*, vol. 50, pp. 2127–2159, 2006.

[25] C. Santivanez et al., "Opportunistic Spectrum Access: Challenges, Architecture, Protocols," in *Proc. Wireless Internet Conf.*, Aug. 2006.

[26] Q. Zhao and A. Swami, "A Decision-Theoretic Framework for Opportunistic Spectrum Access," *IEEE T. Wireless Commun.*, vol. 14, no. 4, pp. 14–20, Aug. 2007.

[27] Q. Zhao, L. Tong, A. Swami, and Y. Chen, "Decentralized cognitive MAC for opportunistic spectrum access in ad hoc networks: A POMDP framework," *IEEE T. Wireless Commun.*, vol. 25, no. 3, pp. 589–600, April 2007.

[28] N. Tewfik and A. Acoustics, "Sequential pilotsensing of ATSC signals in IEEE 802.22 cognitive radio networks Kundargi," in *Proc. IEEE International Conference on Speech and Signal Processing (ICASSP'08)*, April 2008, pp. 2789–2792.

[29] C. Carlos, M. Ghosh, C. Dave, and C. Kiran, "Spectrum Sensing for Dynamic Spectrum Access of TV Bands," in *Proc. International Conference on Cognitive Radio Oriented Wireless Networks and Communications (CrownCom'08)*, Aug. 2007, pp. 225–233.

[30] M. Ghosh, "Text on FFT-based Pilot Sensing," IEEE 802.22 (doc. 22-07-0298-01-0000), July 2007.

[31] H. Chen, W. Gao, and D. Daut, "Spectrum Sensing for OFDM Systems Employing Pilot Tones and Application to DVB-T OFDM," in *Proc. IEEE ICC'08*, May 2008, pp. 3421–3426.

[32] F. Socheleau, P. Ciblat, and S. Houcke, "OFDM System Identification for Cognitive Radio Based on Pilot-Induced Cyclostationarity," in *Proc. IEEE Wireless Communications and Networking Conference (WCNC'09)*, April 2009.

[33] S. Tu, K. Chen, and R. Prasad, "Spectrum Sensing of OFDMA System for Cognitive Radios," in *Proc. IEEE International Symposium on Personal, Indoor and Mobile Radio Communications (PIMRC'07)*, Sep. 2007, pp. 1–5.

[34] X. Wang, H. Chen, Y. Wu, J. Chouinard, and C. Wang, "Identification of PCP-OFDM Signals at Very Low SNR for Spectrum Efficient Communications," in *Proc. IEEE VTC'09 Spring*, April 2009.

[35] B. Shent, L. Huang, C. Zhao, Z. Zhou, and K. Kwak, "Energy Detection Based Spectrum Sensing for Cognitive Radios in Noise of Uncertain Power," in *Proc. International Symposium on Communications and Information Technologies (ISCIT'07)*, Oct. 2008, pp. 628–633.

[36] D. Chen, J. Li, and J. Ma, "Cooperative Spectrum Sensing under Noise Uncertainty in Cognitive Radio," in *Proc. International Conference on Wireless Communications, Networking and Mobile Computing (WiCOM'08)*, Oct. 2008, pp. 1–4.

[37] B. Le, T. W. Rondeau, D. Maldonado, and C. W. Bostian, "Modulation Identification Using Neural Network for Cognitive Radios," in *Proc. Software Defined Radio Forum Technical Conference*, Anaheim, CA, 2005.

[38] T. Yucek and H. Arslan, "OFDM Signal Identification and Transmission Parameter Estimation for Cognitive Radio Applications," in *Proc. IEEE Globecom'07*, Nov. 2007, pp. 4056–4060.

[39] P. D. Sutton, K. E. Nolan and L. E. Doyle, "Cyclostationary Signatures in Practical Cognitive Radio Applications," *IEEE Journal on Selected Areas in Communications*, vol. 26, no. 1, pp. 13–24, Jan. 2008.

[40] C. Wang, X. Wang, H. Li, and P. Ho, "Multi-window Spectrum Sensing of Unsynchronized OFDM Signal at Very Low SNR," in *Proc. IEEE Globecom'09*, Dec. 2009.

[41] P. H. Moose, "A technique for orthogonal frequency division multiplexingfrequency offset correction," *IEEE T. Commun.*, vol. 42, no. 10, pp. 2908–2914, Oct. 1994.

[42] D. S. Han, J. H. Seo, and J. J. Kim, "Fast carrier frequency offset compensation in OFDM systems," *IEEE T. Consumer Electronics*, vol. 47, no. 3, pp. 364–369, Aug. 2001.

[43] T. M. Schmidl and D. C. Cox, "Robust frequency and timing synchronization for OFDM," *IEEE T. Commun.*, vol. 45, no. 12, pp. 1613–1621, Dec. 1997.

[44] B. Ai, J. Ge, Y. Wang, S. Y. Yang, P. Liu, and G. Liu, "Frequency offset estimation for OFDM in wireless communications," *IEEE T. Consumer Electronics*, vol. 50, no. 1, pp. 73–77, Feb. 2004.

[45] M. Hlaing, V. K. Bhargava, and K. B. Letaief, "A robust timing and frequency synchronization for OFDM systems," *IEEE T. Wireless Commun.*, vol. 2, no. 4, pp. 822–839, July 2003.

[46] M. Morelli and U. Mengali, "An improved frequency offset estimator for OFDM applications," *IEEE Commun. Lett.*, vol. 3, no. 3, pp. 75–77, March 1999.

[47] T. Keller, L. Piazzo, P. Mandarini, and L. Hanzo, "Orthogonal frequency division multiplex synchronization techniques for frequency-selective fading channels," *IEEE JSAC*, vol. 19, no. 6, pp. 999–1008, June 2001.

[48] J. J. van de Beek, M. Sandell, and P. O. Borjesson, "ML estimation of time and frequency offset in OFDM systems," *IEEE T. Signal Processing*, vol. 45, no. 7, pp. 1800–1805, July 1997.

[49] T. Keller, and L. Hanzo, "Orthogonal frequency division multiplex synchronisation techniques for wireless local area networks," in *Proc. IEEE PIMRC'96*, Oct. 1996, vol. 3, pp. 963–967.

[50] M. Sandell, J. J. van de Beek, and P. O. Borjesson, "Timing and frequency synchronization in OFDM systems using the cyclic prefix," in *Proc. International Symmposium on Synchronization 1995*, Dec. 1995, pp. 16–19.

[51] P. Chevillat, D. Maiwald, and G. Ungerboeck, "Rapid Training of a Voiceband Data-Modem Receiver Employing an Equalizer with Fractional-T Spaced Coefficients," *IEEE T. Commun.*, vol. 35, no. 9, pp. 869–876, Sep. 1987.

[52] M. L. Lieu and T. D. Chiueh, "A low-power digital matched filter for direct-sequencespread-spectrum signal acquisition," *IEEE J. Solid-State Circuits*, vol. 36, no. 6, pp. 933–943, June 2001.

[53] ETSI Standard, "Digital Video Broadcasting (DVB); Framing structure, channel coding and modulation for digital terrestrial television," EN 300 744 V1.5.1, June 2004, available at http://pda.etsi.org/pda/queryform.asp

[54] M. Dong and L. Tong, "Optimal Design and Placement of Pilot Symbols for Channel Estimation," *IEEE T. Signal Process.*, vol. 50, no. 12, pp. 3055–3069, Dec. 2002.

[55] S. Haykin, *Communication Systems*, 4th Ed. New York: Wiley, 2001.

[56] F. Tufvesson, O. Edfors, and M. Faulkner, "Time and frequency synchronization for OFDM using PN-sequence preambles," in *Proc. IEEE VTC 99' fall*, Sep. 1999, vol. 4, pp. 2203–2207.

[57] M. Lieu, and T. Chiueh, "A low-power digital matched filter for direct-sequencespread-spectrum signal acquisition," *IEEE J. Solid-State Circuits*, vol. 36, no. 6, pp. 933–943, June 2001.

[58] A. Fort, J. W. Weijers, V. Derudder, W. Eberle, and A. Bourdoux, "A performance and complexity comparison of auto-correlation and cross-correlation for OFDM burst synchronization," in *Proc. IEEE International Conference on Acoustics, Speech, and Signal Processing (ICASSP '03)*, April 2003, vol. 2, pp. II- 341–4.

[59] R. van Nee, and R. Prasad, *OFDM for Wireless Multimedia Communications*, Norwood, MA: Artech House Publishers, Jan. 2000.

[60] M. Hsieh and C. Wei, "Channel estimation for OFDM systems based on comb-type pilot arrangement in frequency selective fading channels," *IEEE Transactions on Consumer Electronics*, vol. 44, no.1, pp. 217–225, Feb. 1998.

[61] M. Morelli and U. Mengali, "A comparison of pilot-aided channel estimation methods for OFDMsystems," *IEEE T. Signal Processing*, vol. 49, no. 12, pp. 3065–3073, Dec. 2001.

[62] J. J. van de Beek, O. Edfors, M. Sandell, S. K. Wilson, and P. 0. BGrjesson, "On channel estimation in OFDM systems," in *Proc. IEEE Veh. Tech. Conf. (VTC'95)*, July 1995, pp. 815–819.

[63] O. Edfors, M. Sandell, J. J. van de Beek, S. K. Wilson, and P.O. Brjesson, "OFDM channel estimation by singular value decomposition," *IEEE T. Commun.*, vol. 46, no. 7, pp. 931–939, July 1998.

[64] L. Deneire, P. Vandenameele, L. van der Perre, B. Gyselinckx, and M. Engels, "A low-complexity ML channel estimator for OFDM," *IEEE T. Commun.*, vol. 51, no. 2, pp. 135–140, Feb. 2003.

[65] T. D. Chiueh and P. Y. Tsai, *OFDM Baseband Receiver Design for Wireless Communications*, John Wiley and Sons (Asia) Pte Ltd, 2007, pp. 138–140.